



Ernest Orlando Lawrence
Berkeley National Laboratory
1 Cyclotron Road, 70R0108B
Berkeley CA 94720-8168
(510) 495-2679; fax: (510) 486-4260

March 17, 2014

Mr. Tien Q. Duong
3V/Forrestal Building
Office of Vehicle Technologies
U.S. Department of Energy
1000 Independence Avenue, S.W.
Washington D.C. 20585

Dear Tien,

Here is the first quarter FY 2014 report for the Batteries for Advanced Transportation Technologies (BATT) Program. This report and prior Program reports can be downloaded from <http://batt.lbl.gov/reports/quarterly-reports/>.

Sincerely,

Venkat Srinivasan
Acting Head
BATT Program

edited by: V. Battaglia
M. Foure
S. Lauer
M. Minamihara

cc: J. Barnes DOE/OVT
P. Davis DOE/OVT
D. Howell DOE/OVT
P. Smith DOE/OVT
J. Muhlestein DOE-BSO

SIX FEATURED HIGHLIGHTS

Electrode Architectures

- ✦ Zaghib of HQ demonstrates excellent cycleability of a Si electrode when cycled to just 40% of its theoretical capacity.

Anodes

- ✦ Wang of Penn State and Cui of Stanford demonstrate Si-based electrodes made from nanostructures of > 1600 mAh/g with excellent cycling ability.

Diagnostics

- ✦ Balsara and Prendergast of LBNL perform the first theoretical calculation of the sulfur K-edge XAS of isolated Li_2S_x species solvated in tetraglyme.
- ✦ Kostecki of LBNL uses XANES to show that dissolved Ni and Mn from an NMO cathode appear in the anode SEI as Ni^{2+} and Mn^{2+} .
- ✦ Somorjai and Ross of LBNL use *ex situ* FTIR to demonstrate the formation of Li_2CO_3 on Si during SEI formation.

Modeling

- ✦ Ceder of MIT determines the Li-migration path in a representative Li-rich oxide. This may lead to the development of new, high capacity Li-rich materials.

Task 1.1 - Vincent Battaglia (Lawrence Berkeley National Laboratory)

Electrode Failure and Benchmarking Analysis

PROJECT OBJECTIVE: This project supports the BATT Focus Groups, with emphasis on the High-Voltage Cathode Project and the Si-Anode Project. If the difference in cycleability of NMO and NCM can be understood through identification of a difference in reaction products, then perhaps the cycleability of NCM at higher voltages can be improved. If differences between the side reactions on graphite and Si can be measured, than perhaps the Si surface can be modified to allow for long-term full cell cycleability comparable to that of cells containing graphite.

PROJECT IMPACT: Success with understanding and improving the stability of NCM in the presence of electrolyte at voltages greater than 4.3 V vs. Li/Li⁺ will translate to an increase in capacity and voltage and hence a compounding improvement in energy density. Improvement in the passivating effects of SEI on Si that allows for long term cycleability, would result in larger fractions of Si in the anode and improved energy density of high-capacity cathode cells.

OUT-YEAR GOALS: One goal of this project is to support the High-Voltage Focus Group, formed to understand the limits of cycleability of NCM as the voltage is increased. This project will provide electrochemical and chemical data to support that effort. The second goal is to support the Si-Anode Focus Group, which was formed to effectively use Si in a battery. This project will provide electrochemical and chemical data to support this effort.

COLLABORATIONS: None this quarter.

Milestones

- 1) Make a pouch cell with the same cycling behavior as a coin cell. (Dec. 13) **Complete.**
- 2) Go/No-Go: Generate measurable levels of soluble reaction products. Criteria: Evaluate one of the proposed experimental test set-ups for its ability to generate measurable levels of soluble reaction products. (Mar. 14) **Ongoing**
- 3) Demonstrate a 3-electrode cell where the impedance data of the individual electrodes can be directly assigned to the full cell data. (Jun. 14) **Ongoing**
- 4) Measure the gas composition of a high-voltage cell. (Sep. 14) **Ongoing**
- 5) Measure the gas composition of a Si-anode cell. (Sep. 14) **Ongoing**

Progress Report

As part of a high-voltage study, it may be important to determine if a gas is formed during the initial, middle, or later stages of cycling. Much effort was spent in the previous year to develop a coin cell where gas could be extracted. These experiments proved inconclusive. It was decided that greater success may come from using larger cells. With this in mind, the group set out to make full cells in a pouch cell configuration.

Figure 1 shows the first attempt to make a pouch cell. This is the cycling data of a Graphite/NCM cell to 500 cycles. The cell was cycled between 3 and 4.3 V at a charge rate of C/2 and a discharge rate of C/1. At this rather rapid cycling rate, the coulombic efficiency is near 1. The average capacity fade is approximately 0.23% per cycle. This compares very well with the capacity retention of some coin cells tested in some earlier work. For those cells, the average capacity fade was approximately 0.27% per cycle.

The data presented in Fig. 2 shows the average voltage of the cell on charge and discharge vs. cycle number. This data is more sensitive to resistance rise in the cell than the capacity data and shows very little change with cycling. This indicates that the cells are sealed well enough to prevent incursion of moisture or loss of electrolyte that can lead to resistance rise. Based on this data, it is believed that it should be possible to use these larger format cells for electrode performance evaluation and meaningful gas capture.

The next step to this process will be to develop a method to extract the gas and have it sent directly to a mass spectrometer while cycling. Sealing a cell with an additional port will not be trivial.

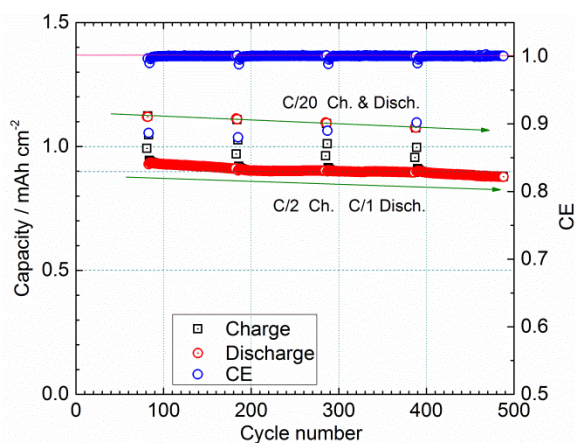


Figure 1. Cycling data of an Gr./NCM cell at a C/2 charge and C/1 discharge rate. The cell is cycled between 3.0 and 4.3 V.

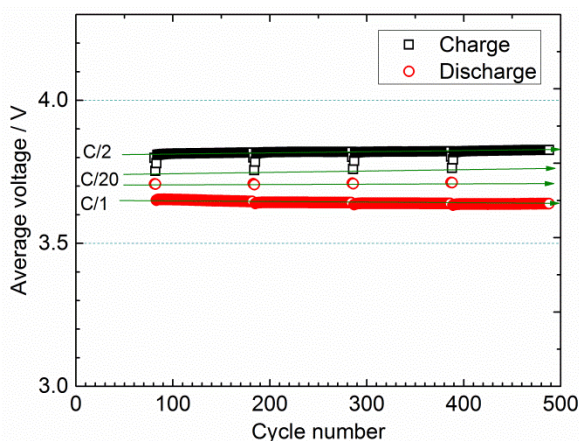


Figure 2. Average voltage on charge and discharge of the cell described in Fig. 1.

Assembly of Battery Materials and Electrodes

PROJECT OBJECTIVE: To develop high-capacity, low-cost electrodes with good cycle stability and rate capability to replace graphite in Li-ion batteries.

The *in situ* analyses of Si-based electrodes showed that the bigger particles (*ca.* 13 μm) start to crack at around 0.1 V. During the charging process, all of the major cracks remained, while some fissures collapsed and others expanded, but the smaller particles ($< 2 \mu\text{m}$) did not crack. Furthermore, the *in situ* study revealed that delamination occurred at the interfaces of the particle/binder and the Cu current collector/electrode. These experiments provided a better understanding of the anode cycling mechanism and the failure mode associated with capacity fade. The results will be helpful to redesign the anode architecture. This study will also be beneficial to design the architecture of the high-voltage cathode (LMNO).

PROJECT IMPACT: This project will have a major impact on the wide spread adoption of EVs by (i) demonstrating scale-up production of nano-Si powders (to kilogram levels) for advanced EV batteries, and (ii) improving electrode performance by the understanding gained from *in situ* SEM and TEM studies.

The success of the project will contribute to the advancement of EV battery technology by developing batteries with increased energy density and improved cycle life, leading to EVs with longer driving range.

OUT-YEAR GOALS: Complete the *in situ* SEM and TEM studies of the Si-anode material during electrochemical cycling and real-time monitoring of structure changes. These analyses will help to understand the failure mode and to guide further improvements in the electrode architecture. These studies will also help to investigate the high-voltage passivation layer to identify the appropriate electrolyte and electrode compositions. In addition, the studies will help to identify an alternative supplier of Si powder material as a base line for the BATT Program.

As a final goal, the optimized Si-anode and LiMnNiO-doped Cr cathode will be evaluated in a laminate 20 Ah Li-ion cell.

COLLABORATIONS: Collaborations with BATT members: V. Battaglia and G. Liu from LBNL and J. Goodenough from the University of Texas at Austin.

Milestones

- 1) Identify Si-based anode materials that can achieve a capacity of 1200 mAh/g. (Dec. 13) **Complete**
- 2) Supply Si powder (1 Kg) from an alternative supplier as a baseline material for BATT PIs. (Mar. 14) **Complete**
- 3) Go/No-Go: Terminate production of Si powder in anode tests that show more than 20% capacity fade in the initial 100 cycles. Criteria: Supply laminates Si-based electrodes to BATT PIs. (Jun. 14) **Ongoing**.
- 4) Supply a 20-Ah Li-ion flat cell based on Si and LiMNO materials to BATT PIs. (Sep. 14) **Ongoing**

Progress Report

During the previous quarter, Si:Alginate:carbon electrodes, between 50:25:25 and 60:20:20, were identified as an optimum range of composition to produce longer cycle life. The porosity of the electrode, which is strongly influenced by the electrode composition, is also an important contribution to the electrode performance. A high carbon content and low Si ratio in the anode composition yielded significantly better performance. To investigate the cycle life of the Si baseline material, the formulation 50:25:25 was adopted. Monitoring the stress on Si particles is another key parameter that affects cycling performance. The stress level was controlled by varying depth of discharge (DoD); at low DoD, the Si particles experience the minimum amount of stress. This study clearly revealed the effect of DoD on cycling stability. When the anode is cycled at a high percent of its DoD, the capacity fade is severe, as a result of experiencing high stress and cracking. At 40% DoD at a C/6 rate, a very stable reversible capacity of around 1670 mAh/g with good coulombic efficiency is obtained after 200 cycles. This result indicates that sacrificing a little capacity may be an acceptable compromise to achieving longer cycle life and sufficient capacity.

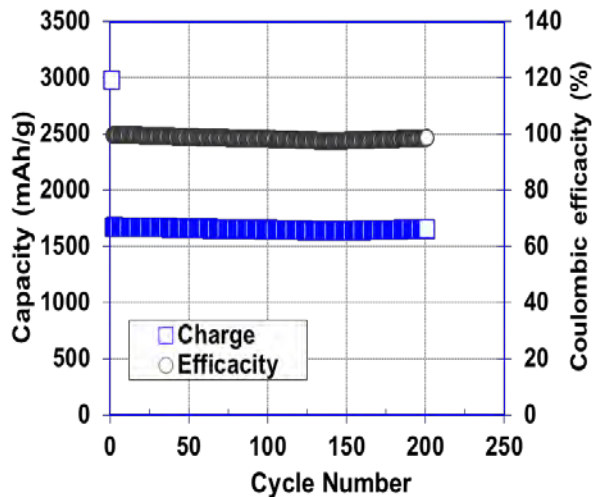


Figure 1. Cycle life at C/6 of Li/EC-DEC-LiPF₆/Si cells at different 40% DoD.

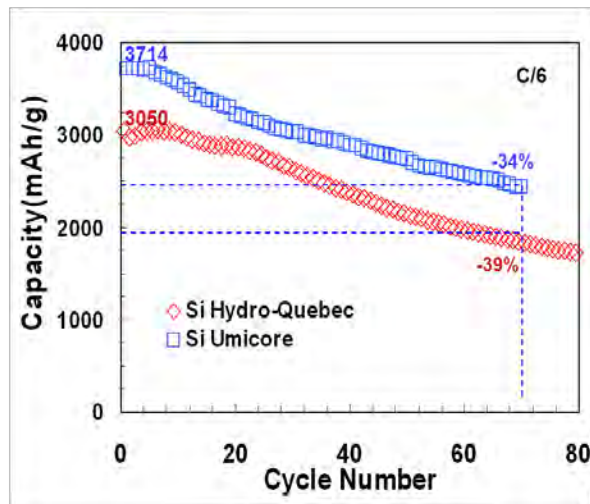


Figure 2. Cycle life at C/6 of HQ Si compared to the baseline in Li/EC-DEC-LiPF₆/Si cells.

In a parallel effort, HQ has initiated a project to produce a new Si material as an alternative source for the BATT Si Focus Group. This material consists of an agglomeration of spherical particles varying from 50 to 120 μm . The primary particles ranged from 80 to 500 nm. The evaluation of this material in an electrode with the formulation 50:25:25 showed a reversible capacity of 3494 mAh/g compared to 3870 mAh/g for the baseline Si. The coulombic efficiency of the 1st and 2nd cycles, respectively, are 84.0% and 97.5% for the HQ material, compared to 85.3% and 97.9% for the baseline material. The cell life at C/6 shows a similar capacity fade for both materials. After 70 cycles at C/6, the Si-HQ shows a capacity fade of 39% compared to 34% for the baseline material (Fig. 2). Investigations to obtain further improvements are ongoing at HQ; preliminary results suggest this material is a promising alternative electrode source for the BATT Program. HQ has supplied 1 kg of the HQ-Si material to the BATT PIs for evaluation.

Design and Scalable Assembly of High Density Low Tortuosity Electrodes

PROJECT OBJECTIVE: Develop a scalable high density binder-free low-tortuosity electrode design and fabrication process to enable increased cell-level energy density compared to conventional Li-ion technology. Characterize and optimize the electronic and ionic transport properties of controlled porosity and tortuosity electrodes as well as densely-sintered reference materials in $\text{Li}(\text{Ni},\text{Co},\text{Al})\text{O}_2$ (NCA), high capacity Li_2MnO_3 - LiMO_2 , and high voltage $\text{LiM}_{1-x}\text{Mn}_2\text{O}_4$ and $\text{LiM}_{1-x}\text{Mn}_2\text{O}_4\text{-yFy}$ spinels in order to elucidate rate-limiting steps.

PROJECT IMPACT: The high cost (\$/kWh) and low energy density of current automotive Li-ion technology is in part due to the need for thin electrodes and associated high inactive materials content. If successful this project will enable use of electrodes based on known families of cathode and anode actives but with at least 3 times the areal capacity (mAh/cm^2) of current technology while satisfying the duty cycles of vehicle applications. This will be accomplished *via* new electrode architectures fabricated by scalable methods with higher active materials density and reduced inactive content, and will in turn enable higher energy density and lower-cost EV cells and packs.

OUT-YEAR GOALS: After downselection of cathodes, identify an anode approach that therefore allows full cells in which both electrodes have high area capacity under EV operating conditions. Anode approach will include identifying compounds amenable to same fabrication approach as cathode, or use of very high capacity anodes such as stabilized Li or Si alloys that in conventional form can capacity-match the cathodes. Use data from best performing electrochemical couple in techno-economic modeling of EV cell and pack performance parameters.

COLLABORATIONS: Within BATT, this project collaborates with Antoni P. Tomsia (LBNL) in fabrication of low-tortuosity high density electrodes by directional freeze-casting and sintering, and with Gao Liu (LBNL) in the Silicon Anode Focus Group on acoustic emission-based characterization of electrochemically-induced microfracture of Si anodes. Outside of BATT, the project collaborates with Randall Erb (Northeastern Univ.) on magnetic-alignment-based fabrication of low tortuosity electrodes.

Milestones

- 1) Measure electronic and ionic conductivities and diffusivity in sintered dense $\text{Li}(\text{Ni},\text{Co},\text{Al})\text{O}_2$ (NCA) and Fe-doped high voltage spinel $\text{Li}_{1-x}\text{Mn}_{1.5}\text{Ni}_{0.5}\text{O}_4$ spinel. Fabricate first freeze-cast samples of at least one cathode composition. (Dec. 13) **Complete**
- 2) Go/No-Go: Downselect one cathode composition for follow-on work. Criteria: Based on transport measurements and cycling tests of freeze-cast and sintered electrodes. (Mar. 14) **Ongoing**
- 3) Demonstrate at least $5 \text{ mAh}/\text{cm}^2$ capacity per unit area at 1C continuous cycling rate for a freeze-cast cathode. (Jun. 14) **Ongoing**
- 4) Demonstrate at least $10 \text{ mAh}/\text{cm}^2$ capacity per unit area for a 2C 30 sec pulse for a freeze-cast cathode. (Sep. 14) **Ongoing**

Progress Report

Transport measurements in single-phase $\text{Li}_x\text{Ni}_{0.8}\text{Co}_{0.15}\text{Al}_{0.05}\text{O}_2$ (NCA) were completed. The Li-ion diffusivity was measured as a function of x using the dc depolarization method and found to vary by over an order of magnitude with x (Fig. 1a). The x -dependence indicates a change in diffusion mechanism, probably between vacancy and interstitial mechanisms, around $x=0.5$. In initial tests of directionally freeze-cast NCA in Swagelok-type half cells (Fig. 1b), voltage-capacity curves at low rates ($C/50$) are as expected for NCA following initial “formation” on charge, which may be related to electrolyte penetration or electronic conductivity enhancement upon delithiation.

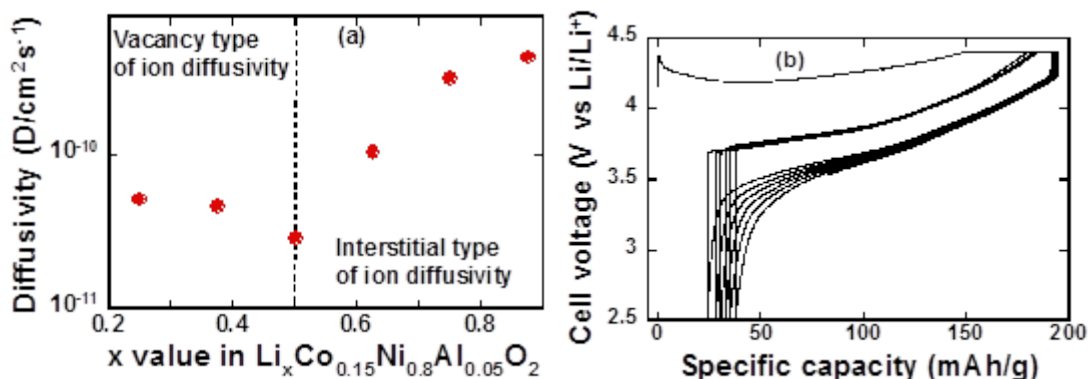


Figure 1. (a) Ion diffusivity vs. Li in NCA. (b) Voltage-capacity for directionally freeze-cast NCA.

Iron doping of the high-voltage spinel LMNO stabilizes against cubic-cubic first-order phase transitions and related mechanical failure/fatigue. Here the impact on Li-ion transport was measured in dense single-phase samples using DC and AC impedance using an electron blocking cell configuration $\text{Li}/\text{PEO}/\text{NCA}/\text{PEO}/\text{Li}$. As shown in Table 1, Fe-doping varies ion diffusivity by less than a factor of two. Previous measurements have shown that Fe-doping enhances electronic conductivity by a factor of 10 to 100, reaching 10^{-4} S/cm. Thus, Fe-doping is expected to improve mechanical reliability and electrochemical performance in sintered LNMO.

Table 1. Ionic transport in ordered $\text{LiMn}_{1.5}\text{Ni}_{0.5}\text{O}_4$ and $\text{LiMn}_{1.5}\text{Ni}_{0.42}\text{Fe}_{0.08}\text{O}_4$ at *ca.* 50°C.

Samples	Ionic conductivity (Scm^{-1})	Ionic diffusivity (cm^2s^{-1})	Techniques used
$\text{LiMn}_{1.5}\text{Ni}_{0.5}\text{O}_4$	<i>ca.</i> 2×10^{-7}	<i>ca.</i> 10^{-7}	DC
$\text{LiMn}_{1.5}\text{Ni}_{0.5}\text{O}_4$	<i>ca.</i> 6×10^{-8}	<i>ca.</i> 5×10^{-8}	AC
$\text{LiMn}_{1.5}\text{Ni}_{0.42}\text{Fe}_{0.08}\text{O}_4$	<i>ca.</i> 8×10^{-8}	<i>ca.</i> 6×10^{-8}	DC
$\text{LiMn}_{1.5}\text{Ni}_{0.42}\text{Fe}_{0.08}\text{O}_4$	<i>ca.</i> 6×10^{-8}	<i>ca.</i> 9×10^{-8}	AC

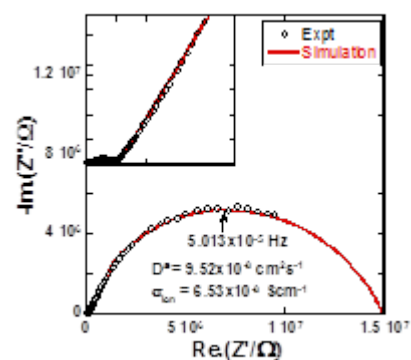


Figure 2. AC impedance data.

Hierarchical Assembly of Inorganic/Organic Hybrid Si Negative Electrodes

PROJECT OBJECTIVE: This proposed work aims to enable Si as a high-capacity and long cycle-life material for negative electrode to address two of the barriers of Li-ion chemistry for EV/PHEV application: insufficient energy density and poor cycle life performance. The proposed work will combine material synthesis and composite particle formation with electrode design and engineering to develop high-capacity, long-life, and low cost hierarchical Si-based electrode. State of the art Li-ion negative electrodes employ graphitic active materials with theoretical capacities of 372 mAh/g. Silicon, a naturally abundant material, possesses the highest capacity of all Li-ion anode materials. It has a theoretical capacity of 4200 mAh/g for full lithiation to the $\text{Li}_{22}\text{Si}_5$ phase. However, Si volume change disrupts the integrity of electrode and induces excessive side reactions, leading to fast capacity fade.

PROJECT IMPACT: This work addresses the adverse effects of Si volume change and minimizes the side reactions to significantly improve capacity and lifetime to develop negative electrode with Li-ion storage capacity over 2000 mAh/g (electrode level capacity) and significantly improve the coulombic efficiency to over 99.9%. The research and development activity will provide an in-depth understanding of the challenges associated with assembling large volume change materials into electrodes and will develop a practical hierarchical assembly approach to enable Si materials as negative electrodes in Li-ion batteries.

OUT-YEAR GOALS: There are three aspects of this proposed work - bulk assembly, surface stabilization and Li enrichment, which are formulated into 10 tasks in a four-year period. 1) Develop hierarchical electrode structure to maintain electrode mechanical stability and electrical conductivity. (Bulk assembly). 2) Form *in situ* compliant coating on Si and electrode surface to minimize Si surface reaction (surface stabilization). 3) Use prelithiation to compensate first cycle loss of the Si electrode. (Li enrichment) In the end of the 4th year, the goal is to achieve a Si based electrode at higher mass loading of Si, and can be extensively cycled cycles with minimum capacity loss at high coulombic efficiency to qualified for vehicle application.

COLLABORATIONS: Vince Battaglia and Venkat Srinivasan (LBNL), Xingcheng Xiao (GM), Jason Zhang (PNNL), Chongming Wang (Penn State), Yi Cui (Stanford), and the Si-Anode Focus Group.

Milestones

- 1) Design and synthesize 3 more PEFM polymers with different EO content to study the adhesion and swelling properties of binder to the Si electrode performance. (Dec. 13) **Complete**
- 2) Go/No-Go: Down select Si vs. Si alloy particles and particle sizes (nano vs. micro.) Criteria: Down select based on cycling results. (Mar. 14) **Ongoing**
- 3) Prepare one type of Si/conductive polymer composite particles and test its electrochemical performance. (Jun. 14) **Ongoing**
- 4) Design and synthesize one type of vinylene carbonate (VC) derivative that is targeted to protect Si surface and test it with Si-based electrode. (Sep. 14) **Ongoing**

*Progress Report

Figure 1 is a schematic of the synthesis of the conductive polymers under study, where P represents polyfluorene with octyl side chains, E represents triethyleneoxide monomethylether side chains, F represents fluorenone, and M represents benzoate ester. The molar ratio among P, E, F, and M is represented by a, b, c, and d. In terms of their functionality, P contributes to the electric conductivity as polyfluorene-type polymer block; E was introduced into the polymer to enhance its polarity, and therefore its electrolyte uptake; F was incorporated to tailor the electronic structure of the polymer, so that the polymer could be cathodically doped under the reduced Li environment to improve its overall electric

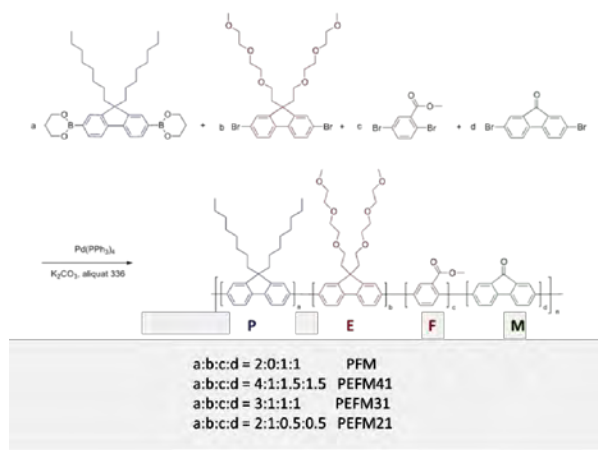


Figure 1. Synthetic scheme and the relative molar ratio of four functional block of polymer binders.

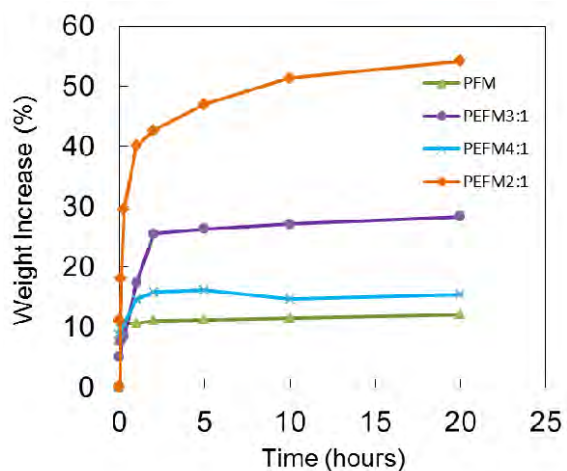


Figure 2. The swelling tests of polymer films in the EC/DEC (1:1) electrolyte.

conductivity; M groups were copolymerized to improve the chain flexibility of the polymer, thereby strengthening the mechanical adhesion force between the active materials and the polymer binder. As shown in Fig. 1, the polarity of the polymers was designed from low to high by controlling the relative molar ratio of the polar side chain E from low to high, and named PFM, PEFM41, PEFM31, and PEFM21, respectively.

An important parameter used to predict the performance of a polymer binder in an anode is the interaction between the polymer with the electrolyte. The swellability of thin films of polymer in ethylene carbonate (EC) and diethylene carbonate (DEC) (1:1 w/w) at room temperature was measured (Fig. 2). Swelling ratio is defined as weight increase with absorbed solvent divided by the weight of the dry polymer film. As shown in Fig. 3., PFM has electrolyte uptake only up to 10% of its dry state; PEFM41 shows a bit higher electrolyte uptake at about 15%; PEFM31 almost triples the electrolyte uptake compared to that of PFM, reaching around 28%. Last, but not least, the polymer binder PEFM21, which has the highest polarity in this system, shows an electrolyte uptake ratio reaching higher than 50%. As can be seen, the trend of the swelling of four polymer binders is consistent with the increase of ethyleneoxide content, indicating that the chemically-attached ether side groups in the binder help to improve the overall electrolyte uptake. The swellability of the polymer binders indicates the level of polymer/electrolyte interaction; higher swellability of polymer binders should also lead to a more deformable material.

Task 1.5 - Vincent Battaglia (Lawrence Berkeley National Laboratory)

Electrode Fabrication and Materials Benchmarking

PROJECT OBJECTIVE: The objective of this task is to bring together a large fraction of the BATT community to work on a single chemistry. Thus, the best combination of materials found will be provided to multiple researchers in the BATT Program for the Focus Groups. The Liu Group will be supplying the Si anodes and the Battaglia group will develop matching cathodes of LiFePO_4 that will be used to benchmark the effect of side reactions at the anode on cell capacity fade. For the High Voltage Focus Group, our group will benchmark (*i.e.*, measure reversible capacity, rate performance, cycle efficiency) the latest NMO material from NEI and an NCM material for comparative testing. This project also serves as a hub for testing new materials developed in the BATT Program.

PROJECT IMPACT: This project supports two focus groups. For the Si-Anode Focus Group, it is critical that the effect of the side reactions in a full cell are quantified as the side reaction on the Si is considered a major flaw of the material. For the High Voltage Focus group, it is important to source good materials and to make good cells in order to compare the effects of side reactions on the performance of the active materials that address critical questions for the BATT Program. This project is the key to demonstrating progress within the Program against industry standards.

OUT-YEAR GOALS: The long-term goal of this project is to support the Focus Groups and to identify and provide quality materials, electrodes, and cell performance data. This effort supplies a benchmark for the rest of the BATT Program to build upon, thus advancing Li-ion chemistry through proper analysis of state-of-the-art materials.

COLLABORATION: Gao Liu (LBNL)

Milestones

- 1) Go/No-Go: Decide if the newest NMO material from NEI should be the baseline material or not.
Criteria: Benchmark the newest NMO material from NEI. (Dec. 13) **Go to use NMO.**
- 2) Identify the NCM baseline material. (Mar. 14) **Ongoing**
- 3) Demonstrate a cyclable LiFePO_4 electrode. (Jun. 14) **Complete**
- 4) Measure the difference in side reactions of graphite and Si when cycled against LiFePO_4 . (Sep. 14) **Ongoing**

Progress Report

Of the two Focus Groups considered for 2014, the one centered on Si-based anodes has launched. The team's responsibility in this Focus Group is to measure the cycleability of Si-based anodes when matched with a cathode of limited capacity for Li ions, *i.e.*, in a full cell. LiFePO₄ was selected for the counter electrode. This material has the advantages of a flat voltage profile, no Mn dissolution, and stable cycling ability. It is unique when compared to other materials previously tested as it consists of sub-micron secondary particles. It is manufactured on a sub-micron scale because it is known to possess poor electronic conductivity and poor Li diffusivity for particles greater than 50 nm in diameter. To circumvent local conductivity issues, the material is typically coated with 5 nm of amorphous carbon, which assists

with the charge transfer kinetics. To address long-range conductivity issues, the electrode is fabricated with greater than typical quantities of carbon black. This allows for continuous particle-to-particle contact as the material's volume increases and decreases with lithiation and delithiation.

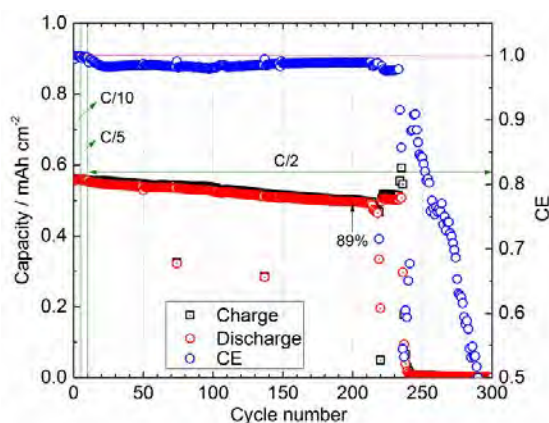


Figure 1. LiFePO₄ cell cycled at C/2 with an electrolyte of 1 M LiFePO₄ in EC:DEC 1:2.

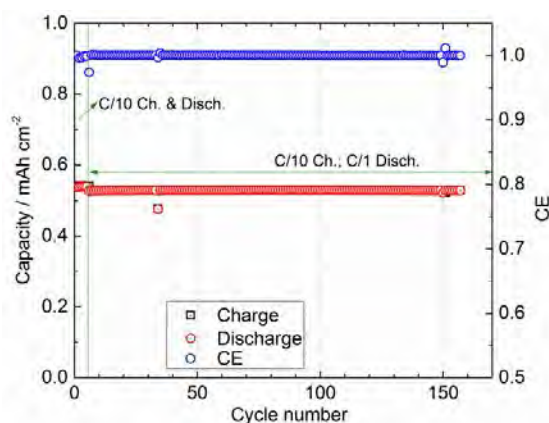


Figure 2. Similar cell as displayed in Fig. 1, but charged at C/10 and discharged at C/1.

Figure 1 shows the cycleability in a half-cell of the first attempt of a LiFePO₄ electrode. This electrode contains 80% active material, 10% carbon black, and PVdF. The capacity steadily declines when cycled at a charge and discharge rate of C/2. Careful inspection of the voltage *vs.* capacity curves indicate that the capacity declines as a result of impedance rise. Interestingly, when a new cell is assembled and charged at C/10 and discharged at C/1, the capacity fade is greatly diminished (Fig. 2). This is not well understood.

In preparation for testing Si-based electrodes, half cells of LiFePO₄ were made with an electrolyte containing FEC. Cell cycling against a Li-counter electrode demonstrated superb cycling ability. Preliminary analysis suggests that the impedance rise of the Li counter electrode with this electrolyte is less than with the baseline electrolyte.

As one can see, the loading of these electrodes is fairly low. It was recently learned that Dr. Liu's group intends to provide electrodes of around 1.5 mAh/cm². Thus, work shall start on electrode formulations of higher loading. This will probably require electrodes of even higher carbon and binder fractions to help maintain good cycle performance.

Novel Anode Materials

PROJECT OBJECTIVE: The project seeks to understand how the cycling of elemental Si in a Li-ion cell configuration affects the local electrode structure, then relate the information garnered to counter-cell failure mechanisms. By using various types of electrode formulations and diagnostic spectroscopies, probing from the surface of the Si to the final complex laminate electrode can take place. Initial work included creation of an all-inorganic electrode that allowed the effects of cycling on the Si to be examined as the electrolyte was the only source of carbon in the cell. This work extended to developing thin-film deposition techniques that allow tailoring of the surface chemistry of the Si that influence how the binder and Si interact. In addition to normal cycling, imaging, and impedance spectroscopies tomography studies of conventional electrodes were initiated to examine how electrode porosity and particle size influenced the isolation of Si particles on cycling, a major cause of capacity fade.

PROJECT IMPACT: The project utilizes a combination of synthesis and characterization to discern how the cycling of elemental Si in a Li-ion cell affects the surrounding electrode structure and how this can be modified to increase cycle life and stability. Results from these studies will be of interest to cell builders and end-users as degradation of the electrode structure can often be traced as the root cause of inconsistent results and premature cell failure. These goals are in line with EERE and OVT goals of furthering development of novel electrode materials and energy storage systems.

OUT-YEAR GOALS:

- Using the new BATT-standard Si source, design and formulate Si-based electrodes that allow for volume expansion in a less rigid environment than a porous Cu substrate.
- Design and evaluate alternative structures that integrate the role of the current collector with the conductive additive requirement of the electrode to reduce materials requirements.

COLLABORATIONS: Fikile Brushett (MIT), Lynn Trahey and Fulya Dogan (ANL)

Milestones

- 1) Synthesize and evaluate a Si-based electrode that utilizes a multilayer structure to stabilize the active Si. (Dec. 13) **Complete**
- 2) Synthesis and evaluation of at least three alternative electrode structures based on non-Cu porous substrates. (Mar. 14) **Ongoing**
- 3) Utilize surface sensitive techniques to develop a model of the Si- substrate interface in the alternative electrodes created. (Jun. 14) **Ongoing**
- 4) Evaluate optimized electrode structure against BATT-standard Si electrode for rate capability and stability on cycling. Make recommendations to improve BATT standard electrode. (Sep. 14) **Ongoing**

Progress Report

Studies have continued on the stability and role of the Si surface on the cycling properties of Si anodes. It was previously shown that the surface of Si was very dependent on its history and could be either hydroxyl, oxide, or proton terminated. These functional groups interact with the electrolyte and have been shown to have an effect on the specific SEI phases that form, and potentially on issues critical to commercializing Si, namely cycling efficiency and capacity fade. The Q1 deliverable involves establishing if the surface of Si can be tempered (mediate its interactions with the electrolyte) in order to better understand how this affects the cycling efficiency of the system.

Experimentally, previous work was built upon Cu-Si coatings and films and a series of physical vapor deposition (PVD) generated multilayers were created, (1) Si on Cu, and (2) Cu on Si on Cu (Si sandwich). In both cases, the amount of Si deposited was approximately the same (0.1 mg/cm^2). A top-down image (SEM) of the Cu-Si-Cu film is shown in Fig. 1. The multilayers were deposited on a stainless steel substrate appropriate for button cell electrochemical testing. Analysis of the multilayers indicated that there probably was some formation of Cu_3Si at the interface between the Si and Cu, consistent with previous observations.

Electrochemical cycling of the multilayers was performed in a manner consistent with the literature. A Li metal anode, Gen2 electrolyte, and conventional 2032 cell hardware were used. A comparison of the representative cycling of each cell type is shown in Fig. 2. Besides the loss in capacity going to a capped Si multilayer (partially due to active Si loss owing to increased Cu_3Si formation and diffusional problems), the role of the active surface on cycling efficiency can be partially inferred. In these systems, the surface is probably a mix of hydroxyl and oxide terminations. Comparing the cycling of the two different films, the capacity retention of the sandwich multilayer after cycle 5 is approximately 96% and for the simple Si on Cu film, approximately 86%. Although not as good as previous electrodeposited films in terms of capacity fade (>99.4%), the initial results show that mediating the contact of the electrolyte with the Si can have beneficial effects on the cycling performance of Si anodes. This, in part, comes from inhibiting material loss and electronic isolation by controlling the surface of the electrode. Similar results on a related system were recently reported by Goldman, *et al.*, (*JES*, **160**, (2013) A1746) on a series of porous Cu/Si/Cu and porous Cu/Si/polymer multilayer electrodes made by a photolithography and etching process.

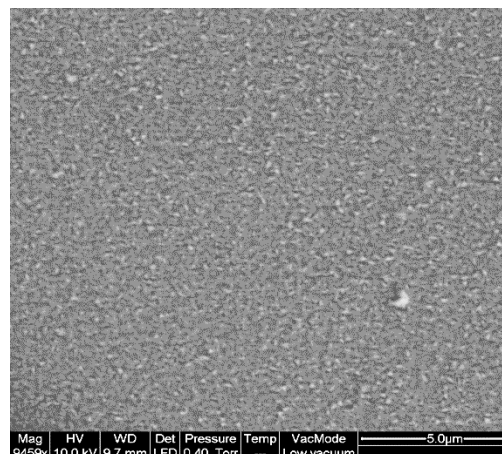


Figure 1. Top down view of the Cu surface of the Cu-Si-Cu multilayer.

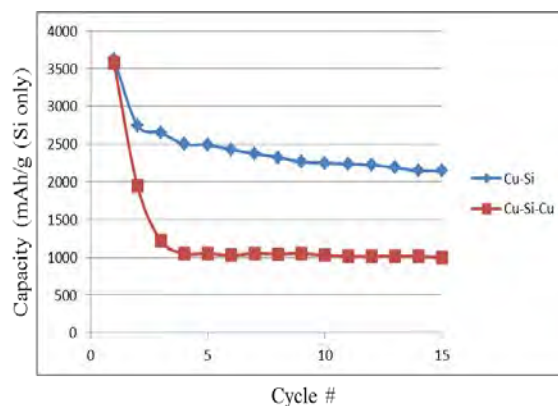


Figure 2. Cycling comparison of the two different Cu/Si electrode multilayers.

Task 2.2 - Stanley Whittingham (SUNY Binghamton)

Metal-Based High Capacity Li-Ion Anodes

PROJECT OBJECTIVE: To replace the presently used carbon anodes with safer materials that have double the volumetric energy density and will be compatible with low-cost layered oxide and phosphate cathodes and the associated electrolyte.

Specifically, the primary objectives are to:

- Increase the volumetric capacity of the anode by a factor of two over today's carbons
 - 1.6 Ah/cm^3
- Increase the gravimetric capacity of the anode
 - $\geq 500 \text{ Ah/kg}$
- Lower the cost of materials and approaches

PROJECT IMPACT: The volumetric energy density of today's Li-ion batteries is limited primarily by the low volumetric capacity of the carbon anode. If the volume of the anode could be cut in half, then the cell energy density can be increased by over 50% to approach 1 kWh/liter (actual cell). In addition, alloys with higher Li diffusivity than carbon would minimize the possible formation of cell-shortening dendritic Li under high charging rates or low temperature conditions. Moreover, smaller cells using lower cost manufacturing will lower the cost of tomorrow's batteries.

OUT-YEAR GOALS: The long-term goal of this project is to replace the present carbon used in Li-ion batteries with lower cost anodes that have double the volumetric energy density of carbon. This will be accomplished by using Sn- and/or Si-based materials. By the end of this project it is anticipated that a new Sn anode will be available that can exceed the charging and discharging rates of carbon thereby making it safer, that will have minimal excess capacity on the first cycle, and that can be cycled at greater than 99% efficiency over 200 cycles.

COLLABORATIONS: National Synchrotron Light Source (BNL) and Advanced Photon Source (ANL)

Milestones

- 1) Identify the two most promising approaches for nano-Si. (Dec. 13) **Complete**
- 2) Reduce the first cycle excess capacity to less than 20% for nano-Sn. (Mar. 14) **Ongoing**
- 3) Go/No-Go: Decision on solvothermal approach for nano-Sn. Criteria: Identify the optimum synthesis approach for nano-Sn anode material. (Jun. 14) **Ongoing**
- 4) Achieve more than 200 cycles on nano-Sn at double the capacity of carbon at the 1C rate. (Sep. 14) **Ongoing**

Progress Report

The goal of this project is to synthesize Sn- and Si-based anodes that have double the volumetric capacity of the present carbons without diminishing the gravimetric capacity.

Milestone (1): In this quarter, synthesis approaches for nano-Si narrowed to the two most promising. In the first, nano-Si is formed from a readily available Al-Si alloy by leaching out most of the Al; around 3 to 5% Al remains dissolved in the nano-Si and it is believed that this favorably impacts the electrochemical behavior. In the second, nano-Si is made by the Ti reduction of “SiO”, similar to the method used for the formation of the nano-Sn material reported below.

Milestone (2): The Ti/Sn molar ratio used in the synthesis of the nano-sized Sn-Fe-C composite was varied to reduce the first-cycle excess-capacity (first-cycle capacity loss). As shown in Fig. 1a, as the Ti/Sn ratio increases from 0 to 1, the first-cycle capacity loss decreases from 610 to 390 mAh/g. This decrease mainly occurs when the Ti/Sn ratio varies from 0 to 0.5, and after that (*i.e.*, Ti/Sn ratio from 0.5 to 1) the decrease is less. This observation indicates that the Ti content of this material has a marked impact on the chemistry/electrochemistry on the initial reaction with Li; however, it is not the only contributor to the capacity. From an overall capacity-retention point of view, an optimum Ti/Sn ratio appears to be between 0.25 and 0.5 (Fig. 1b). Other causes for the first-cycle excess-capacity will be investigated.

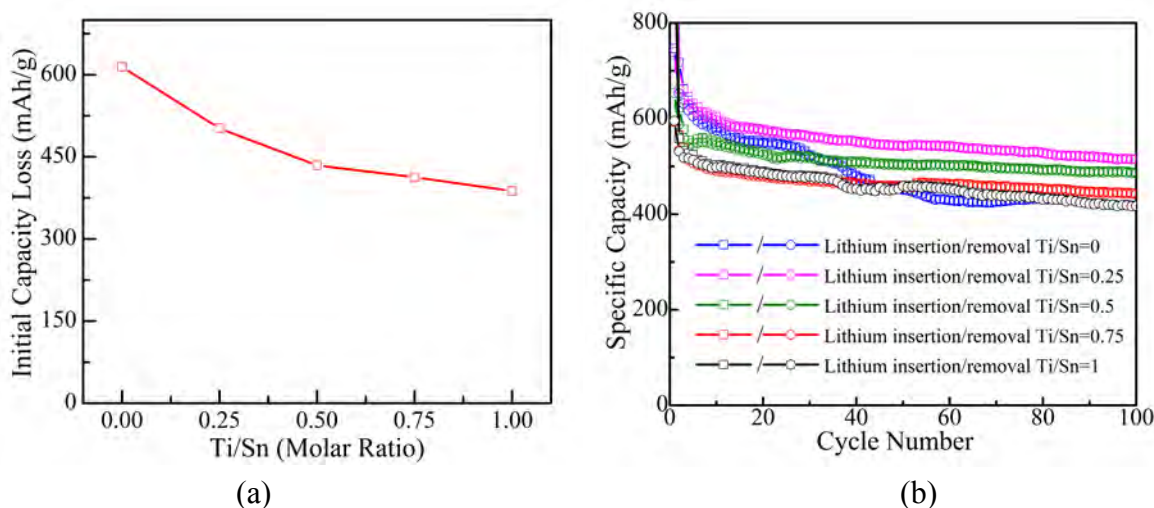


Figure 1. (a) First-cycle capacity loss and (b) electrochemical performance of nano-sized Sn-Fe-C synthesized by mechanochemical method with different Ti/Sn ratios.

Milestone (3): Effort will be increased on this milestone in the 2nd and 3rd quarters.

Milestone (4): This is ongoing, and as shown in Fig. 1b, 100 cycles have been achieved; this will be extended to 200 cycles and the rate capability of this material will be determined.

Nanoscale Composite Hetero-structures and Thermoplastic Resin Binders: Novel Li-Ion Anode Systems

PROJECT OBJECTIVE: The objectives are to identify novel materials and configurations, improved polymeric binders, and cost-effective scalable strategies to generate these systems to overcome the Si-anode limitations. The goals of the present project are to identify inexpensive nanoscale composites, new classes of polymeric binders and electrode configurations displaying higher capacity (>1200 mAh/g) than carbon while exhibiting similar first-cycle irreversible loss ($<15\%$), higher coulombic efficiency ($>99.9\%$), and excellent cyclability to replace graphite.

PROJECT IMPACT: Identification of new Si-based systems displaying higher gravimetric and volumetric energy densities than graphite will likely result in new commercial battery systems that are more robust, capable of delivering better energy and power densities, and will be more lightweight than current Li-ion battery packs utilizing graphite anodes for identical performance specifications. New Si-anode-based strategies and configurations will also lead to more compact battery designs for the same energy and power density specifications as current Li-ion systems. Commercialization of these new Si anode based Li-ion battery packs will represent fundamentally, a major hallmark contribution of the BATT Program and the BATT community.

OUT-YEAR GOALS: This is a multi-year project comprised of four major phases to be successfully completed in four years. Phase 1: Development of cost-effective, high-energy mechanical milling (HEMM) and direct mechano-chemical reduction (DMCR) approaches to generate nanocrystalline and amorphous Si and Li_xSi ($x>3.5$) alloys exhibiting capacities in the ~ 1600 mAh/g range and higher. This phase was completed in year 1. Phase 2: Use of chemical vapor deposition (CVD) to generate amorphous and nanocrystalline Si on vertically-aligned carbon nanotubes (VACNT)-based nano-scale heterostructures exhibiting specific capacity in the ~ 2000 - 2500 mAh/g range. This phase was completed in Year 2. Phase 3: Identify interface control agents (ICA) and surface electron-conducting additives (SECA) to lower the first-cycle irreversible (FIR) loss ($<15\%$) and improve the coulombic efficiency (CE) ($>99.9\%$). This phase was completed in Year 3. Phase 4: Develop elastic and high-strength polymeric binders, to be completed in Year 4.

COLLABORATIONS: Ayyakkannu Manivannan (NETL), Spandan Maiti (U. Pittsburgh), Shawn Lister and Amit Acharya (Carnegie Mellon U.)

Milestones

- 1) Go/No-Go: Stop microwave approach if it fails to generate nanoscale electrochemically-active architectures of Si and C resulting in capacities greater than or equal to 1200 mAh/g. Criteria: Develop and optimize the different parameters involved in the cost-effective scalable solution approach for generation of Si nanoscale architectures. (Dec. 13) **Discontinued**
- 2) Demonstrate generation of *a*-Si hollow nanotubes using cost effective ($< \$65/\text{kg}$) chemical approaches. (Dec. 13) **Complete**
- 3) Develop interface control agents (ICA) to reduce the first-cycle irreversible loss to $<15\%$. (Mar. 14) **Ongoing**
- 4) Develop surface electron-conducting additives (SECA) to improve the coulombic efficiency to $>99.9\%$. (Jul. 14) **Ongoing**
- 5) Develop multilayered *a*-Si/M (M = Matrix) composite films to lower the first-cycle irreversible loss ($<15\%$) and improve the active mass loadings ($2\text{-}3\text{mg}/\text{cm}^2$). (Oct. 14) **Ongoing**

Progress Report

Previously, thin films of amorphous silicon (*a*-Si) on Cu substrate, synthesized using electrodeposition from electrolyte containing SiCl₄ (report Q4-2011), exhibited a reversible capacity *ca.* 1300 mAh/g with excellent capacity retention. In this quarter, the effect of pulse plating conditions on the morphology and stability of these thin films has been studied. Electrodeposition was carried out at a constant duty cycle of 50% and at different frequencies (defined as the number of the pulsing cycles per second) of 0, 500, 1000, 2000, 3000, 4000, and 5000 Hz. SEM studies indicated a drastic change in the morphology of the Si deposits obtained from different deposition frequencies (Fig. 1). While the galvanostatic deposition (0 Hz) showed a mud-crack (island) morphology, the 500 Hz deposition showed a cracked morphology with the islands consisting of agglomerated discrete particle deposits and the 1000 Hz deposition showed a continuous thin layer comprised of Si particles. At higher frequency of deposition (2000, 3000, 4000, and 5000 Hz) the deposited *a*-Si film was continuous, without any major change in the morphology of the deposits. The variation in the morphology is due to the decrease in the depletion layer thickness formed at the electrode-electrolyte interface and the increase in the diffusion of Si⁴⁺ ions during the off-time of the current cycle when there is no deposition current. The electrodeposited *a*-Si thin films were cycled at a current density of 0.4 A/g in the voltage range of 0.01 to 1.2 V *vs.* Li⁺/Li in 1M LiPF₆ in EC:DEC (1:2) electrolyte. The capacity fade or the percentage loss of capacity per cycle (calculated for 10 cycles) indicated a decreasing trend with increase in the frequency of the deposition, reaching a saturation value for higher frequencies (Fig 2). This indicates an increase in the stability of the *a*-Si thin films with an increase in frequency of the deposition. A decrease in the first cycle irreversible loss (not significant) was observed with increase in the frequency of deposition. The lithiation and delithiation of the *a*-Si films deposited at 5000 Hz pulsing frequency exhibited a stable cycling capacity of *ca.* 980 mAh/g after 50 cycles at a current density of 0.4 A/g (Fig 3). A significant decrease in the charge capacity was observed in the first 10 cycles (*ca.* 1.6% loss per cycle) of lithiation and delithiation for all the films obtained at different deposition frequencies following which there was minimal loss (*ca.* 0.2% loss per cycle) in the charge capacity of the *a*-Si thin films. Efforts are currently being directed to understand the origin of the first-cycle irreversible loss and these results will be reported in future quarterlies.

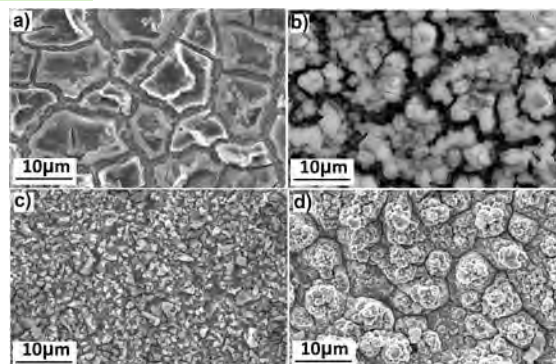


Figure 1. SEM images of electrodeposited amorphous Si films at different frequencies a) 0Hz/galvanostatic condition, b) 500Hz, c) 1000Hz and d) 5000Hz.

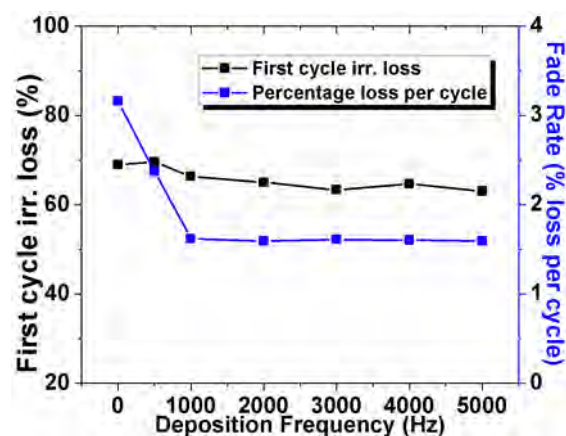


Figure 2. First cycle irreversible loss and percentage loss per cycle vs frequency of electrodeposition for *a*-Si films.

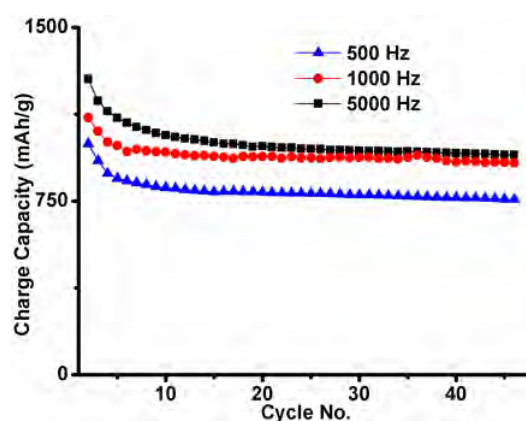


Figure 3. Charge capacity of *a*-Si thin films deposited at 500, 1000 and 5000Hz.

Development of Silicon-Based High Capacity Anodes

PROJECT OBJECTIVE: The objective of this project is to develop high-capacity, low-cost electrodes with good cycle stability and rate capability to replace graphite in Li-ion batteries. The porous Si and the rigid-skeleton supported Si/C composite anode (B₄C/Si/C) will be further optimized. The optimized B₄C/Si/C material will be used as the baseline material for both thick electrode fabrication and studies to advance our fundamental understanding of the degradation mechanism in Si-based anodes. New electrolyte additives, binders, and artificial SEI layers will be investigated to further improve the performance of anodes. New approaches will be developed to pre-lithiate Si-based and other Li-alloy anodes to minimize their first-cycle losses. Fundamental understanding on the formation and evolution of SEI layer, the effect of electrolyte additives and electrode thickness will be investigated by *in situ* microscopic analysis.

PROJECT IMPACT: Si-based anodes have much larger specific capacities compared with conventional graphite anodes. However, the cyclability of Si-based anodes is limited because of the large volume expansion that is characteristic of these anodes. This work will develop a low-cost approach to extend the cycle life of high-capacity, Si-based anodes. The success of this work will further increase the energy density of Li-ion batteries and accelerate market acceptance of EVs, especially for plug-in hybrid electrical vehicles (PHEV) required by the EV Everywhere Grand Challenge proposed by DOE/EERE.

OUT-YEAR GOALS: The main goal of the proposed work is to enable Li-ion batteries with a specific energy of >96 Wh/kg (for PHEVs), 5000 deep-discharge cycles, 15-year calendar life, improved abuse tolerance, and less than 20% capacity fade over a 10-year period

COLLABORATIONS:

Collaboration on anode development will continue with the following battery groups:

- Prof. Jim Zheng (Florida State University) – pre-lithiation of Si-based anode.
- Prof. Michael Sailor (UCSD) —preparation of porous Si.
- Dr. Gao Liu (LBNL) — binders.
- Prof. Yi Cui (Stanford) — failure mechanism study.
- Dr. M.V. Yakovleva(FMC Corp) — SLMP
- Dr. Chunmei Ben (NREL) — surface protection and failure mechanism study.
- Prof. David Ji (Oregon State University) — preparation of porous Si by thermite reactions.

Milestones

- 1) Identify the fading mechanism in the thick Si electrode vs. thin electrode (PNNL). (Dec. 13). **Delayed, due Mar. 14**
- 2) Achieve coulombic charge efficiency of the electrode >90% during the first cycle, through application of SLPMs and sacrificial Li electrode to PNNL's B₄C/Si/C anode (FSU). (Mar. 14) **Ongoing**
- 3) Achieve high loading Si-based anode capacity retention of >1.2 mAh/cm² over 150 cycles using new binders/electrolyte additives (PNNL). (Jun. 14) **Complete**
- 4) Achieve improved cycling stability of thick electrodes (> 3 mAh/cm²) (PNNL). (Sep. 14) **Ongoing**
- 5) Achieve a specific energy greater than 30 Wh/kg and the specific power greater than 5 kW/kg, and cycle life greater than 30,000 cycles for Li ion capacitors (FSU). (Sep. 14) **Ongoing**

Progress Report

Through additional modifications of our rigid, skeleton-supported Si nanocomposite, the cycling stability of thick electrodes was further improved. Figure 1a illustrates the cycling stability of a typical cell with *ca.* 2 mg/cm² loading. The capacity after 150 cycles is *ca.* 1.21 mAh/cm². The battery was cycled using the BATT protocol: 0.005 to 1 V; three formation cycles at 0.06 mA/cm²; followed by 0.75 mA/cm² for delithiation and 0.5 mA/cm² for lithiation. The highest capacity after formation cycles is 1.42 mAh/cm². Capacity retention after 150 cycles is *ca.* 85%. The first-cycle irreversible-capacity loss in this thick electrode is still large (*ca.* 30%). Prelithiation treatment will be used in further investigations.

In another effort, good cycling stability of porous Si obtained by thermite reactions (in collaboration with Oregon State University) was demonstrated. Figure 1b shows that a porous Si with a capacity of *ca.* 1.85 mAh/cm² with *ca.* 87% capacity retention after 100 cycles. The BATT protocol described above was used in this study. Nanostructured Si has demonstrated very good cycling stability when the electrode is thin. For thick electrodes of high mass loading, the interaction between different components (active materials, conductive carbon, and binder) may lead to more complicated mechanical/electrical failure of the electrode. To enable the stable operation of thick Si-based electrodes will be the focus of the work in the next quarter.

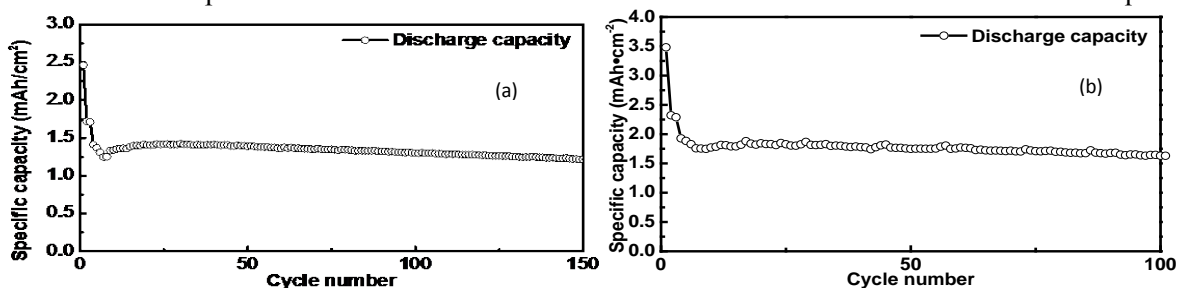


Figure 1. (a) Cycling stability of the modified rigid-skeleton supported Si nanocomposite. (b) Cycling stability of the porous Si by thermite reactions.

To investigate the effect of pre-lithiation of anodes for Li-ion batteries and Li-ion capacitors, *in situ* ⁷Li NMR experiments were conducted on a Li-ion capacitor comprised of a hard-carbon anode with stabilized Li-metal powder (SLMP) applied to the surface and a double-layer capacitor-type activated carbon cathode. The NMR spectra (Fig. 2) were recorded *in situ* while the capacitor was cycled galvanostatically at regular intervals (0.25 V step). A broad Li-metal peak appearing around 270 ppm always exists, pointing to the SLMP layer. A sharp peak around 0 ppm is attributed to the Li ions in the electrolyte and trapped in the SEI layer. During the discharge process, the intercalation peak at around 12 ppm continuously decreases in intensity while slightly moving downfield. During the charge process from 2 to 4 V, an intercalation peak in the hard-carbon electrode reappears as a separate broad peak around 12 ppm. Figure 3 shows the contribution of each electrode (see inset for the assembled capacitor). The SLMP Li-metal peak appears only on the anode side. The intercalation peak expectedly appears on the anode side pointing towards the Li intercalated in the hard-carbon electrode. The application of the *in situ* NMR technique enables the monitoring of the electrochemical activity in an energy-storage device in real time.

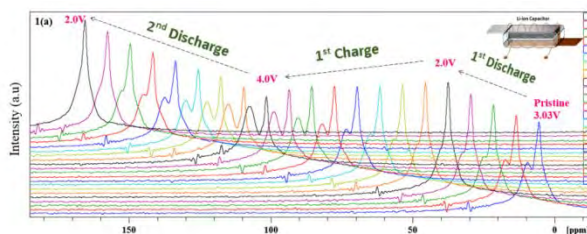


Figure 2. Stacked NMR plots from *in situ* cycled polyethylene-bag capacitor.

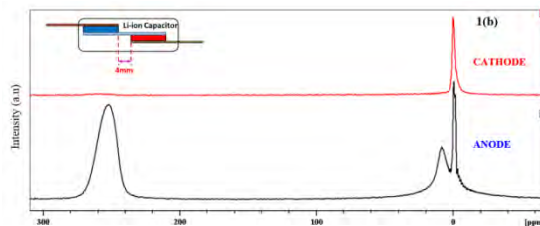


Figure 3. Stacked NMR plots from pristine 4-mm gap capacitor showing electrode contributions.

Atomic Layer Deposition for Stabilization of Amorphous Silicon Anodes

PROJECT OBJECTIVE: The objective of the project is to develop a low-cost, thick, high-capacity silicon anode with sustainable cycling performance. Our specific objectives are to develop a novel conductive and elastic scaffold by using Atomic Layer Deposition (ALD) and Molecular Layer Deposition (MLD), demonstrate durable cycling by using the new coating and electrode design, and investigate the effect of atomic surface modification on irreversible capacity loss and cycling performance.

PROJECT IMPACT: Due to its high theoretical capacity and natural abundance, Si has attracted much attention as a promising Li-ion anode material. However, progress towards a commercially-viable Si anode has been impeded by Si's rapid capacity fade caused by large volumetric expansion. In this project, new ALD/MLD conformal nanoscale coatings with desirable elastic properties and good conductivity will be developed to accommodate the volumetric expansion and protect the surface from reactive electrolytes, as well as to ensure the electronic paths through the composite electrodes. Successful completion of this project will enable the coated Si anodes to have high Coulombic efficiency, as well as durable high-rate capability. This project supports the goals of the DOE *EV Everywhere* Grand Challenge and EERE's OVT to develop high-energy batteries for wider adoption of EVs to reduce consumption of imported oil and generation of gaseous pollutants.

OUT-YEAR GOALS:

- Demonstrate durable cycling performance of thick Si anodes (>15 μm) by using new ALD/MLD coatings and electrode designs.
- Explore the importance and mechanism of various coatings *via* the BATT coating group.
- Collaborate within the BATT Program with the aim of developing high-rate PHEV-compatible electrodes (both anodes and cathodes).

COLLABORATIONS: P. Ross and G. Liu (LBNL), J. Zhang (PNNL), Q. Yue (MSU), X. Xiao (GM), and P. Balbuena (Texas A&M)

Milestones

- 1) Identify the impact of Alucone MLD coating on the structure and morphology of Si anodes during cycling. (Dec. 13) **Complete**
- 2) Develop Al_2O_3 /carbon composite coatings by pyrolysis of Alucone MLD film. (Mar. 14) **Ongoing**
- 3) Go/No Go: Test coated electrodes in coin cells. Criteria: Stop the development of Al_2O_3 /carbon composite coatings if the coating cannot help the performance of Si anodes. (Jun. 14) **Ongoing**
- 4) Synthesize and characterize novel AlF_3 /Alucone hybrid coating by using ALD and MLD. (Sep. 14) **Ongoing**

Progress Report

The polymeric aluminum glycerol (Alucone) coating, fabricated by MLD in FY13, has shown great impact on the electrochemical performance of thick Si anodes. The alucone coatings enable the thick Si anodes (*ca.* 15 μm) to deliver a high reversible cycling capacity of 1500 mAh/g, or 0.9 mAh/cm² in areal capacity, at a cycling rate of 350 mA/g. In the first quarter of FY14, research has been focused on the effect of this coating on the structure and interfacial reactions and the development of new alucone coatings composed of metal oxide and conductive aromatic rings.

Alucone coating enhances the cohesion of the composite electrodes. Figure 1 presents the TEM images of bare and coated electrodes after first delithiation. The severance of nano-Si particles from the electrode network was observed after delithiation (during volumetric contraction), as shown in Fig. 1 a and b. As depicted in Fig. 1c, the massive volume change during lithiation/delithiation of Si particles contributes to the isolation of Si particles, that results in rapid capacity degradation. On the contrary, the alucone-coated electrode shows intimate adherence between Si particles and the surrounding network during cycling. The alucone coating grown by MLD was covalently bound to the surface of the electrode, which dramatically enhanced the cohesion of the components in the electrode. It is the covalent coating that ensures the continuous and conductive matrix even while large volume changes occur during cycling.

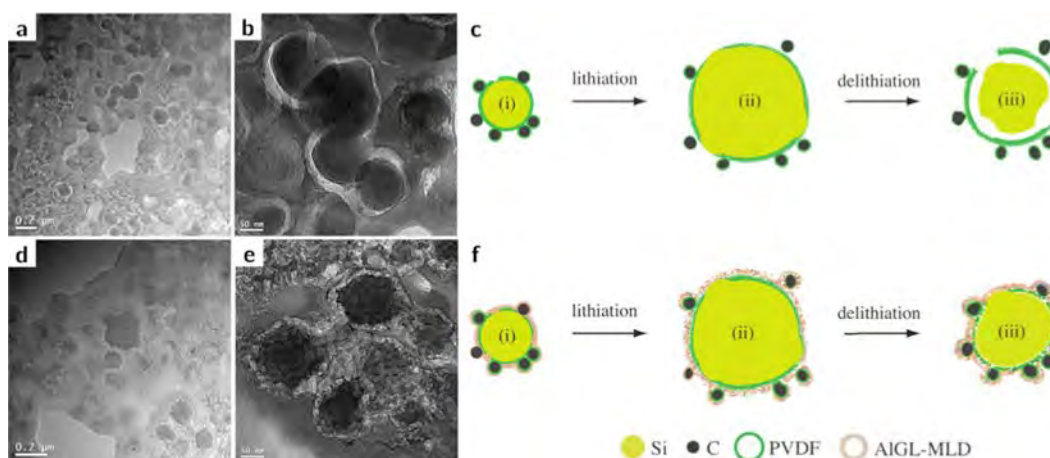


Figure 1. TEM images of the bare electrode (a and b) and coated electrode (d and e); schematics of the bare and coated electrodes during lithiation/delithiation (c and f).

MLD synthesis of conductive alucone coating. A new alucone coating was developed for the Si anode by using MLD sequential reactions of trimethylaluminum (TMA) and hydroquinone (HQ, C₆H₄(OH)₂). This is an aromatic diol that has a rigid structure with a central benzene ring, which can potentially increase electronic conductivity due to the conjugated π -electrons in the aromatic rings. As illustrated in Fig. 2, the aromatic rings enclose the AlO_x and appear polymerized after annealing above 200°C. The cross-linked alucone coating has shown greatly improved critical tensile strain from 1.0 to 1.8%. The improved mechanical properties of this conductive coating can ensure the structural integrity of the composite electrodes, which is critical to high-capacity Si anodes with massive volume change. This coating has been applied to the Si anodes and is presently under electrochemical evaluation.

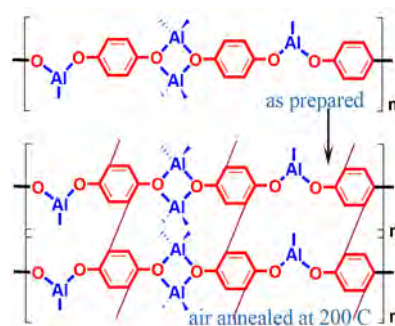


Figure 2: Chemistry structure of TMA-HQ MLD coating: as-prepared coating (top) and the cross-linked coating after annealing at 200°C.

New Layered Nanolaminates for Use in Lithium Battery Anodes

PROJECT OBJECTIVE: Replace graphite with a new material selected from a group of layered (two-dimensional) binary carbides and nitrides known as MXenes, which may offer combined advantages of graphite and Si anodes with a higher capacity than graphite, less expansion, longer cycle life, and a lower cost than Si nanoparticles.

PROJECT IMPACT: As a result of this project, a new family of two-dimensional materials (MXenes) was discovered. Using MXenes as anode materials would result in higher capacity than graphite with an excellent ability to handle high cycling rates that graphite anodes cannot handle. Since each MXene has its own voltage window, considering the rich chemistry of MXenes and the possibility of solid solutions, MXene compositions can be selected and tuned for certain voltages to produce high-performance batteries with improved safety.

OUT-YEAR-GOALS: The project's long-term goal is to produce new anode materials (MXenes) that may replace graphite in anodes of Li-ion batteries.

FY2014 - Improvement of the cycle-life of the anodes. Optimization and modification of the material manufacturing process to enable large-volume, low-cost production.

COLLABORATIONS:

Xiao-Qing Yang and Kyung-Wan Nam, *BNL*

Yu Xie and Paul Kent, *ORNL*

Jun Lu, Lars Hultman, and Per Eklund, *Linkoping University, Sweden*

Jérémy Come, Yohan Dall'Agnese, and Prof. Patrice Simon, *Université Paul Sabatier, Toulouse, France*

Milestones

- 1) Produce MXene anodes with capability of delivering a stable performance at 10 C cycling rates. (Dec. 13) **Complete**
- 2) Complete *in situ* and *ex situ* studies of the lithiation and delithiation of MXenes and determine the most promising materials. (Dec. 13) **Delayed to Jun. 14**
- 3) Maximize capacity of MXenes and test newly-discovered MXenes (Mo_2C) that have shown the highest capacity so far. (Mar. 14) **Ongoing**
- 4) Predict the theoretical capacity and Li insertion potential of MXenes, and synthesize and test MXenes that are expected to have the largest Li uptake (>600 mAh/g theoretical capacity) and the lithiation/delithiation potential below 1 V. (Jun. 14) **Ongoing**
- 5) Demonstrate charge/discharge behavior by controlling particle size and surface chemistry of MXenes. (Sep. 14) **Ongoing**

Progress Report

Several MXenes (Ti_2C , Ti_3C_2 , Nb_2C , and V_2C) were tested at high cycling rates (*e.g.*, 10 C), and in all cases a stable performance (less than 5% change in capacity) was obtained for more than 100 cycles.

For further understanding of the lithiation and delithiation mechanisms, X-ray absorption spectroscopy (XAS) and X-ray photoelectron spectroscopy (XPS) were used. *In situ* XAS during electrochemical lithiation and delithiation for Ti_3C_2 was carried out through a collaboration with Yang and Nam at BNL. The X-ray absorption near edge spectroscopy (XANES) for Ti K edge after lithiation (Fig. 1a) showed a shift to lower energy, which means a lower oxidation state. The XANES spectrum shifts back to higher energies (higher oxidation state), but not to the initial state, after delithiation. This is evidence of a redox reaction. No evidence for a conversion reaction was observed. The variation of the Ti edge (Fig. 1a) during lithiation (Fig. 1b) shows two distinct regions. In the first, a continuous decrease in energy was observed, then in region II, the energy did not change with further lithiation. Similar behavior was observed during delithiation (regions III and IV in Fig. 1b). The independence of the energy in regions II and III can be explained by the formation of a second Li layer on the $\text{Ti}_3\text{C}_2\text{O}_2\text{Li}_2$ layers. Theoretical calculations showed that the formation of additional atomic layers of Li on $\text{Ti}_3\text{C}_2\text{O}_2\text{Li}_2$ is possible; however, this needs to be confirmed experimentally by *in situ* NMR.

An *ex situ* study of the lithiation and delithiation processes during electrochemical cycling of Ti_3C_2 was performed using XPS. Upon full lithiation, down to 5 mV, and delithiation to 3 V, it was found that an irreversible peak corresponding to LiF and a partially irreversible peak corresponding to $\text{ROCO}_2\text{Li}/\text{Li}_2\text{O}$ appear in the Li1s and C1s regions of the XPS spectra (Fig. 2). LiF is most likely formed by extraction of F atoms from the MXene surface, which is supported by the partial irreversible loss of Ti(IV)/Ti-F signal in Ti_{2p} region (not shown). The latter also could be due to formation of TiF-Li. Thus, it can be concluded that the 1st cycle irreversibility is affected mostly by formation of LiF and Li_2O and partially by ROCO_2Li and/or TiF-Li by the end of the cycle. It implies that the formation of a SEI is not the strongest contributor in the 1st-cycle irreversibility. On the other hand, the shift to higher binding energy values in the Li 1s (Fig. 2b), O 1s, and F 1s regions could be assigned to Li interacting with/absorbing onto the MXene O and F surface groups that could correspond to the reversible lithiation and delithiation mechanisms. Additionally, XPS peaks after 8 cycles (not shown) were not too different than those after the 1st cycle. Only a slight increase of LiF peak intensity and decrease of TiO-Li was observed indicating a small drop in capacity with cycling.

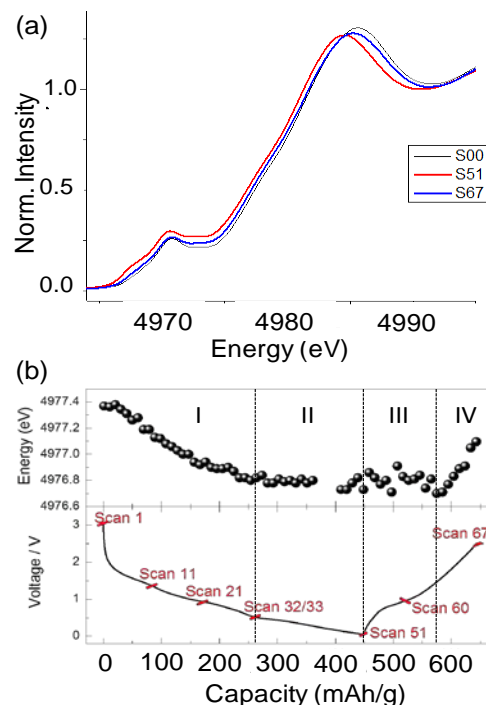


Figure 1. (a) *In situ* Ti K-edge XANES analysis of lithiation and delithiation of Ti_3C_2 (b) Variation of Ti edge energy vs. capacity during lithiation and delithiation combined with the voltage profile.

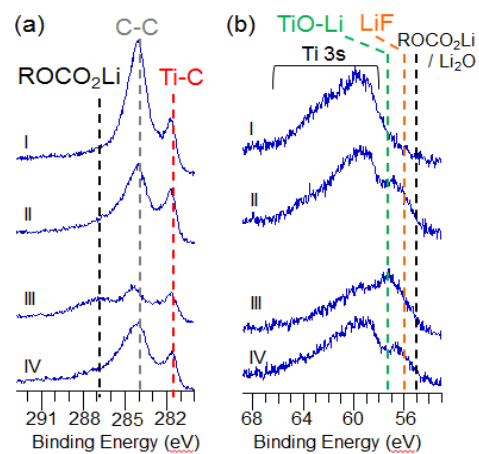


Figure 2. *Ex situ* XPS spectra in C1s region (a) and Li1s region (b) for Ti_3C_2 after electrochemical cycling: I (initial Ti_3C_2 soaked in the electrolyte), II (lithiated from OCV to 1 V), III (lithiated from OCV to 5 mV), IV (lithiated from OCV to 5 mV, then delithiated to 3 V).

Synthesis and Characterization of Si/SiO_x-Graphene Nanocomposite Anodes and Polymer Binders

PROJECT OBJECTIVE: Novel-structured Si/SiO_x-carbon nanocomposites and polymer binders will be designed and synthesized to improve Si-based anode electrode kinetics and cycling life, and decrease initial irreversible capacity loss in high capacity Li-ion batteries. By combining the new Si-based anode materials and new polymer binders and investigating their structure-performance relationships, a high-performance Si anode can be achieved.

1. Synthesize and characterize Si/SiO_x-based nanocomposite Li-ion battery anodes.
2. Identify and evaluate the electrochemical performance of the Si/SiO_x-based nanocomposite and the polymer binder.
3. Develop understanding of long-lifetime Si anodes for Li-ion batteries by considering both the Si active phase and the polymer binder and surface interactions between the electrode components.

PROJECT IMPACT: The proposed collaborative effort closely integrates synthesis of Si-based composite anodes with controlled structure and composition, development of novel functional polymer binders, and materials characterization and electrochemical evaluation. The resulting optimized Si anode electrode will provide electrochemical performances which are essential to achieving higher energy densities in PHEV and EV applications.

OUT-YEAR GOALS: According to the accomplishments of the project, several types of Si-based composite with promising electrochemical performance will be developed and demonstrated. New functional polymer binders will be developed. The mechanical and chemical influences of the structure, chemical composition, and surface modification on electrochemical performance of those materials will be identified and demonstrated, thus to provide systematic fundamental understanding to guide the Si-based anode material design. The Si-based electrode design, including the selection of materials and polymer binders, will be demonstrated in cell testing at Penn State and with BATT Program partners.

COLLABORATIONS: Gao Liu (LBNL), Chunmei Ban (NREL), Nissan R&D Center

Milestones

- 1) **Go/No-Go:** Stop the metal composites coating approach and focus on carbon coating approach if the capacities are less than 1500 mAh/g. **Criteria:** Synthesize, characterize and evaluate Si-based composite with novel coating (*e.g.*, non-oxidic metal composites). (Dec. 13) **Go for carbon coating**
- 2) Identify and demonstrate the optimized composition, structure and surface modification of micro-sized Si/C and porous Si/C composites. (Mar. 14) **Ongoing**
- 3) Synthesize acidic/semiconducting polymer binders using grafting approach. (Jun. 14) **Ongoing**
- 4) **Go/No-Go:** Determine if semiconducting polymer approach can generally be applied to Si anodes. **Criteria:** Synthesis and electrochemical evaluation of Si/Si alloy composites. Fully characterize acidic/semiconducting polymer binders. Supply laminates of the optimized Si/Si alloy electrodes with electrode capacity of 800 mAh/g that cycle 100 cycles to BATT PIs. (Sep. 14) **Ongoing**

Progress Report

Si-based anode materials: Hierarchical silicon-carbon (Si-C) composites have been prepared, which consists of primary carbon-coated sub-10 nm Si particles aggregated to secondary micron-sized particles, as shown in the SEM image (Fig. 1). The synthesis process involves facile thermal annealing of silsesquioxane with size-controlled formation of Si primary particles and subsequent C coating steps. The C was found to uniformly coat the Si particles as a similar intensity of Si (red) and C (blue) was observed in the same regions by EDS analysis (Fig. 2). These Si-C composites exhibited a high reversible capacity of 1660 mAh/g and excellent cycling stability for 150 cycles. They also deliver a relatively high initial coulombic efficiency of 76%, that quickly increases to *ca.* 97.8% by the third cycle, 99% by the tenth cycle, and eventually stabilizes to *ca.* 99.5% in subsequent cycles. A high reversible capacity of *ca.* 800 mAh/g can be achieved at a high current density of 8 A/g. This Si-C composite with micron-sized secondary aggregation exhibits a high tap density of 0.68 g/cm³, which leads to a high volumetric capacity of 1088 mAh/cm³.

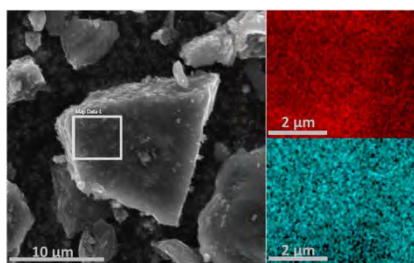


Figure 1.

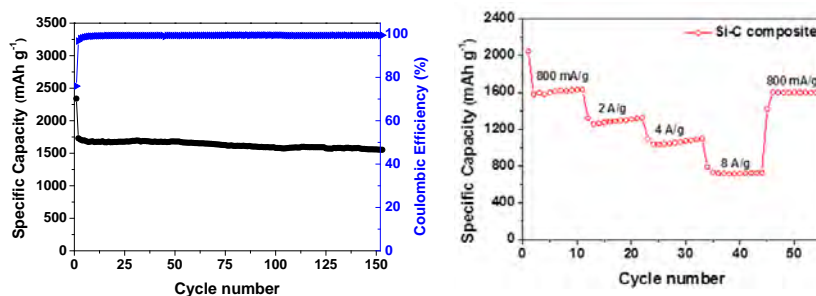


Figure 2.

Semiconducting binders: Based on the success of conductive polymers as Si-based anode binders, a new structure for backbone grafting of semiconducting functional units is proposed. This strategy will provide robust mechanical support to the anode structure as well as impart semiconducting functionality. As shown Fig. 3, an aromatic polymer backbone will be brominated and then the aryl bromides complexed with a Pd-based Suzuki catalyst. This catalyst-complexed polymer will then be subject to catalyst transfer chain growth polymerization, grafting semiconducting moieties from the backbone. Using this strategy, it will be possible to modify both the mechanical properties of the binder as well as its semiconducting functionality. Currently, initial materials have been demonstrated using this approach and are gathering testing feedback on binder performance. The chemistry outlined above and work towards demonstrating this concept in Si-anodes will be optimized.

Mechanically Robust Backbone

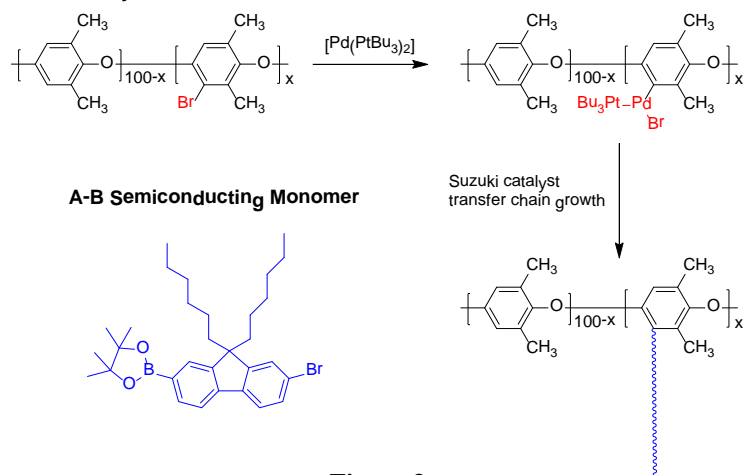


Figure 3.

Wiring up Silicon Nanoparticles for High Performance Lithium Ion Battery Anodes

PROJECT OBJECTIVE: The charge capacity limitations of conventional carbon anodes are overcome by designing optimized nano-architected Si electrodes.

This study pursues two main directions:

- 1) fabricating novel nanostructures that show improved cycle life, and
- 2) developing methods to study the lithiation/delithiation process to understand volume expansion for higher efficiency.

PROJECT IMPACT: The Li-ion storage capacity, as well as the cycling stability of Si anodes, will be dramatically increased. This project's success will make Si the high performance Li-ion battery anode material toward high energy batteries to power vehicles.

OUT-YEAR GOALS: Mass loading, cycling life and first cycle Coulombic efficiency (1st CE) will be improved and optimized (over 1 mg/cm² and >85%) by varying material synthesis and electrode assembly. Fundamentals of volume expansion as well as SEI formation in Si nanostructures will be identified. A detailed study of inter-particle interactions during electrochemical reaction will be performed by *in situ* and *ex situ* microscopy.

COLLABORATIONS: None this quarter.

Milestones

- 1) Utilize Si particles as an anode with capacity >1000 mAh/g, mass loading of 1mAh/cm², and cycle life >100 cycles (Dec. 13) **Complete**
- 2) Go/No-Go: Try other conducting coating materials. Criteria: If the first-cycle coulombic efficiency cannot go >80%. (Mar. 14) **Ongoing**
- 3) Complete *in situ* TEM and *ex situ* SEM studies of two or multiple Si nanostructures during lithiation/delithiation to understand how neighboring particles affect each other and volume changes. (Jun. 14) **Ongoing**
- 4) Increase mass loading of Si material to achieve 2 mAh/cm² and first cycle coulombic efficiency (>85%) and cycle life >300 cycles. (Sep. 14) **Ongoing**

Progress Report

Much effort by our group has been devoted towards designing Si-nanostructure-based anodes with long cycle life, as detailed in previous reports and publications. Although nanostructured Si anodes have been successful in extending the cycle life, they introduced new challenges like low mass loading. At high mass loading, the electrical contact between nanoparticles is easily destroyed by volume change during cycling that decreases the cycle life of the electrode.

To this end, two porous Si structures were used as anode materials with areal mass loadings of about 1 mg/cm^2 . The first Si structure was prepared from rice husk. Rice husks were first converted to pure silica by burning them in air and then reducing the remaining metal to Si. This results in an interconnected network of nanoparticles, as shown in the SEM image in Fig. 1a. These nanoparticle domains were physically connected with each other in the synthesis, resulting in good contact during cycling. The gaps between the particles provide the space for volume expansion during lithiation. Galvanostatic curves of these Si structures are shown in Fig. 1b. The stable capacity of later cycles is about 1700 mAh/g with an areal mass loading 0.6 mg/cm^2 . Thus, an anode with areal capacity above 1 mAh/cm^2 and cycle life above 100 cycles was demonstrated.

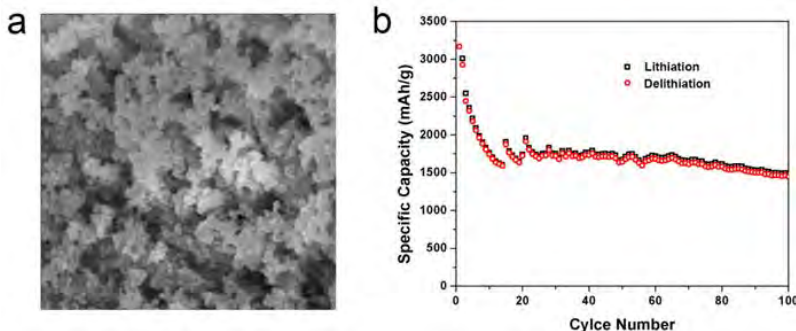


Figure 1. (a) SEM images of porous Si structure from rice husk. (b) Lithiation/delithiation capacity of the first 100 galvanostatic cycles. The rate was C/20 for the first cycle, C/2 for the later cycles.

A second porous Si microstructure was synthesized from Si microparticles by combining an electroless Ag deposition *via* a galvanic displacement reaction, with a metal-assisted chemical etching process. This synthesis yields a porous microparticle with a large amount of macropores and nanopores (Fig. 2a). This pore space should allow for accommodation of volume change during electrochemical cycling. The porous microparticles were converted to slurry-type electrodes and tested in half-cells *vs.* Li metal. Galvanostatic cycling curves are shown in Fig. 2b. The electrode demonstrates an areal capacity around 1 mAh/cm^2 and a cycle life of 100 cycles with over 85% capacity retention.

In summary, porous Si microstructures show promising performance at relatively high mass loadings; future work will involve increasing the cycle life by combining the materials with our protection layer design *via* different coating methods.

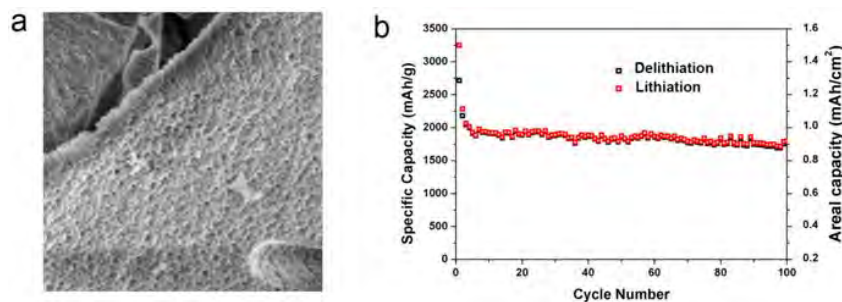


Figure 2. (a) SEM images of porous Si structure prepared by HF etching. (b) Lithiation/delithiation capacity of the first 100 galvanostatic cycles. The rate was C/20 for the first cycle, then C/5 for the later cycles.

Synthesis and Characterization of Silicon Clathrates for Anode Applications in Lithium-ion Batteries

PROJECT OBJECTIVE: Current Li-ion batteries with graphite anodes are inadequate for PHEV or EV applications because of low energy density, short calendar life, and high cost. The energy density and power density of current Li batteries must be doubled for EV applications. Despite extensive research, Li-ion batteries with Si anodes suffer from limited cyclability due in part to the large dimensional changes and pulverization of the Si anode after a few tens of charging and discharging cycles. This major obstacle can be overcome by using silicon clathrate, Si_{46} , whose cage structure is amenable to Li insertion as the anode material without incurring a significant volume change. The objectives of this project are to synthesize and characterize the electrochemical performance of Si clathrate anodes designed to exhibit little or no volume expansion during lithiation, high specific energy density, no capacity fading, and improved abuse tolerance.

PROJECT IMPACT: The significant impacts of this project include (1) developing a processing method for synthesizing Si_{46} particles with suitable purity and size range for use as anode materials, (2) generation of a fundamental understanding of the lithiation and delithiation processes in Si_{46} , (3) identifying the potential of, and scalable synthetic pathways toward, the development of Si clathrate anodes for concept demonstration, and (4) development of prototype Li-ion batteries with Si clathrate anodes for use in a high-energy, high-power, and durable Li-ion battery with a long calendar life.

OUT-YEAR GOALS: The goals are (1) to arrive at an improved and scalable solvothermal synthetic pathway for Si_{46} devoid of non-Li guest atoms as synthesized, (2) to optimize the electrochemical performance of Si clathrates in the context of electrode engineering and electrolyte selection, and (3) to design and fabricate a complete, small-scale battery construct based on the Si-clathrate anode developed in this project. Cathode materials will be selected and a cathode construct will be fabricated to match the Si clathrate anode. After forming the anode-cathode battery assembly, at least two prototype battery cells will be evaluated to determine the performance metrics of the battery: capacity, discharge rate, and cycle life.

COLLABORATIONS: Participated in the Si-Anode Focus Group and collaborated with V. Battaglia at LBNL on electrochemical testing of silicon clathrate anodes. Collaborated with C. Chan at Arizona State University on silicon clathrate characterization and electrochemical measurements.

Milestones

- 1) **Go/No-Go:** Continue project. **Criteria:** Achieve either a) Ba-containing clathrate: capacity of 1,500 Ah/g at 50 cycles after cycling at C/5, or b) Si clathrates: capacity of 750 mAh/g at 50 cycles after cycling at c/5. (Dec. 13) **Complete**
- 2) Arrive at an improved and scalable solvothermal synthetic pathway to produce 50 g Si_{46} devoid of non-Li guest atoms as synthesized. (Mar. 14) **Ongoing**
- 3) Submit ≥ 50 g silicon clathrate material selected in Q2 to LBNL for independent verification of anode performance predicated on the use of standard protocols for cell construction and measurement. (Jun. 14) **Ongoing**
- 4) Construct ≥ 2 prototype full cells consisting of best-case (and verified) silicon clathrate anode matched with best-case cathode material and electrolyte, then demonstrate ≥ 100 cycles with $\leq 20\%$ fade in capacity. (Sep. 14) **Ongoing**

Progress Report

Long-term cycling tests of an intermetallic clathrate, $Ba_8Al_8Si_{38}$, combined with Super-P carbon (20 wt%) and EC/DEC/FEC electrolyte were completed. The effects of higher than previously-used carbon loading (25 vs. 20 wt.%) on overall capacity fade and coulombic efficiency were recorded. The results are shown in Figs. 1 and 2 for the first 50 and subsequent 1000 cycles, respectively.

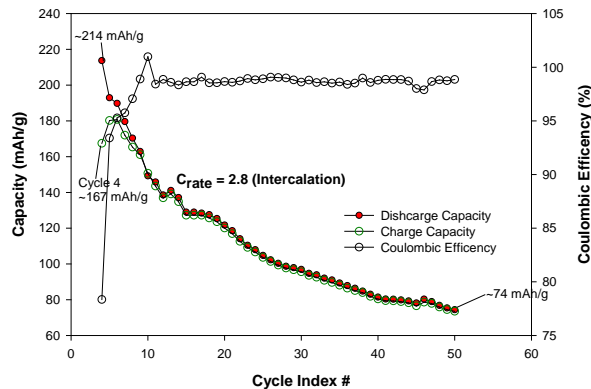


Figure 1. Cyclic capacity and coulombic efficiency profiles for the intermetallic clathrate $Ba_8Al_8Si_{38}$ showing cycles 4-50. Electrode: 25/20 wt% Super-P/PVDF; 1M $LiPF_6$ in EC/DEC/FEC (45:45:10).

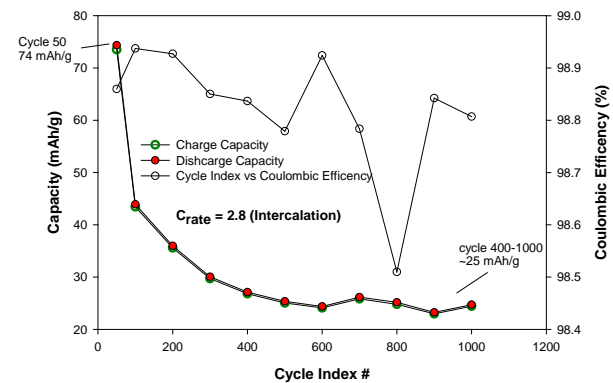


Figure 2. Cycles 50 to 1000 for same system shown in Fig. 1.

It is evident from Figs. 1 and 2 that significant capacity fade is exhibited by this intermetallic clathrate even while the coulombic efficiency remains reasonably high (98.8%) up to the 50th cycle. After that, the capacity and coulombic efficiency drop precipitously until the cell is no longer responsive. The root cause for this behavior may be attributed to the large Ba guest atoms which act to inhibit Li transport by occluding the connecting cage volumes within the framework due to atomic-species “crowding”, much akin to a one-way ball valve. To overcome this problem, experimental efforts focused more intently on synthesizing the empty, pure-Si clathrate (Si_{146}) using a solvothermal reaction developed earlier in the project. Sufficient quantities were successfully synthesized this quarter for structural and electrochemical characterization, and the results of long-term durability tests are illustrated in Figs. 3 and 4. The differences in performance between this and the intermetallic clathrate are extraordinary (809 mAh/g and 99.0% efficiency at 50 cycles; 553 mAh/g and 99.8% efficiency at 1000 cycles after cycling at C/1), which demonstrates the importance of making most, if not all, the cage volume for intercalation/deintercalation of Li. On this basis, the Go/No-Go milestone for this quarter has been successfully met.

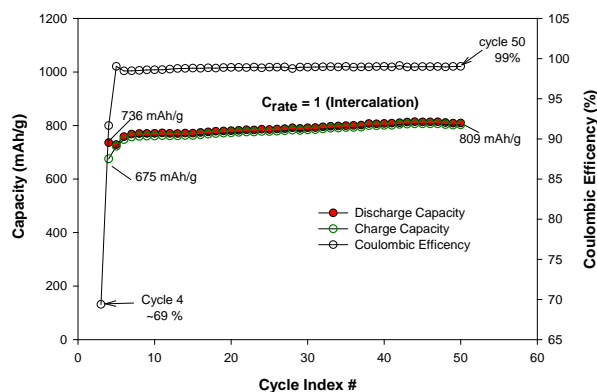


Figure 3. Cyclic capacity and coulombic efficiency profiles for Si_{146} showing cycles 4 to 50. Electrode: 25/20 wt% Super-P/PVDF; 1M $LiPF_6$ in EC/DEC/FEC (45:45:10).

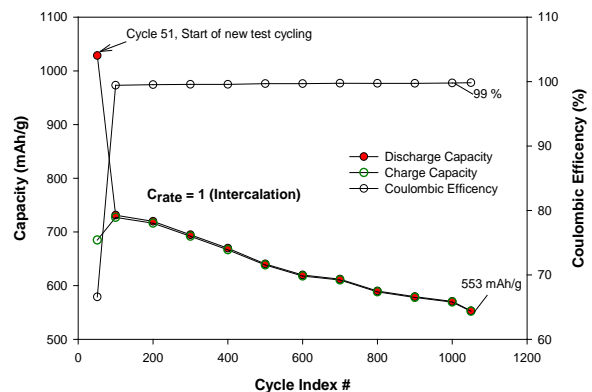


Figure 4. Cycles 50 to 1000 for same system as that shown in Fig. 3.

Fluorinated Electrolyte for 5-V Li-ion Chemistry

PROJECT OBJECTIVE: The objective of this project is to develop a new advanced electrolyte system with outstanding stability at high voltage and high temperature and improved safety characteristic for an electrochemical couple consisting of the high voltage $\text{LiNi}_{0.5}\text{Mn}_{1.5}\text{O}_4$ (LNMO) cathode and graphite anode. The specific objectives of this proposal are the design, synthesis and evaluation of (1) non-flammable high voltage solvents to render intrinsic voltage and thermal stability in the entire electrochemical window of the high-voltage cathode materials, and (2) electrolyte additives to enhance the formation of a compact and robust solid electrolyte interphase (SEI) on the surface of the high voltage cathode. A third objective is to gain fundamental understanding of the interaction between electrolyte and high voltage electrode materials, the dependence of SEI functionality on electrolyte composition, and the effect of high temperature on the full Li-ion cells using the advanced electrolyte system.

PROJECT IMPACT: This innovative fluorinated electrolyte is intrinsically more electrochemically stable due to the fluorine substitution; therefore it would be applicable to cathode chemistries based on TM oxides other than LNMO. Therefore, the results of this project can be further applied to a wide spectrum of high-energy battery systems oriented for PHEVs that operate at high potentials, such as LiMPO_4 (M=Co, Ni, Mn), or battery systems that require a high-voltage activation process, such as the high-capacity Li-Mn-rich $x\text{Li}_2\text{MnO}_3 \cdot (1-x)\text{Li}[\text{Ni}_x\text{Mn}_y\text{Co}_z]\text{O}_2$. Therefore, this electrolyte innovation will push the U.S. supply base of batteries and battery materials past the technological and cost advantages of foreign competitors, thereby increasing economic value to the USA. ANL's new fluorinated electrolyte material will enable the demand for more PHEVs and EVs, which directly transforms to much less gasoline consumption and less pollutant emissions.

OUT-YEAR-GOALS: The goal of this project for the 2nd year is to deliver a new fluorinated electrolyte system with outstanding stability at high voltage and high temperature with improved safety characteristic for an electrochemical couple consisting of 5-V Ni-Mn spinel $\text{LiNi}_{0.5}\text{Mn}_{1.5}\text{O}_4$ (LNMO) cathode and graphite anode. The specific objectives of this proposal are the design, synthesis, and evaluation of (1) non-flammable high voltage fluorinated solvents to attain intrinsic voltage stability in the entire electrochemical window of the high-voltage cathode material and (2) effective electrolyte additives that form a compact and robust solid-electrolyte interphase (SEI) on the surfaces of the high voltage cathode and graphitic anode.

COLLABORATIONS: Dr. Kang Xu, Co-PI, U.S. Army Research Laboratory; Dr. Xiao-Qing Yang, Co-PI, Brookhaven National Laboratory; Dr. Ganesh Skandan, NEI Corporation; Dr. Brett Lucht, University of Rhode Island; Dr. Libo Hu, Dr. Andrew Jansen, Dr. Ira Bloom and Dr. Gregory Krumbick, Argonne National Laboratory.

Milestones

- 1) Complete theoretical calculation of electrolyte solvents (fluorinated carbonate, fluorinated ether) and additives (fluorinated phosphate, fluorinated phosphazene); Validate the electrochemical properties of the available fluorinated solvents by CV and leakage current experimnt. (Dec. 13) **Complete**.
- 2) Synthesize and characterize the Gen-1 electrolyte (3 linear/cyclic F-carbonate solvents + 1 additive) by NMR, FT-IR, GC-MS, DSC. (Mar. 14) **Ongoing**.
- 3) Evaluate the LNMO/graphite cell performance of Gen-1 electrolyte [Solvent(s) + Additive(s)]. (Jun. 14) **Ongoing**.
- 4) Optimize the Gen-1 high voltage F-electrolyte; Deliver 10 baseline pouch cells. (Sep. 14) **Ongoing**.

Progress Report

In the first quarter of FY14, molecular modeling by density functional theory (DFT) calculations was performed to predict the potentials and the molecular orbital energies of two fluorinated solvents and compared with their non-fluorinated counterparts. The oxidation potentials were calculated by subtracting the absolute free energies of the neutral species from those of the corresponding cations, and 1.46 V was subtracted to obtain values relative to a Li⁺/Li reference electrode. Calculations of the energies for the HOMO and LUMO with the B3LYP/6-311+G(3df,2p) basis set are also provided. Based on the results, fluorine substitution on carbonates and ethers lowers both HOMO and LUMO levels, resulting in simultaneously higher oxidation stability. Fluoroethylene carbonate (FEC) has a P_{ox} = 7.16 V, while the value for EC is only 6.91 V. An even larger difference was observed for the linear carbonate. Methyl 2,2,2-trifluoroethyl carbonate's (F-EMC) theoretical oxidation value is 7.10 V, a 0.47 V increase compared with that of its non-fluorinated counterpart. 1,1,2,2-Tetrafluoroethyl 2,2,3,3-tetrafluoropropyl ether (F-EPE) showed the highest oxidation potential of 7.24 V among the first compound list, indicating the fluorinated ethers are more thermodynamically stable. It is worth noting that the oxidation potential of the methyl ethyl sulfone, a representative of a class of high oxidation solvents, was calculated by Shao and coworkers using the same DFT method to be around 6.0 V, which is much lower than those of the fluorinated solvents.

The synthesis, characterization, and purification of the above calculated F-EMC are first performed in this quarter. The reaction involved is illustrated in Fig. 1a and the compound purity was monitored by ¹H, ¹³C, and ¹⁹F-NMR and GC-MS (Fig. 1b). Based on the GC-MS results, a high purity level of 99.9% was obtained after repeated fractional distillations.

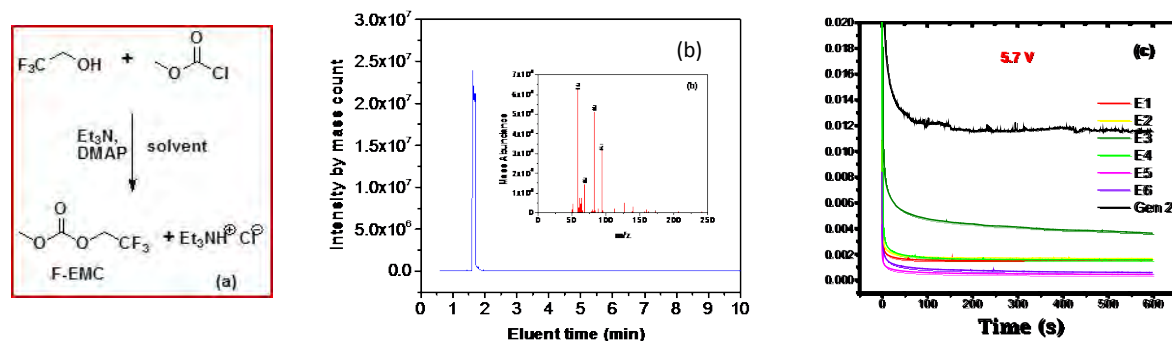


Figure 1. (a) Synthesis reaction of methyl 2,2,2-trifluoroethyl carbonate (F-EMC), (b) GC-MS spectrum (inset of MS) of the synthesized F-EMC, and (c) leakage current profiles at 5.7 V in Pt/Li/Li electrochemical cell using fluorinated electrolyte formulations with the synthesized F-EMC as a major component.

To validate the DFT calculations, an electrochemical floating test was performed using a Pt/Li/Li cell with a potential range from 5.3 to 5.7 V vs. Li⁺/Li. Figure 1c illustrated the 5.7 V test results. Clearly, the incorporation of the fluorinated carbonate and ether component into the electrolyte formulation greatly improved the voltage stability over the conventional electrolyte. By varying the ratio of the components in the formulation, it clearly indicates that the predominant potential-limiting factor arises from the non-fluorinated linear carbonate rather than the cyclic one. However, this does not mean that the cyclic carbonate plays a trivial role in the electrolyte oxidative decomposition under high potentials. Additive study and interphasial characterization were also initiated at the end of this quarter. LNMO cell performance using the first-developed High Voltage Electrolyte (HVE-1) will be reported in the second quarter.

Task 3.2 – Joe Sunstrom and Hitomi Miyawaki (Daikin America, Inc.)

Daikin America High Voltage Electrolyte

PROJECT OBJECTIVE: Development of a stable (300 – 1000 cycles), high-voltage (at 4.6 V), and safe (self-extinguishing) formulated electrolyte.

Exploratory Development (Budget Period #1 – October 1, 2013 to January 31, 2015)

- Identify promising electrolyte compositions for high-voltage (4.6 V) electrolytes via the initial experimental screening and testing of selected compositions

Advanced Development (Budget Period #2 – February 1, 2015 to September 31, 2015)

- Detailed studies and testing of the selected high-voltage electrolyte formulations and the fabrication of final demonstration cells

PROJECT IMPACT: Fluorinated small molecules offer the advantage of low viscosity along with high chemical stability due to the strength of the C-F bond. Due to this bond strength, Daikin fluorochemical materials are among the most electrochemical stable materials that still have the needed performance attributes for a practical electrolyte. Such an electrolyte will allow routine operating voltages to be increased to 4.6 V. This technological advance would allow significant cost reduction by reducing the number of cells needed in a particular application and/or allow for greater driving range in PHEV applications.

OUT-YEAR-GOALS: This project has a clearly defined goals for both temperature and voltage performance which are consistent with the deliverables of this proposal. Those goals are to deliver an electrolyte capable of 300 - 1000 cycles at 3.2 - 4.6 V at nominal rate with stable performance. An additional goal is to have improved high temperature (> 60°C) performance. An additional safety goal is to have this electrolyte be self-extinguishing.

COLLABORATIONS: At present, the team is collaborating with and receiving great advice from Vince Battaglia's group at Lawrence Berkeley Laboratory. In addition, there are plans to collaborate with another group (TBD) for electrode surface analysis.

Milestones

Budget Period #1 – Oct. 1, 2013 to Jan. 31, 2015

- 1) Complete identification of promising electrolyte formulations. Experimental design completed with consistent data sufficient to build models. Promising electrolyte formulations are identified which are suitable for high-voltage battery testing. **Ongoing**
- 2) Successful fabrication of 10 interim cells and delivery of cells to DOE laboratory to be specified. **Ongoing**
- 3) Electrochemical and battery cycle tests are completed and promising results are obtained which demonstrate stable performance at 4.6 V. **Ongoing**

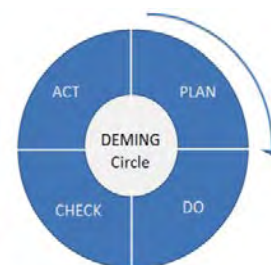
Progress Report

The technical approach to achieve the milestones is based on an iterative plan following a sound scientific method, also sometimes referred to as a Plan-Do-Check-Act (PDCA) cycle, shown in the figure below.

Technical Approach: Exploratory Development

Using a stable, established cell chemistry (4.6 V LMNO/graphite), 4 PDCA cycles will be conducted to develop a high-voltage electrolyte.

1. 2 PDCA cycles to identify optimum base solvent and salt formulation utilizing basic property measurements
2. 1 PDCA cycle to identify best available fluorinated anode/cathode additives which form stable SEI layers at high cell voltage
3. 1 PDCA cycle to identify and optimize out gassing/acid scavenger additives
4. Each PDCA cycle includes basic property measurements (conductivity, viscosity, electrochemical measurements and brief cycle testing in full cell test batteries)



Status: The first PDCA cycle is underway.

Following the three month plan summarized here, progress on these tasks is as described below:

Materials for fabrication of high voltage cell fabrication have been identified. The electrochemistry which will be used for the study is the LMNO spinel/graphite. In addition, another cathode material, NMC is being evaluated as a side-by-side countermeasure.

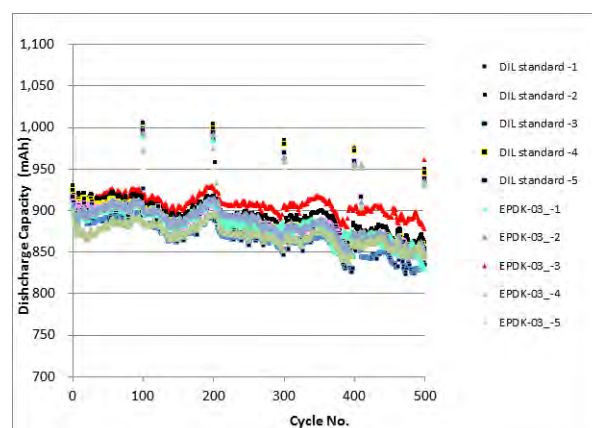
A visit was made to Oak Ridge National Laboratory to determine their electrode fabrication capability. A quote and work plan was received and is under consideration.

Quotes have been solicited from Bren-tronics, Hydro-Québec, and Electrodes & More for electrode fabrication.

A pertinent review of the literature was completed and merged with Daikin internal data.

Two standard formulations have been decided for initial evaluation. The first cycle of experiments will explore variations of base solvents mixtures to these standard formulations. The first formulation is a base hydrocarbon formulation used in the battery industry and the second has been studied extensively within the BATT Program under code name BDK-03.

Baseline RT cycling data has been collected for both of the standard samples. The cycling is 1 C-rate charge/discharge cycles with a capacity check completed every 100 cycles. Within error there is no performance difference between the two samples even though one contains a substantial (40%) fluorochemical level. The data is shown here. The periodic oscillations in the data is due to room temperature and this artifact will be eliminated in future data sets.



Novel Non-Carbonate Based Electrolytes for Silicon Anodes

PROJECT OBJECTIVE:

The objective of this project is to develop non-carbonate electrolytes that form a stable solid electrolyte interphase (SEI) on silicon alloy anodes, enabling substantial improvements in energy density and cost relative to current lithium ion batteries (LIBs). These improvements are vital for mass market adoption of electric vehicles. At present, commercial vehicle batteries employ cells based on LiMO_2 ($M = \text{Mn, Ni, Co}$), LiMn_2O_4 , and/or LiFePO_4 coupled with graphite anodes. Next generation cathode candidates include materials with higher specific capacity or higher operating voltage, with a goal of improving overall cell energy density. However, to achieve substantial increases in cell energy density, a higher energy density anode material is also required. Silicon anodes demonstrate very high specific capacities, with a theoretical limit of 4200 mAh/g and state-of-the-art electrodes exhibiting capacities greater than 1000 mAh/g. While these types of anodes can help achieve target energy densities, their current cycle life is inadequate for automotive applications. In graphite anodes, carbonate electrolyte formulations reductively decompose during the first cycle lithiation, forming a passivation layer that allows lithium transport, yet is electrically insulating to prevent further reduction of bulk electrolyte. However, the volumetric changes in silicon upon cycling are substantially larger than graphite, requiring a much more mechanically robust SEI film.

PROJECT IMPACT:

Silicon alloy anodes enable substantial improvements in energy density and cost relative to current lithium ion batteries. These improvements are vital for mass market adoption of electric vehicles, which would significantly reduce CO_2 emissions as well as eliminate the US dependence on energy imports.

OUT-YEAR-GOALS:

Development of non-carbonate electrolyte formulations that

- form stable SEIs on 3M silicon alloy anode, enabling coulombic efficiency > 99.9% and cycle life > 500 cycles (80% capacity) with NMC cathodes;
- have comparable ionic conductivity to carbonate formulations, enabling high power at room temperature and low temperature;
- are oxidatively stable to 4.6V, enabling the use of high energy NMC cathodes in the future; and
- do not increase cell costs over today's carbonate formulations.

COLLABORATIONS: Wildcat is working with 3M on this project. To date, 3M is supplying the silicon alloy anode films and NMC cathode films for use in Wildcat cells.

Milestones

- 1) Assemble materials, establish baseline performance with 3M materials (Dec. 13) **Complete**
- 2) Develop initial additive package using non-SEI forming solvent. (Mar. 14) **Ongoing**
- 3) Screen initial solvents with initial additive package. (Jun. 14) **Ongoing**
- 4) Design/build interim cells for DOE (Sep. 14) **Ongoing**

Progress Report

The first quarter of this project focused on developing a high-throughput workflow using electrode materials supplied by 3M. Wildcat proprietary high-throughput cells can be varied in a number of ways to match cell formats. In order to better guarantee that results of our high-throughput screening will result in discoveries that translate across cell formats, Wildcat tested 3M materials using a variety of conditions and cell architectures.

An example of the effect of electrode drying conditions is shown in Fig. 1, where significantly better results were observed using shorter, lower temperature conditions.

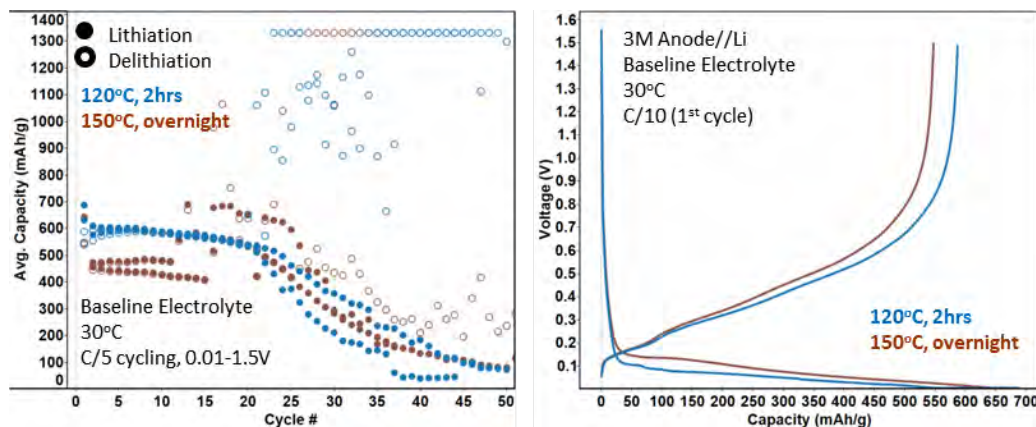


Figure 1. Example of sensitivity to film drying process.

Using these results, a set of conditions were established for high throughput that showed good correlation using 3M cells. The baseline full-cell cycle life is shown in Fig. 2.

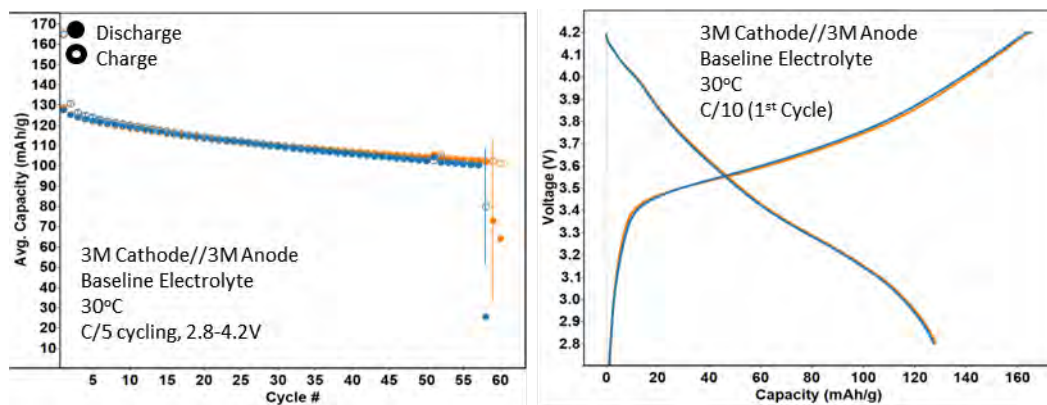


Figure 2. Baseline data for 3M materials in Wildcat high-throughput workflow and cell architecture.

Once baseline data were obtained, initial library designs were completed on additives. The first design consists of approximately 100 additives from broad chemistry families that were previously screened in graphite cells. The objective of running this initial library is to determine if there are correlations between effective chemistries on graphite and Si.

Electrolytes – Development of Electrolytes for Lithium-Ion Batteries

PROJECT OBJECTIVE: The objective of the project is to develop an understanding of the mechanism of improved capacity retention for Si-nanoparticle electrodes in the presence of electrolyte additives, fluoroethylene carbonate (FEC) and/or vinylene carbonate (VC). A direct comparison of the cycling performance of electrolytes with different concentrations of added FEC and/or VC will be conducted and the results will allow the determination of an optimized electrolyte for use with Si-nanoparticle electrodes. This formulation will be suggested as a standard formulation for BATT researchers to allow for better cross comparison of electrochemical cycling data for different novel Si-anode materials. After cycling Si-nanoparticle electrodes with different electrolyte formulations, the electrodes will be extracted and *ex situ* surface analysis will be conducted. The surface analysis and cycling data will be used to develop a mechanism for capacity retention enhancement *via* addition of FEC or VC.

PROJECT IMPACT: Due to the large volume expansion and subsequent surface area changes for Si-anode materials, the reactions of the electrolyte to generate a stable SEI are critical to the cycling stability of the electrode. This project is being conducted to develop a better understanding of the role of the electrolyte in capacity fade for Si-nanoparticle electrodes. Developing an understanding of the effect of mechanism of stabilization of currently utilized additives, VC and FEC, can lead to the development of superior additives which afford improved cycling performance.

OUT-YEAR-GOALS: This is the final year of this project.

COLLABORATIONS: V. Battaglia, G. Chen, and J. Kerr (LBNL), P. Balbuena (TAMU), A. Manthiram (UT), Silicon-Anode Focus Group, P. Guduru (Brown U.), A. Garsuch (BASF).

Milestones

- 1) Complete electrochemical cycling of Si-nanoparticle electrodes with electrolytes containing added VC or FEC. (Dec. 13) **Complete**
- 2) Determine the best electrolyte formulation for Si-nanoparticle electrodes and suggest as standard for BATT researchers. (Mar. 14) **Ongoing**
- 3) Complete surface analysis of Si-nanoparticle electrodes with electrolytes containing VC or FEC. (Jun. 14) **Ongoing**
- 4) Develop mechanism for the beneficial cycling performance for electrolytes with added FEC or VC for Si-nanoparticle electrodes. (Sep. 14) **Ongoing**

Progress Report

Silicon is one of the most promising candidates for an anode material in LIBs due to its high theoretical capacity, 3580 mAh/g. This theoretical capacity is *ca.* 10 times that of commercial graphite (372 mAh/g) currently used in Li-ion batteries. However, Si electrodes have a very large volume expansion (300-400%) during lithiation resulting in instability of the SEI and poor capacity retention. The two most frequently utilized SEI stabilizing additives are VC and FEC. A systematic comparison of the effects of added FEC or VC at multiple concentrations is being conducted with uniform Si-nanoparticle electrodes.

Capacity retention of Li/Si-nanoparticle cells with different concentrations of VC and FEC in 1.2 M LiPF₆ in 1:1 EC/DEC is depicted in Fig. 1. The capacity fades very rapidly for the baseline electrolyte. Incorporation of FEC at any of the concentrations investigated (5, 10, 15, or 25%) results in significant improvements in capacity retention. Interestingly, intermediate concentrations of FEC 10 and 15% give the best capacity retention suggesting that lower concentrations do not generate a sufficiently stable SEI while higher concentrations may result in increased cell resistance. Cells containing added VC do not have significantly better performance than the cells containing the baseline electrolyte. Incorporation of 3% VC results in cells with very similar capacity fade to the baseline electrolyte, while cells containing 6% VC have an odd intermittent behavior which may be due to high cell impedance as evidenced by electrochemical impedance spectroscopy. The cycling efficiencies correlate very well with the capacity retention. Cells containing 10 and 15% FEC have the best efficiencies (*ca.* 99% for cycles 10 to 50), while cells containing the baseline electrolyte or electrolyte with added VC have lower efficiencies (<98% for cycles 10 to 50). *Ex situ* surface analysis of the electrodes after cycling is currently being conducted by a combination of SEM, XPS, and FT-IR. Preliminary investigations suggest incorporation of VC and FEC results in the generation of different polymeric structures on the Si surface.

The structural and compositional information obtained from the *ex situ* surface analysis in conjunction with collaborative computational efforts (P. Balbuena) will afford the development of a mechanism for the beneficial cycling performance of silicon nano-particle electrodes with electrolytes containing added FEC. An understanding of the mechanism of stabilization of the Si SEI will allow a systematic development of superior electrolyte additives.

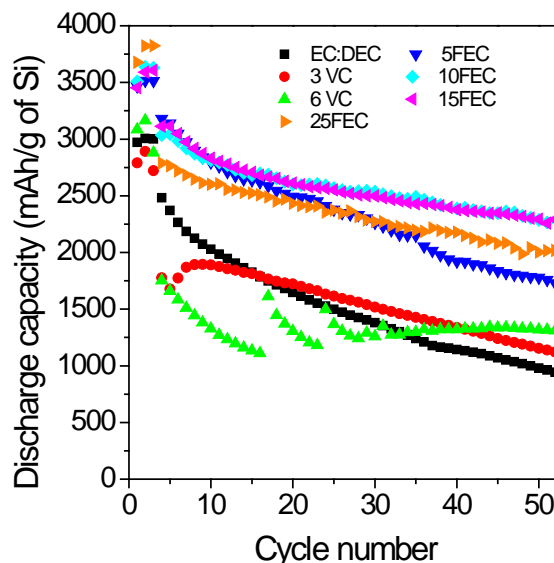


Figure 1. Capacity retention for Li/Si nanoparticle cells with electrolytes containing different concentrations of VC or FEC.

Electrolytes - Interfacial and Bulk Properties and Stability.

PROJECT OBJECTIVE: To demonstrate the advantages of single-ion conductor (SIC) electrolytes for prevention of concentration polarization in Li battery composite electrolytes. The performance requirements are bulk conductivities $>10^{-4}\text{S/cm}$ at the operating temperatures and interfacial impedances $<100\text{ ohm.cm}^2$ and preferably $<10\text{ ohm.cm}^2$. The use of SIC electrolytes also leads to improved stability, more control of the passivating layers (*e.g.*, SEI) and hence longer lifetime and improved safety. It is also anticipated that the use of SIC electrolytes will significantly improve the performance of Li metal electrodes with respect to dendrite growth. The two major technical objectives are:

1. Determine the role of electrolyte structure upon bulk transport and intrinsic electrochemical kinetics and how it contributes to cell impedance (Energy/power density).
2. Determine chemical and electrochemical stability of electrolyte materials to allow elucidation of the structure of and the design of passivating layers (*e.g.*, SEI)

PROJECT IMPACT: Elimination of concentration polarization while minimizing the interfacial impedance is required to allow high rate discharge and charging. In fact rapid charging of high-energy batteries with large capacities is impossible if the electrolyte undergoes concentration polarization. Prior results have already demonstrated that SIC electrolytes allow double the energy density to be discharged at high rates compared to conventional binary salt electrolytes. This project aims to more clearly demonstrate the advantages so that more appropriate resources may be focused on the topic by DOE.

OUT-YEAR-GOALS: The project lead by this P.I. will terminate in FY2014 but the out-year goals will be to encourage other teams of investigators to address the topic with appropriately-sized resources.

COLLABORATIONS: Collaboration with LANL and LBNL Fuel Cell groups on electrode ink formulation will continue. Collaboration with cell building group in BATT needed to test and scale up electrolytes.

Milestones

- 1) Test high voltage composite cathode electrode cells using gel electrolyte (Apr. 14). **Ongoing**
- 2) Optimize single-ion conductor solid state cells with no free solvents and composite anodes and cathodes (Jun. 14). **Ongoing**
- 3) Define dendrite formation on Li metal with single-ion conductors (Sep. 14). **Ongoing**

Progress Report

Two SIC electrolytes were prepared, one with a stiff, polysulfone backbone (Fig. 1a) and one with a flexible, polyether backbone (Fig. 1b). These are materials whose electrochemical performance were reported on in FY2012. The polysulfone has no conductivity in the absence of added solvent as it contains no solvating groups, whereas the polyether SIC has conductivity in the dry form as well as when solvent is added. The polysulfone, when ethylene carbonate/ethylmethyl carbonate solvent is added, exhibits excellent conductivity and greatly improved interfacial impedance, which is sufficient to allow fabrication and testing of composite electrodes. These tests demonstrated the improvements in performance resulting from the lack of concentration polarization. The performance of the polyether material improves with added solvent but not by as much as the polysulfone material, which clearly has the better conductivity and interfacial behavior when used as a gel with carbonate solvents. Both materials exhibit excellent stability at elevated temperatures, largely due to the absence of any Lewis acidity in the anionic groups.

Small Angle X-ray Scattering (SAXS) can be used to observe morphological structures in polymers and Beam line 7.3.3 at the Advanced Light Source (ALS) at LBNL was employed to measure the SAXS behavior of the polymers in the dry form, and over time as solvent was absorbed by the material. Figure 1a shows the SAXS results for the polysulfone material (in this case a fluoroalkylsulfonate or triflate anion) in the dry form and over time after the addition of the carbonate solvent (see arrow). Initially the material shows little or no signs of phase separation but after addition of solvent a peak grows that indicates an ionic multiplet of about 5.5 nm in diameter. For comparison, Nafion[®] has a multiplet size of about 4.3 nm. The polyether polymer, by contrast, exhibits a peak at about 2.5 nm in the dry form, which is not affected by the addition of solvent. This behavior can be rationalized by the presence of the ether groups which solvate the Li ions so that the ionic groups are already dissociated and have already undergone phase separation to some extent. The multiplet in this case is smaller, perhaps indicating less phase separation. In the polysulfone case, the ions are not dissociated in the dry form, but dissociated in the presence of solvent, which also plasticizes the backbone leading to rearrangement and phase separation. The larger multiplet size is consistent with a more liquid-like environment for the ions leading to liquid-like electrochemical performance that has previously been reported.

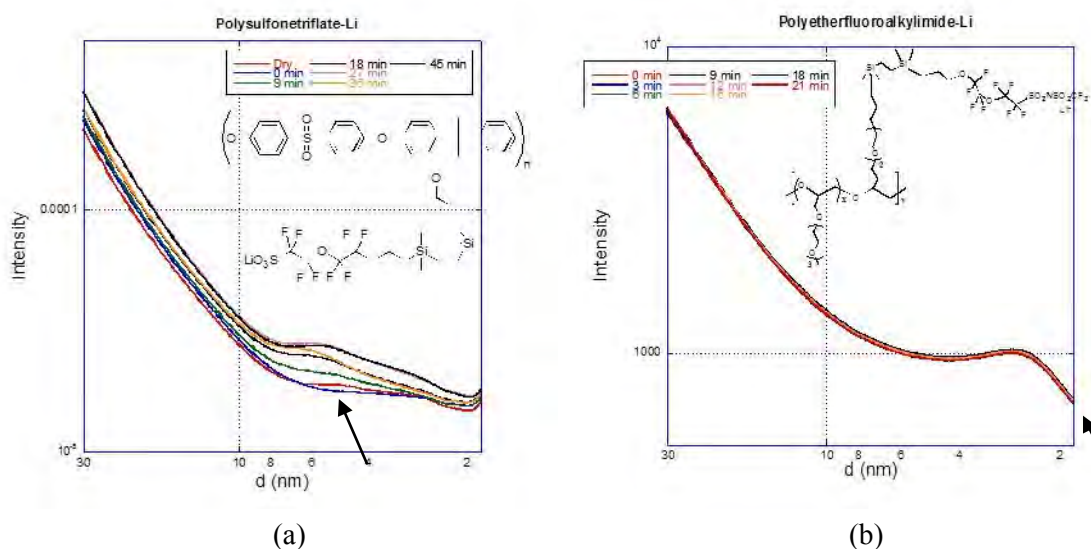


Figure 1. Small Angle X-ray Scattering of ionomeric polymers in the dry form and over time with EC/EMC solvent (Time after solvent added given in legend). (a) Polysulfone, (b) Polyether.

Electrolytes – Sulfones with Additives as Electrolytes

PROJECT OBJECTIVE: To devise new electrolyte types (sulfone mixtures and superionic glasses or plastic solid derivatives) that will permit cell operation at high voltages without solvent oxidation and with adequate overcharge protection, and to provide optimized nanoporous supporting membranes for this electrolyte.

PROJECT IMPACT:

OUT-YEAR-GOALS: Project will terminate in FY 2014.

COLLABORATIONS: None this quarter.

Milestones

- 1) Go/No-Go: On cathode half cells with sulfone electrolytes with HFiP additive. (Dec. 13) **Complete**
- 2) Produce new plastic Li-conducting phases of $\sigma(25^{\circ}\text{C}) > 10$ mS/cm. (Dec. 13) **Delayed, due Mar. 14.**
- 3) Achieve glassy or viscous liquid single-ion Li-conducting versions of 2). (Dec. 13) **Delayed, due Mar. 14.**
- 4) Make mixed 3- and 4-bonding covalent nanoporous nets (amorphous MOFs). (Jun. 13) **Complete**
- 5) Go/No-go: Develop mechanically robust nanoporous covalent networks for novel solution and plastic alkali-ion conductors. (Dec. 13) **Delayed, due Mar. 14.**

Progress Report

(a) Go-no-go on cathode half-cells with sulfone electrolytes (*Milestone met*).

Previously, results were presented on half-cell testing of the capacity retention and coulombic efficiency of sulfone-carbonate electrolytes with LNMO cathodes, finding 97% capacity retention, and 99 to 100% coulomb efficiency over 100 cycles. Our last report showed data with both molecular and ionic additives that led to slight improvements only. A modification of the sulfone component is reported that provides 100% capacity retention at 130 mAhg^{-1} over the same number of cycles, though at the expense of a decrease in coulombic efficiency to 98% (Fig. 1.) The conductivity of the improved electrolyte is significantly higher than that of EMS-DMC, as seen in Fig. 2. These data were obtained at 25°C .

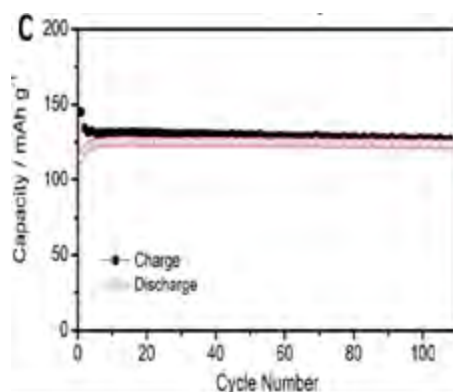


Figure 1. No capacity loss in 100 c.

As expected, raising T to 55°C lead to cell failure. To test the expectation that this is due to PF_6^- thermal instability, additional half-cells with the more stable LiBF_4 and LiAsF_6 salts are being studied. With LiBF_4 (of uncertain purity), both discharge capacity and coulomb efficiency are lower but, importantly, there is no deterioration in discharge capacity on passing from 25 to 55°C . LiAsF_6 based half-cells are currently being tested.

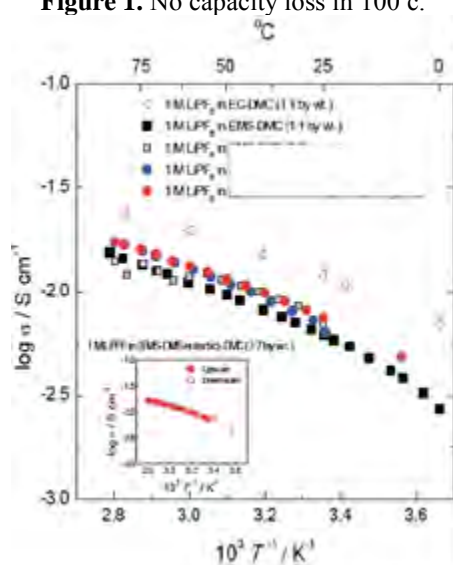


Figure 2. Improved conductivity

(b) Production of new plastic Li-conducting phases of $\sigma(25^\circ\text{C}) > 10 \text{ mS/cm}$, by June 2013. (*Milestone not met*).

Previously, there was a setback in this research initiative that required a fully revamped (now closed system) synthesis procedure for preparing precursor acids of novel character – soft, waxy materials that are highly acidic (attacking stainless steel conductivity cells). Proton conductivities at 25°C are 100x higher than any found in the literature. They may have applications to fuel cells, but this is not our objective. Cautious lithiation with LiNH_2 , (vigorous, despite the solid-state character of the reaction), leads to a beige material similar to those reported last year, but less pliable, and less conductive. However, a recent breakthrough in synthesis procedures, that will reduce the reaction times by up to 10,000x, and provide much greater flexibility in the products obtainable, is being introduced, with the prospect of new materials for the next quarterly report.

Revised milestone March 31, 2014.

(c) Achievement of glassy single ion Li-conducting versions of (b) by Dec. 2013. (*Delayed to Mar. 14*)

(d) Production of new mixed 3 and 4-bonding covalent nanoporous nets (amorphous MOFs) by Dec. 2013. (*Milestone met*).

However while these have been achieved, they so far fail to satisfy mechanical robustness requirements.

(e) Go-no-go development of mechanically robust nanoporous covalent networks for novel solution and plastic alkali-ion conductors, by Dec. 2013. (*Delayed, due Mar. 14*).

Reinforcement by long chain polymers has been attempted without notable success and the coworker on the project has departed.

Novel Cathode Materials and Processing Methods

PROJECT OBJECTIVE:

The end-goal of this project is the development of low-cost, high-energy and high-power, Mn-oxide-based cathodes for PHEV and EV vehicles. Improvement of design, composition, and performance of advanced electrodes with stable architectures, facilitated by an atomic-scale understanding of electrochemical and degradation processes, is a key objective of this work. New processing routes as well as ANL's comprehensive characterization facilities will be used to explore novel, surface and bulk structures both *in situ* and *ex situ* in the pursuit of advancing Li-ion battery cathode materials.

PROJECT IMPACT:

Standard Li-ion technologies are currently unable to meet the demands of next-generation PHEVs and EVs. Battery developers and scientists alike will take advantage of the knowledge, both applied and fundamental, generated from this project to further advance the field. In particular, it is expected that this knowledge will significantly enable progress towards meeting the DOE goals for 40-mile, all-electric range, PHEVs.

OUT-YEAR-GOALS:

- Identify composite electrode structures that mitigate or eliminate voltage fade.
- Identify and characterize surface chemistries and architectures that allow fast Li-ion transport, are stable to ~5 V, and mitigate or eliminate transition-metal dissolution.
- Scale-up, evaluate and verify promising cathode materials using ANL's Scale-up and Cell Fabrication facilities.
- Take advantage of ANL's user facilities (*e.g.*, the Advanced Photon Source (APS), the Center for Nanoscale Materials (CNM), the Electron Microscopy Center (EMC) and the Leadership Computing Facility (ALCF) to build on the fundamental knowledge gained to promote and implement the rational design of new electrode materials.
- Use complementary theoretical approaches to further the understanding of electrode structures and electrochemical processes to accelerate the progress of materials development.

COLLABORATIONS: Jason Croy, Brandon Long, Joong Sun Park, Kevin Gallagher, Mahalingam Balasubramanian (APS), Dean Miller (EMC), and William David (Rutherford Appleton Laboratory, UK).

Milestones

- 1) Evaluate the stabilization and performance of near end-member, Li_2MnO_3 -containing composite electrodes. Specifically, high and low Li_2MnO_3 -content electrodes. (Dec. 13) **Go for low Li_2MnO_3 ; No-go for high Li_2MnO_3**
- 2) Evaluate new synthetic routes using layered LiMO_2 (M = Mn, Ni, Co) precursors to prepare composite electrode materials. (Mar. 14) **Ongoing**
- 3) Synthesize and characterize unique surface architectures that enable >200 mAh/g at a $>1\text{C}$ rate with complementary theoretical studies of surface structures. (Jun. 14) **Ongoing**
- 4) Identify structures and compositions, including surface and bulk, that can deliver ~ 230 mAh/g at an average discharge voltage of ~ 3.5 V on extended cycling. (Sep. 14) **Ongoing**

Progress Report

The link between voltage fade and hysteresis in composite electrodes has been studied and a model proposed that points to partially reversible migration of cations between the Li and transition metal layers. As such, the tetrahedral sites of the Li layers, which link the octahedral sites of the migration pathways, may play a crucial role in the overall degradation mechanisms. It has been shown that both voltage fade and hysteresis increase as a function of Li_2MnO_3 content, x , in $x\text{Li}_2\text{MnO}_3 \cdot (1-x)\text{LiMO}_2$ ($M = \text{Mn, Ni, Co}$) electrode structures. However, it is the excess Li contained within the transition metal layers of the Li_2MnO_3 component that gives these composite materials their alluring properties (*e.g.*, capacities of *ca.* 250 mAh/g). Therefore, understanding the electrochemical role of Li_2MnO_3 -like domains and the mitigation of voltage fade, through various routes (theory, synthesis, experiment, and optimization), is crucial to the commercial success of these materials.

A study was undertaken on both low- and high-content Li_2MnO_3 electrodes to assess their stability limits with respect to electrochemical cycling. While $x\text{Li}_2\text{MnO}_3 \cdot (1-x)\text{LiMO}_2$ materials with $x > 0.5$ yielded capacities > 250 mAh/g, their structural stability was found to be untenable. However, electrodes with lower values of x (*i.e.*, $x \leq 0.33$) were found to have promising electrochemical attributes. In order to explore the possibility of stabilizing low Li_2MnO_3 -content electrodes to counter voltage fade and hysteresis, a $0.33\text{Li}_2\text{MnO}_3 \cdot 0.67\text{LiMn}_{0.375}\text{Ni}_{0.375}\text{Co}_{0.25}\text{O}_2$ composite was chosen as a baseline composition and doped with 2 mol% Mg^{2+} or Al^{3+} . Mg^{2+} and Al^{3+} are both electrochemically inactive ions and can occupy and/or move through both tetrahedral and octahedral sites. It can be anticipated, therefore, that a small amount of mobile, electrochemically inactive ions in these sites could impact the stability of cycled electrodes. Figures 1a and b show the cycling performance of baseline and $\text{Mg}^{2+}/\text{Al}^{3+}$ -doped electrodes, cycled between 4.45–2.0 V at 15 mA/g, after activation to 4.6 V. All cells delivered more than 200 mAh/g with capacity values converging after *ca.* 10 cycles to *ca.* 210 mAh/g. Figure 1b shows the dQ/dV plots of the 15th cycle for each cell; they reveal a larger redox activity in the lower voltage region (< 3.3 V) for the undoped electrode relative to the Mg^{2+} - and Al^{3+} -doped electrodes. Interestingly, the hysteresis, which manifests itself by the redox processes at *ca.* 4.3 V on charge and *ca.* 3.3 V on discharge, was significantly less for the doped electrodes. The rate performance of the cells, shown in Fig. 1c, demonstrates that all three electrodes were able to deliver more than 200 mAh/g at a 150 mA/g rate ($\sim C/1.3$) after being charged to 4.6 V at 15 mA/g. Figure 1c also shows that at a low charge and discharge rate (15 mA/g), a discharge capacity of 240 to 250 mAh/g was obtained, and that at higher discharge rates there was greater polarization when Mg^{2+} - and Al^{3+} -doped electrodes were used. This finding suggests that Li^+ diffusion is hindered as a result of tetrahedral site occupancy by Mg^{2+} and Al^{3+} ions. Note that the polarization is highest for the Mg^{2+} -doped electrodes. Further structural analyses as well as high-voltage, long-term cycling of these materials are currently being undertaken.

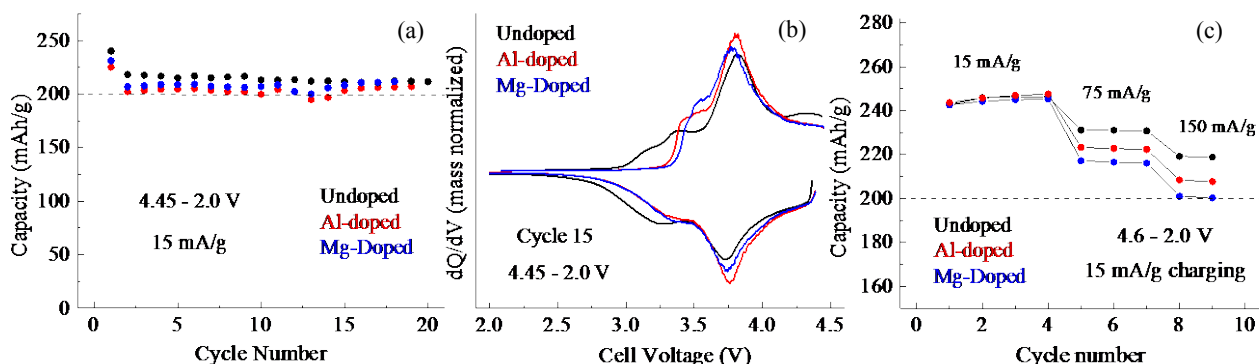


Figure 1. (a) Capacity, (b) dQ/dV , and (c) rate data for $0.33\text{Li}_2\text{MnO}_3 \cdot 0.67\text{LiMn}_{0.375}\text{Ni}_{0.375}\text{Co}_{0.25}\text{O}_2$ baseline and Mg^{2+} - and Al^{3+} -doped (2 mol%) electrodes in Li half-cells at room temperature

Design of High Performance, High Energy Cathode Materials

PROJECT OBJECTIVE: To develop high-energy, high-performance cathode materials including composites and coated powders, using spray pyrolysis and other synthesis techniques. The emphasis is on two systems: modified NMC materials and the high-voltage spinel, $\text{LiNi}_{0.5}\text{Mn}_{1.5}\text{O}_4$ (LNMO). Partial substitution of Ti for Co in NMCs results in higher discharge capacities (up to 225 mAh/g) without the need for a formation reaction and without risk of structural change during cycling. Experiments are directed towards optimizing the synthesis, improving cycle life, and understanding the effect of Ti substitution. For LNMO, particle size and morphology are controlled during spray pyrolysis synthesis by varying residence time, temperature, precursors, and other synthetic parameters. By exploiting differences in precursor reactivity, coated materials can be produced; composites can be prepared by post-processing techniques such as infiltration. These approaches are expected to improve cycling due to reduced side reactions with electrolytes.

PROJECT IMPACT: To increase the energy density of Li-ion batteries, cathode materials with higher voltages and/or higher capacities are required, but safety and cycle life cannot be compromised. In the short term, the most promising materials are based on high voltage spinels or modified NMCs that do not require formation cycles or undergo structural transformations during cycling. Ti-substituted NMCs exhibit increased discharge capacity, due to improved first-cycle efficiencies and are not expected to undergo structural changes or voltage decay during cycling. Optimizing LNMO particle morphologies, utilizing coatings and composites, is expected to improve coulombic efficiencies and safety as well as cycle life.

OUT-YEAR GOALS: Two high-energy cathode systems will have been optimized for this work; LNMO and high capacity Ti-substituted NMC cathodes, which do not require activation *via* charge to high potentials. Materials will be synthesized by a simple, low cost spray pyrolysis method, which has potential for commercialization. This technique produces phase-pure, unagglomerated powders and allows for excellent control over particle morphologies, sizes, and distributions. Coated materials will also be produced in either one or two simple steps by exploiting differing precursor reactivities during the spray pyrolysis procedure, or by first preparing hollow spheres of an electroactive material, infiltrating the spheres with precursors of the high voltage cathodes, and subsequent thermal treatment. The final result is expected to be a high energy density cathode material with good safety and cycling characteristics suitable for use in vehicular applications, which can be made by a low-cost process that is easily scalable.

COLLABORATIONS: Huolin Xin of BNL, Dennis Norlund and Tsu-Chien Weng of SLAC National Accelerator Laboratory, Mark Asta (U.C. Berkeley).

Milestones

- 1) Complete optimization of Ti-NMC synthesis with TiOSO_4 precursor (Dec. 13) **Discontinued. This effort has been transferred to the ABR Program.**
- 2) Go/No-Go: Decision on infiltration of LiFePO_4 into LNMO. Criteria: A “no go” decision will be made if attempts to prevent reaction of LiFePO_4 with LNMO during processing fail (Mar. 14) **Delayed until Sep. 14. The effort has been postponed due to a recent lab move.**
- 3) Complete soft XAS experiments on Ti-NMCs (Jun. 14) **Complete**
- 4) Go/No-Go: Decision on spray pyrolysis of NMCs. Criteria: A “no go” decision will be made if the electrochemical performance of the spray-pyrolyzed material does not equal that of the material made by co-precipitation. (Sep. 14). **Ongoing**

Progress Report

Due to the recent move of our laboratories, work was delayed on milestones 2 and 4 and concentrated instead on milestone 3, which has now been completed earlier than anticipated. Work directed towards milestone 1 has been transferred to the ABR Program and is discontinued under the BATT Program.

Efforts to understand the surface chemistry of NMC electrodes have led to the successful elucidation of the structure-performance relationship of NMC and Ti-substituted NMC materials. The state-of-the-art techniques applied include high-throughput synchrotron XAS and atomic resolution STEM. For example, ADF-STEM imaging was performed to directly visualize the atomic packing for the NMC particles in a certain state of charge - the representative images are shown in Figs. 1a and 1b. Structural disorder is clearly observed in the NMC particle shown in Fig. 1a and the inset. Furthermore, significant changes in atomic packing were also observed for the top few nanometers. Three structurally distinct regions were selected for fast Fourier transform (FFT); the corresponding FFT patterns are shown in Fig. 1i to 1iii. It is determined from the FFT patterns that the surface of the NMC particle consists of either completely rock salt structure (Region i in Fig. 1b) or layered/rock salt hybrid structure (Region ii in Fig. 1b). Since all transition metals coexist at the top surface, as revealed by spectroscopic techniques (EELS, XAS and XPS, data not shown), the rock salt structure is most likely a solid solution of NiO, MnO, and CoO, *i.e.*, (Ni, Mn, Co)O. The slight mismatch between the lattice spacings of $Fm\bar{3}m$ (111) and $R\bar{3}m$ (003) allows for the epitaxial growth of the rock salt structure on the layered structure, as shown in Fig. 1c. Two publications have been submitted on related NMC work; one to *Nature Communications*, and a second to *Scientific Reports*, and are currently under review.

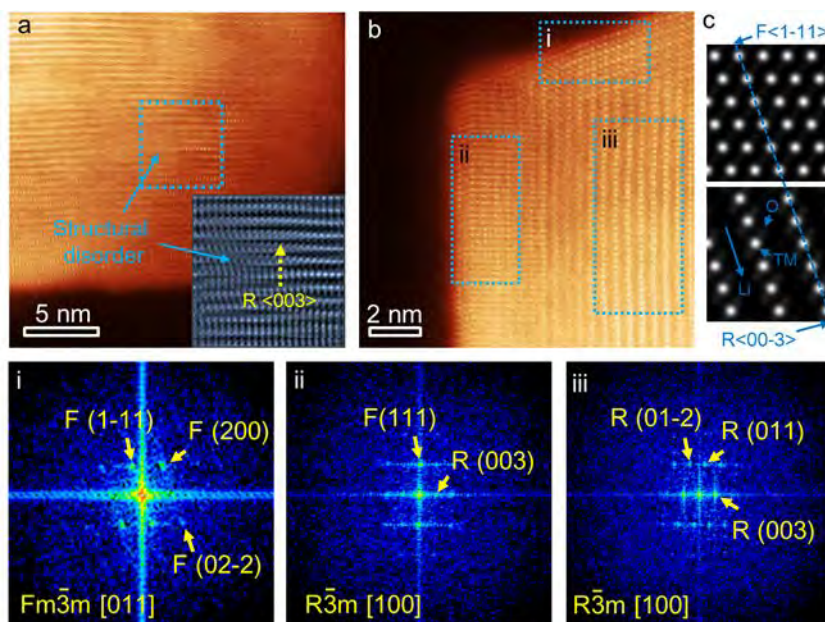


Figure 1. STEM investigation of NMC particles in the fully charged state. (a) High-resolution STEM image; the inset shows the inversed FFT image for the selected region, where the structural disorder is clearly observed. (b) Atomic-resolution STEM image for the surface region; FFT was performed for the selected area, shown in (i), (ii), (iii). (c) Schematic illustration for the semi-coherent growth of rock-salt structure on layered structure. The $Fm\bar{3}m$ (111) crystal plane matches up with the $R\bar{3}m$ (003) plane.

High-capacity, High-voltage Cathode Materials for Lithium-Ion Batteries

PROJECT OBJECTIVE: A significant increase in capacity and/or operating voltage is needed to make the lithium-ion technology viable for vehicle applications. This project addresses this issue by focusing on the design and development of cathode materials based on polyanions that have the possibility for reversibly inserting/extracting more than one Li ion per transition-metal ion and/or operating above 4.3 V. Specifically, high-capacity and/or high-voltage Li transition-metal phosphate, silicate, and carbonophosphate cathodes are investigated. The major issue with the phosphate and silicate cathodes is the poor electronic and ionic transport, which limits the practical capacity, energy density, and power density. To overcome these difficulties, novel microwave-assisted solvothermal, microwave-assisted hydrothermal, and template-assisted synthesis approaches are pursued to realize controlled morphology with smaller particle size and to integrate conductive additives, like graphene, in a single synthesis step.

PROJECT IMPACT: The critical requirements for the widespread adoption of Li-ion batteries for vehicle applications are high energy, high power, long cycle life, low cost, and acceptable safety. The currently available cathode materials do not adequately fulfill these requirements. The polyanion cathodes with the novel synthesis approaches pursued in this project have the potential to significantly increase the energy and power. More importantly, the covalently-bonded polyanion groups can offer excellent thermal stability and enhanced safety. The microwave-assisted synthesis approaches pursued also lower the manufacturing cost of the cathodes through a significant reduction in reaction time and temperature.

OUT-YEAR GOALS: The overall goals are to enhance the electrochemical performances of high-capacity, high-voltage polyanion cathode systems, and to develop a fundamental understanding of their structure-composition-performance relationships. Specifically, the project is focused on enhancing the electrochemical performance of systems such as LiMPO_4 , $\text{Li}_2\text{MP}_2\text{O}_7$, Li_2MSiO_4 , $\text{Li}_3\text{V}_2(\text{PO}_4)_3$, $\text{Li}_9\text{V}_3(\text{P}_2\text{O}_7)_3(\text{PO}_4)_2$, $\text{Li}_3\text{M}(\text{CO}_3)(\text{PO}_4)$, and their solid solutions with $\text{M} = \text{Mn, Fe, Co, Ni, and VO}$. Advanced structural, chemical, surface, and electrochemical characterizations of the materials, synthesized by novel approaches, are anticipated to provide in-depth understanding of the factors that control the electrochemical properties of the polyanion cathodes. For example, the possible segregation of certain cations to the surface in solid-solution cathodes consisting of multiple transition-metal ions and the role of conductive graphene integrated into the polyanion cathodes can help design better-performing cathodes.

COLLABORATIONS:

Wanli Yang (LBNL): to understand the variations in the characteristics of LiMnPO_4 cathodes on doping with V; Feng Wang (BNL): to determine the oxidation state of V and Mn in doped LiMnPO_4 by X-ray absorption near edge spectroscopy (XANES)

Milestones

- 1) Establish whether or not LiMnPO_4 can be aliovalently doped with V^{3+} and determine its effect on electrochemical performance. (Dec. 13) **Complete**
- 2) Demonstrate >200 mAh/g capacity with LiVOPO_4 prepared by novel synthesis approaches. (Mar. 14) **Ongoing**
- 3) Establish whether or not LiCoPO_4 can be aliovalently doped with V^{3+} and determine its effect on electrochemical performance. (Jun. 14) **Ongoing**
- 4) Go/No-Go: Stop the microwave-assisted synthesis if capacities are <150 mAh/g. Criteria: Demonstrate >150 mAh/g capacity with $\text{Li}_3\text{M}(\text{CO}_3)(\text{PO}_4)$ prepared by microwave-assisted synthesis. (Sep. 14) **Ongoing**

Progress Report

This quarter the focus was on the aliovalent doping of LiMnPO_4 with vanadium and determining its effect on electrochemical performance. Single-phase $\text{LiMn}_{1-3x/2}\text{V}_x\text{□}_{x/2}\text{PO}_4$ ($0 \leq x \leq 0.2$ and \square refers to cation vacancy) samples, in which the Mn^{2+} ions are substituted by V^{3+} ions, were obtained by a microwave-assisted solvothermal (MW-ST) synthesis process at 300°C . As seen in Fig. 1, SEM showed rod-like morphology with lengths of 20 to 200 nm for the doped samples. Similar morphology was observed for the undoped sample (not shown). Moreover, a homogenous distribution of Mn, V, and P was observed with energy dispersive spectroscopy (EDS) on the doped samples. The oxidation state of the cations in the doped samples was analyzed with XANES.

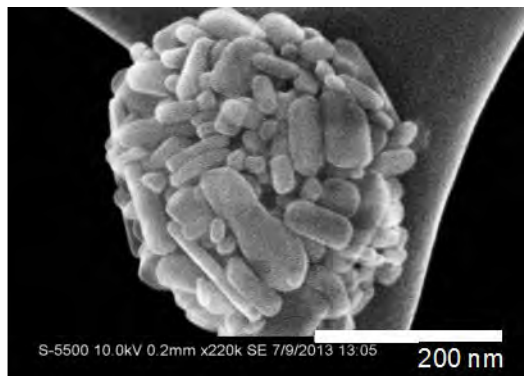


Figure 1. SEM micrograph of the rod-like $\text{LiMn}_{0.7}\text{V}_{0.20}\text{□}_{0.10}\text{PO}_4$ sample.

The Mn oxidation state was found to be $2+$, as expected. Employing LiVOPO_4 and $\text{Li}_3\text{V}_2(\text{PO}_4)_3$ as standards, respectively, for V^{4+} and V^{3+} , the XANES data indicated an oxidation state of near $3+$ for V. Furthermore, the pre-edge feature indicated that the VO_6 octahedra in the V-doped samples is less distorted than in LiVOPO_4 , but more distorted than in $\text{Li}_3\text{V}_2(\text{PO}_4)_3$, which is similar to what was found previously with the V-doped LiFePO_4 .

The typical voltage range for LiMnPO_4 is 3.0 to 4.5 V. However, the electrochemical activity of V could be above or below this voltage range. Therefore, the electrochemical measurements were carried out in the voltage range of 1.5 to 5.0 V. Figure 2 compares the electrochemical charge-discharge profiles of the undoped ($x = 0$) and the V-doped ($x = 0.05$ and 0.20) samples. The first charge/discharge capacity increases as the amount of V increases from 0 to 0.2, demonstrating the influence of V doping. Even with a small amount of V ($x = 0.05$), the first discharge capacity increases drastically from *ca.* 40 to 105 mAh/g. The discharge capacity increases further to 135 mAh/g on increasing the V doping to 0.2, which is *ca.* 80% of the theoretical capacity. It should be noted that the electrochemical data presented in Fig. 2 are without any carbon coating. Although carbon coating is generally needed to extract/insert Li at practical levels from/into LiMnPO_4 due to its poor electronic conductivity, the V-doped samples exhibited high capacity without carbon coating. Moreover, the irreversible capacity loss dropped from *ca.* 20 mAh/g in the undoped ($x = 0$) sample to *ca.* 0 mAh/g in the $x = 0.2$ sample. Preliminary soft XAS data collected at the Advanced Light Source at LBNL indicated an increase in Mn-O covalency with V doping, thereby improving the electrochemical performance. However, the capacity fades on cycling, even when the material is coated with carbon.

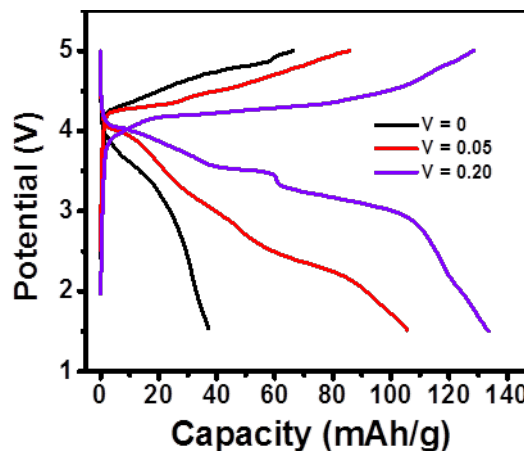


Figure 2. First charge-discharge profiles of the $\text{LiMn}_{1-3x/2}\text{V}_x\text{□}_{x/2}\text{PO}_4$ ($0 \leq x \leq 0.20$) samples, showing the advantage of aliovalent V doping on the electrochemical performance.

The phase stability of the V-doped samples at elevated temperatures was also analyzed by heating the $x = 0.20$ sample to 525, 575, 625, and 725°C and then analyzing by XRD at ambient temperature. While the sample heated to 525°C retained the single-phase character, those heated to 575°C or above indicated the formation of LiVP_2O_7 and/or $\text{Li}_3\text{V}_2(\text{PO}_4)_3$, revealing the metastable nature of the doped samples. Overall, the results demonstrate that LiMnPO_4 can indeed be aliovalently doped to a significant level by low-temperature synthesis.

Development of High Energy Cathode Materials

PROJECT OBJECTIVE: The objective of this project is to develop high-energy, low-cost, and long-life cathode materials. Synthesis of Li-Mn-rich (LMR) layered composite cathodes will be further optimized by using the novel approaches developed at PNNL for high-voltage spinel in FY 2013. The working mechanism of the identified electrolyte additive will be systematically explored to reveal key factors that enable stable cycling of the LMR cathode. Advanced characterization techniques will be combined with electrochemical measurements to understand and mitigate the challenges in the LMR cathode.

PROJECT IMPACT: Although state-of-the-art cathode materials such as LMR-layered composites have very high energy densities, their voltage fade and long-term cycling stability still need further improvement. In this work, the fundamental fading mechanism of LMR cathodes will be investigated and new approaches to reduce the energy loss of these high-energy cathode materials will be developed. The success of this work will increase the energy density of Li-ion batteries and accelerate market acceptance of EVs, especially for PHEVs required by the *EV Everywhere* Grand Challenge proposed by DOE/EERE.

OUT-YEAR GOALS: The long-term goal of the proposed work is to develop Li-ion batteries with a specific energy of >96 Wh/kg (for PHEVs), 5000 deep-discharge cycles, 15-year calendar life, improved abuse tolerance, and less than 20% capacity fade over a 10-year period.

COLLABORATIONS:

- M.S. Whittingham (SUNY Binghamton): characterization of cathode materials
- X.Q. Yang (LBNL): *in situ* XRD characterization during cycling
- K. Zaghbi (Hydro-Québec): material synthesis
- K. Xu (ARL): new electrolyte

Milestones

- 1) Perform preparatory work on stable cycling of 80% capacity retention after 150 cycles high-energy cathode based on $x\text{Li}_2\text{MnO}_3 \cdot (1-x)\text{LiMO}_2$ ($M = \text{Mn, Ni, Co}; 0 \leq x \leq 1$) (Dec. 13). **Complete**
- 2) Obtain stable cycling of 80% capacity retention after 150 cycles from high-energy cathode based on $x\text{Li}_2\text{MnO}_3 \cdot (1-x)\text{LiMO}_2$ ($M = \text{Mn, Ni, Co}; 0 \leq x \leq 1$). (Mar. 14) **Ongoing**
- 3) Identify the fundamental mechanism responsible for electrolyte-additive-induced performance improvement of LMR cathode. (Jun. 14) **Ongoing**
- 4) Demonstrate the effects of elemental doping to improve the cycling stability to >200 cycles. (Sep. 14) **Ongoing**

Progress Report

During FY 2013, a new electrolyte additive, tris (pentafluorophenyl) borane ($(C_6F_5)_3B$, TPFPB), that can effectively stabilize the cycling ability of an LMR cathode was identified. The effects of TPFPB in mitigating the voltage fading of the LMR cathode was further investigated during the first quarter of FY 2014. The proposed working mechanism of TPFPB is described below and illustrated in Fig. 1.

1. As an effective anion receptor, TPFPB captures the intermediate O anions or radicals released during activation of the Li_2MnO_3 component. Without this O-capturing additive, O species released during the charge process (especially during the first charge) should quickly decompose the carbonate-based electrolyte as is reported for Li- O_2 batteries.
2. The increased O solubility in TPFPB prevents direct contact of the O with the carbonate solvents, greatly suppressing the side reactions.
3. Other byproducts, such as Li_2CO_3 and LiF, formed at high voltages also are partially soluble in the presence of TPFPB, thereby reducing the passivation layer on the LMR material.

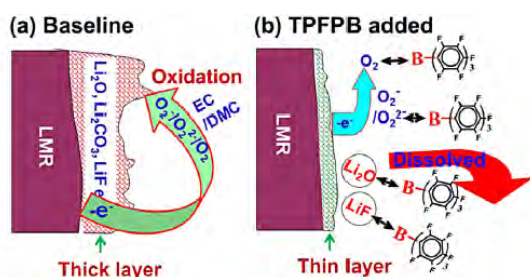


Figure 1. Scheme of the functioning mechanism of TPFPB. (a) Thick passivation layer formation in baseline electrolyte; (b) significantly reduced passivation layer formation in TPFPB added electrolyte.

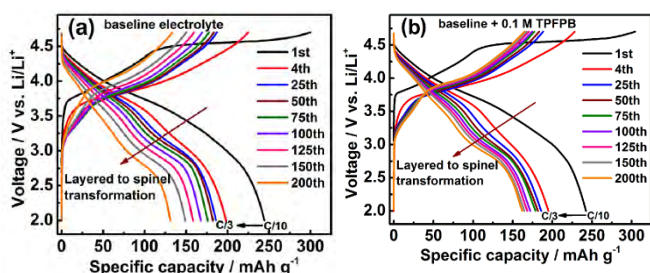


Figure 2. Voltage profiles of cathode material $Li[Li_{0.2}Ni_{0.2}Mn_{0.6}]O_2$ in (a) baseline electrolyte and (b) electrolyte added with 0.1M TPFPB. LMR loading: 3 mg/cm^2 . Testing conditions: 2.0 to 4.7 V at C/3 rate (1C = 250 mA/g).

Figure 2 further compares the charge-discharge curves of the LMR cathode at different cycles in the baseline electrolyte (Fig. 2a) and in the presence of TPFPB (Fig. 2b). Without the additive, the discharge curves show continuous voltage degradation with cycling (Fig. 2a). It is generally believed that the gradual phase transformation of the Li_2MnO_3/MnO_2 component from layered to spinel leads to the voltage fading. Considering the fact that the LMR cathode has to be charged to high voltage (*i.e.*, 4.6 to 4.8 V), the instability of electrolyte at high voltage gets worse by the generation of O_2^{2-} and O_2 from the activation of the Li_2MnO_3 -component during charging. The unavoidable formation of a passivation film covering the cathode rapidly and continuously increases the cell impedance. In the presence of TPFPB (Fig. 2b), the voltage degradation is effectively alleviated because the thickness of the passivation film is reduced, which is consistent with the proposed TPFPB function illustrated in Fig. 1. This additive work also implies that, in addition to the intrinsic layered-to-spinel phase transformation, interfacial reactions also significantly affect electrode polarization, which aggravates the voltage hysteresis and the capacity degradation of LMR cathodes. Table 1 shows that capacity loss of the samples after 300 cycles was reduced from 43% to less than 20% with addition of TPFPB additive. On the other hand, voltage fade was only reduced from *ca.* 11% to *ca.* 9%. Therefore, other approaches are needed to further suppress the voltage of LMR cathode for their long term applications.

Table 1. Capacity and voltage fade after long term cycling

	Baseline Electrolyte	0.1 M TPFPB	0.2 M TPFPB
Capacity fade after 300 cycles	43.0%	19.4%	19.0%
Voltage Fade after 300 cycles	11.2%	9.1%	9.5%

In situ Solvothermal Synthesis of Novel High Capacity Cathodes

PROJECT OBJECTIVE: Develop low-cost cathode materials that offer high energy density (≥ 660 Wh/kg) and electrochemical properties (cycle life, power density, safety) consistent with USABC goals.

PROJECT IMPACT: Present-day Li-ion batteries are incapable of meeting the 40-mile all-electric-range within the weight and volume constraints established for PHEVs by DOE and the USABC. Higher energy density cathodes are needed for Li-ion batteries to be widely commercialized for PHEV applications. This effort will focus on increasing energy density (while maintaining the other performance characteristics of current cathodes) using synthesis methods that have the potential to lower cost. The primary deliverable for this project is a reversible cathode with an energy density of about 660 Wh/kg or higher.

OUT-YEAR GOALS: In FY14, work on Cu-V-O cathodes will be concluded, and efforts will be directed to the synthesis and electrochemical characterization of V-based (fluoro)phosphates. Hydrothermal-based synthesis techniques for preparing ternary and/or quaternary Li-V-PO₄(-X) type cathodes will be explored, either *via* direct chemical reaction or through ion exchange. By the end of FY14, structural and electrochemical characterization of two different types of Cu-V-O compounds will be completed, as well as the preparation of multiple Li-V-PO₄(-X) cathodes. *In situ* x-ray analysis will be used to determine the precursors and reaction conditions for optimal synthesis procedures. Electrochemical testing, along with material characterization (*in situ* and *ex situ*), will be used to identify Li-reaction mechanisms and limitations to cycling stability of synthesized cathodes.

COLLABORATIONS: Arumugam Manthiram (U. Texas at Austin), Brett Lucht (U. Rhode Island), Jordi Cabana (U. Illinois at Chicago), Zaghbir Karim (Hydro-Quebec), Jason Graetz (HRL), Peter Khalifah (Stony Brook U.), Kirsuk Kang (Seoul Nat. U., Korea), Jianming Bai, Lijun Wu, and Yimei Zhu (BNL).

Milestones

- 1) Complete the structural and electrochemical characterization of ϵ -Cu_xV₂O₅ cathodes. (Dec. 13) **Complete**
- 2) Develop synthesis procedures to prepare Li-V-PO₄ cathodes. (Mar. 14) **Ongoing**
- 3) Optimize the synthesis and characterize the structural and electrochemical properties of 2nd class of Cu-V-O cathode. (Jun. 14) **Ongoing**
- 4) Develop synthesis procedures to prepare Li-V-PO₄-X cathodes, and electrochemically characterize at least one Li-V-PO₄-X compound. (Sep. 14) **Ongoing**

Progress Report

In FY13, significant progress was made in preparing and evaluating ϵ - $\text{Cu}_x\text{V}_2\text{O}_5$ (ϵ -CVO) cathodes. In particular, an optimal procedure was established for synthesis of high-quality ϵ -CVO electrodes that can deliver high capacity (*ca.* 300 mAh/g) and reasonable cycling reversibility. In this quarter, advanced TEM and synchrotron X-ray techniques were applied to study the correlation between structural ordering (both *short-range* and *long-range*) and electrochemical behavior of ϵ -CVO cathodes, aiming to understand the structural origin of the electrochemical cycling reversibility in this material.

In addition to bulk analysis using synchrotron XRD, detailed TEM studies were conducted on individual ϵ -CVO nanorods *via* high-resolution imaging and electron diffraction, along with simulations. Representative results are given in Fig. 1. The consistency between the TEM and XRD measurements is good, and show that the as-synthesized material has a monoclinic structure (C2/m), but the local ordering is much different from the ϵ - $\text{Cu}_{0.95}\text{V}_2\text{O}_5$ phase, most likely due to Cu-deficiency in ϵ - $\text{Cu}_x\text{V}_2\text{O}_5$. TEM studies were also performed on cycled electrodes, showing that a new ordered structure is formed after the 1st cycle, and remains invariant with subsequent cycling.

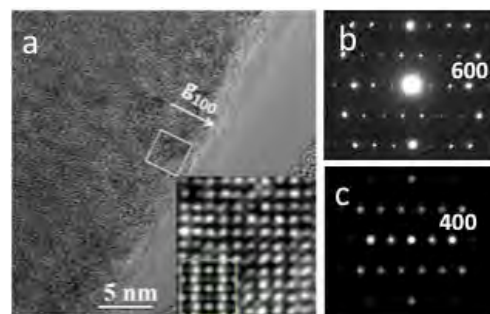


Figure 1. Studies of local structural ordering of ϵ -CVO, by (a) high-resolution TEM imaging (inset: comparison to simulation), and (b, c) electron diffraction compared with simulation (Ref.: Rozier, *et al.*, *J. Solid State Chem.* **182**, 1481, 2009).

Galvanostatic Intermittent Titration Technique (GITT) and *in situ* XAS studies on ϵ -CVO electrodes were used to identify Cu/V redox reactions and local structural evolution during the 1st two cycles. As illustrated in Fig. 2a, there is a clear separation of Cu and V reduction reactions in the 1st discharge, but they become largely overlapped (shaded region) in the 2nd discharge, which is consistent with the observation of a simultaneous shift of Cu and V K-edges in the XANES measurements. At the same time, the reaction kinetics of Cu reduction are significantly improved compared to that during the 1st discharge. This implies that the *long-range order* of ϵ -CVO was changed during the 1st lithiation/delithiation, while the *local structural ordering* is reversible, as shown by EXAFS studies (Fig. 2b). For example, VO_6 octahedra are recovered after one cycle (despite slight increase in symmetry), and the coordination of V in the lithiated electrodes after 1st discharge is nearly identical to that after the 2nd discharge.

The detailed structural analysis provides direct experimental evidence on the abrupt change in the long-range ordering while stabilized short-range ordering during initial lithiation and delithiation, and in concert with electrochemical studies, explains the origin of the cycling reversibility found in ϵ -CVO.

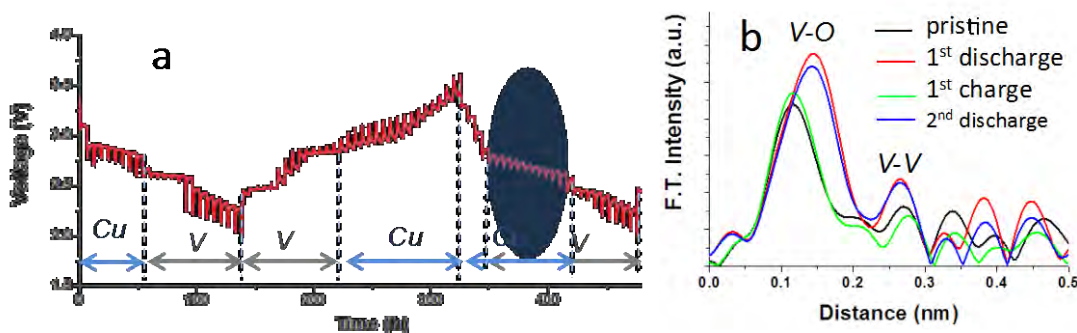


Figure 2. Li reaction pathways and reversibility of ϵ -CVO cathode, *via* (a) GITT and (b) V K-edge EXAFS.

Lithium-bearing Mixed Polyanion (LBMP) Glasses as Cathode Materials

PROJECT OBJECTIVE: Develop mixed polyanion glasses as potential cathode materials for Li-ion batteries with superior performance to lithium iron phosphate for use in EV applications. Modify compositions of mixed polyanion glasses to provide higher electrical conductivities, specific capacities, and specific energies than similar crystalline polyanionic materials. Test mixed polyanion glasses in coin cells for electrochemical performance and cycleability. The final goal is to develop mixed polyanion glass compositions for cathodes with specific energies up to near 1,000 Wh/kg.

PROJECT IMPACT: The projected performance of glass cathode materials addresses the Vehicle Technology Multi-Year Plan goals of higher energy densities, excellent cycle life, and low cost. Mixed polyanion glasses offer the potential of exceptional cathode energy density up to 1,000 Wh/kg, excellent cycle life from a rigid polyanionic framework, and low cost conventional glass processing.

OUT-YEAR GOALS: The composition of successful mixed polyanion glasses with multivalent transitions will be used as the basis to model, produce, and electrochemically test glasses from multiple polyanion systems (*e.g.*, phosphates, borates, silicates), polyanion substitutions (*e.g.*, vanadate, molybdate), and transition metal contents. The electrochemical performance of these compositionally varied glasses will be used to develop optimized glass compositions to obtain maximum specific energy within a desirable voltage window. Cathode processing of the most promising mixed polyanion glasses will be refined to obtain desired cycling and rate performance. Complex mixed polyanion glasses will be modeled, and those glasses with excellent predicted properties will be produced and tested. In-depth electrochemical testing will be performed on the most successful mixed polyanion glasses. The predicted and experimentally verified electrochemical performances from computational thermodynamic models for different glass systems will be used to develop a summary perspective on the design of mixed polyanion glasses for use as cathodes.

COLLABORATIONS: Worked with Kyler Carroll from MIT to perform XAS analysis of glass cathodes using the National Synchrotron Light Source at BNL.

Milestones

- 1) Synthesize, characterize, and perform electrochemical testing on a mixed polyanion glass that is theoretically capable of a multi-valent transition. (Dec. 13) **Complete**
- 2) Demonstrate the effect of submicron particle size on the electrochemical performance of mixed polyanion glass cathodes. (Mar. 14) **Ongoing - powders prepared; experiments in progress.**
- 3) Measure the electrical conductivities of a series of mixed polyanion glasses as a function of polyanionic substitution. (Jun. 14) **Ongoing**
- 4) Synthesize, characterize, and perform electrical testing on at least four different glass cathode compositions with theoretical specific energies exceeding lithium iron phosphate. (Sep. 14) **Ongoing - completed 2 out of 4 glass cathode materials.**

Progress Report

Dr. Kyler Carroll from MIT worked with the project team at the National Synchrotron Light Source at BNL to perform *ex situ* XAS experiments on glass cathodes. XAS was used to track the transition-metal valence changes which occurred during the charge and discharge of iron pyrophosphate glass ($\text{Fe}_4(\text{P}_2\text{O}_7)_3$) and iron pyrophosphate pyrovanadate glass ($\text{Fe}_4(0.5 \text{P}_2\text{O}_7 \cdot 0.5 \text{V}_2\text{O}_7)_3$). Iron glass cathodes have demonstrated two electrochemical reactions: an intercalation reaction and a high capacity 2nd reaction. XAS analysis showed that the Li intercalation into $\text{Fe}_4(0.5 \text{P}_2\text{O}_7 \cdot 0.5 \text{V}_2\text{O}_7)_3$ involved primarily an Fe valence change (Fe^{3+} to Fe^{2+}), but a V valence change did occur also to a limited extent. The 2nd reaction was identified as an Fe-based conversion reaction (Fig. 1) with no noticeable changes in V valence. XRD data of charged and discharged $\text{Fe}_4(0.5 \text{P}_2\text{O}_7 \cdot 0.5 \text{V}_2\text{O}_7)_3$ cathodes was consistent with the formation of Fe nanoparticles during the 2nd reaction, which agreed with conclusions from XAS analysis. A conversion reaction does not occur with crystalline phosphate materials; therefore, the identification of glass-state conversion reactions opens up new options for producing high-capacity glass cathodes.

Lithium copper phosphate vanadate glass ($\text{LiCu}(0.5 \text{PO}_3 \cdot 0.5 \text{VO}_3)_3$) was successfully produced using both splat quenching and graphite mold casting. Cathodes of $\text{LiCu}(0.5 \text{PO}_3 \cdot 0.5 \text{VO}_3)_3$ were electrochemically tested. This glass did not demonstrate multivalent intercalation as hoped (Cu^{3+} to Cu^{1+}). However, the glass did undergo a reversible glass-state conversion reaction with high capacity (Fig. 2). The glass-state conversion discharge reaction in $\text{LiCu}(0.5 \text{PO}_3 \cdot 0.5 \text{VO}_3)_3$ occurs a full volt higher than previously studied in iron phosphate vanadate glass. Currently, the project modeling effort is working to predict the voltages of the glass-state conversion reactions for different candidate glasses in order to obtain high-voltage glass cathodes.

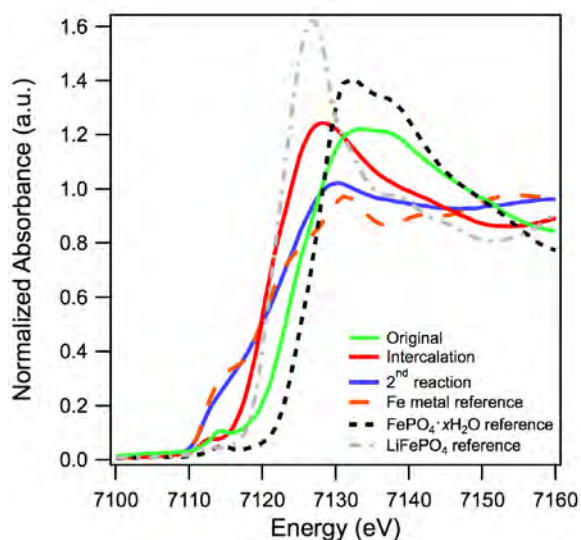


Figure 1. X-ray absorption spectroscopy analysis of $\text{Fe}_4(0.5 \text{P}_2\text{O}_7 \cdot 0.5 \text{V}_2\text{O}_7)_3$ glass cathodes showed how Fe changes from Fe^{2+} to Fe metal during the 2nd reaction (as-produced glass in green, full intercalated glass in red, glass with completed 2nd reaction in blue).

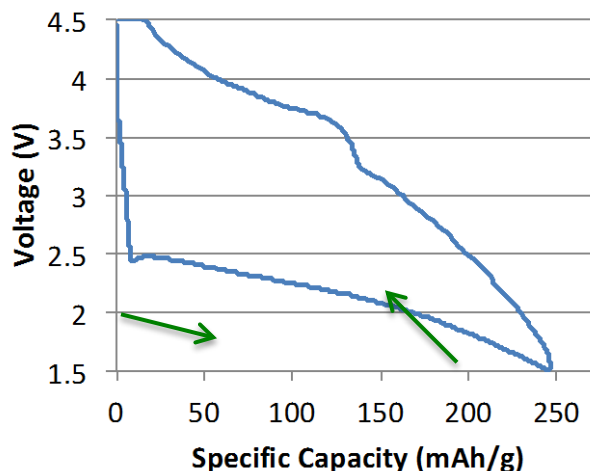


Figure 2. Discharge and charge curve for $\text{LiCu}(0.5 \text{PO}_3 \cdot 0.5 \text{VO}_3)_3$ cathodes at 12 mA/g. A high capacity glass-state conversion reaction occurs at 2.5V.

Lithium Batteries of Higher Capacity and Voltage

PROJECT OBJECTIVE: To develop a solid Li^+ electrolyte that (1) can block dendrites from a Li^0 anode, (2) has a Li^+ conductivity $\sigma_{\text{Li}} > 10^{-4} \text{ S cm}^{-1}$, (3) is stable in different liquid electrolytes at anode and cathode, (4) has a low impedance for Li^+ transfer across a solid/liquid electrolyte interface, (5) is capable of low-cost fabrication as a thin, mechanically robust film.

PROJECT IMPACT: A solid Li^+ -electrolyte separator would permit use of a Li^0 anode, thus maximizing energy density for a given cathode, and liquid flow-through and air cathodes of high capacity as well as high-voltage solid cathodes given two liquid electrolytes having different windows.

OUT-YEAR-GOALS: Prepare an oxide/polymer composite Li^+ electrolyte having a $\sigma_{\text{Li}} > 10^{-4} \text{ S cm}^{-1}$ that can be fabricated at low cost as a mechanically robust membrane and can demonstrate a viable performance of a test cell with a Li^0 anode and a variety of solid, liquid, and air cathodes. Prepare dense garnet membranes with $\sigma_{\text{Li}} \approx 5 \times 10^{-4} \text{ S cm}^{-1}$ that have a reduced impedance for Li^+ transfer across the oxide interface with a liquid electrolyte.

COLLABORATIONS: Li/S cell with A. Manthiram, UT Austin, and membrane characterization with K. Zaghib, Hydro-Québec.

Milestones

- 1) Go-No/Go: Polymer composite membrane project will stop if demonstration of a liquid cathode without crossover of the redox molecule and blocking of Li dendrites with a PEO/ Al_2O_3 membrane fails. Criteria: Suppression of drying of anolyte with an Al_2O_3 /PEO membrane. Elimination of redox-molecule crossover to anolyte. Demonstration that Li dendrites are blocked. (Dec. 13) **Complete**
- 2) Determine TEM garnet surface structure in contact with a liquid electrolyte. Design of a surface coat of a garnet membrane to minimize impedance of Li^+ transfer across garnet surface. (Mar. 14) **Ongoing**
- 3) Prepare dense garnet membrane with surface coatings to test impedance of Li^+ transfer across garnet interface. (Jun. 14) **Ongoing**
- 4) Construct and test a Li/S cell with a solid Li^+ -electrolyte separator. (Sep. 14) **Ongoing**

Progress Report

A critical safety issue is whether a $\text{Al}_2\text{O}_3/\text{PEO}$ membrane can block dendrite penetration from an alkali anode during cycling. A symmetric $\text{Li}|\text{Al}_2\text{O}_3/\text{PEO}|\text{Li}$ cell was galvanostatically charged to generate extensive Li dendrites on one side of the membrane. The dendrites dented the membrane surface (Fig. 1a), but did not penetrate the membrane. This result was further confirmed by an electrochemical-cell test in a Na cell, which provided a severe dendrite condition.

Since the membrane also transports Na^+ , a charged half-cell with a Na anode and a cathode of a transition-metal cyanide ($\text{Na}_2\text{MnFe}(\text{CN})_6$ and $\text{Fe}_2(\text{CN})_6$) were prepared (Fig. 1b). In a conventional half-cell with a porous glass-fiber separator, dendrites from the Na anode penetrate the separator to short-circuit the cell after a relatively few cycles. The $\text{Al}_2\text{O}_3/\text{PEO}$ membrane is seen to improve significantly the cycle performance. Even after 400 cycles, there was no capacity fade with $\text{Fe}_2(\text{CN})_6$ as cathode. The initial capacity at 2C is 75.3 mAh g^{-1} and the 400th capacity is 75.6 mAh g^{-1} with the $\text{Al}_2\text{O}_3/\text{PEO}$ membrane, whereas with the glass-fiber separator, it drops from 71.3 to 21.8 mAh g^{-1} .

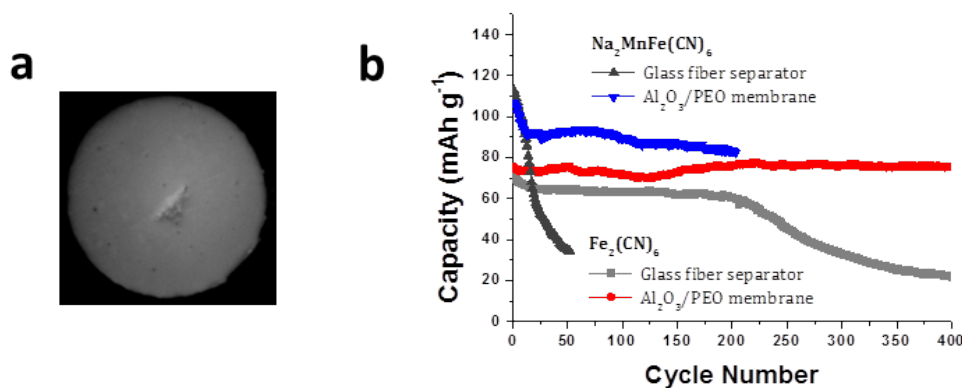


Figure 1. (a) Surface morphology of the $\text{Al}_2\text{O}_3/\text{PEO}$ membrane after contact with electrochemically grown Li dendrites. (b) Charge/discharge performances of $\text{Na}_2\text{MnFe}(\text{CN})_6$ and $\text{Fe}_2(\text{CN})_6$ with a glass fiber separator and the $\text{Al}_2\text{O}_3/\text{PEO}$ membrane soaked with 1 M NaClO_4 in EC/DEC (1/1) liquid electrolyte.

A hybrid redox-flow battery has been tested with the $\text{Al}_2\text{O}_3/\text{PEO}$ membrane and 6-bromohexyl ferrocene as the catholyte redox molecule. To block crossover of the redox molecule and osmosis across the membrane owing to the concentration gradient, two strategies were adopted to solve these problems: (1) large spectator molecules such as poly(ethylene glycol) dimethyl ether were introduced into the anolyte to balance the concentrations in the anolyte and catholyte; (2) a thin film of a mixed electronic/ Li^+ conductor was added to the cathode side of the $\text{Al}_2\text{O}_3/\text{PEO}$ membrane to block the catholyte molecule from crossing the membrane. A conducting polymer, poly(3,4-ethylene dioxythiophene):poly(styrene sulfonate) (PEDOT:PSS), was coated on the PP separator by spin coating. A defect-free PEDOT:PSS film was introduced on the cathode side of the $\text{Al}_2\text{O}_3/\text{PEO}$ membrane, and the cell was discharged/charged galvanostatically. The conducting polymer thin film is seen to block crossover of the 6-bromohexyl ferrocene molecule from the catholyte to provide a stable cycle life without capacity fade for 50 charge/discharge cycles. After cycling, the cell was disassembled and the $\text{Al}_2\text{O}_3/\text{PEO}$ membrane cross sectioned to see whether there was any color change owing to crossover of the redox molecule. The membrane cross section remained white, which suggests no crossover of the ferrocene molecule.

Interfacial Processes

PROJECT OBJECTIVE: The main objective of this task is to obtain detailed insight into the dynamic behavior of molecules, atoms, and electrons at electrode/electrolyte interfaces of intermetallic anodes (Si) and high-voltage Ni/Mn-based materials at a spatial resolution that corresponds to the size of basic chemical or structural building blocks. The aim of these studies is to unveil the structure and reactivity at hidden or buried interfaces and interphases that determine battery performance and failure modes. To accomplish these goals novel far- and near-field optical multifunctional probes must be developed and deployed *in situ*. The proposed work constitutes an integral part of the concerted effort within the BATT Program and it attempts to establish clear connections between diagnostics, theory/modelling, materials synthesis, and cell development efforts.

PROJECT IMPACT: This project provides a better understanding of the underlying principles that govern the function and operation of battery materials, interfaces and interphases, which is inextricably linked with successful implementation of high energy density materials such as Si and high-voltage cathodes in Li-ion cells for PHEVs and EVs. This task also involves the development and application of novel innovative experimental methodologies to study and understand the basic function and mechanism of operation of materials, composite electrodes, and Li-ion battery systems for PHEV and EV applications.

OUT-YEAR GOALS: Design and employ novel and sophisticated *in situ* analytical methods to address the key problems of the BATT baseline chemistries. The proposed experimental strategies combine imaging with spectroscopy aimed at probing electrodes at an atom, molecular, or nanoparticulate level to unveil structure and reactivity at hidden or buried interfaces and determine electrode performance and failure modes in baseline LixSi-anodes and high-voltage LMNO cathodes. The main goal is to gain insight into the mechanism of surface phenomena on thin-film and monocrystal Sn and Si intermetallic anodes and evaluate their impact on the electrode long-term electrochemical behavior. Comprehensive fundamental study of the early stages of SEI layer formation on polycrystalline and single crystal face Sn and Si electrodes will be carried out. *In situ* and *ex situ* far- and near-field scanning probe spectroscopy will be employed to detect and monitor surface phenomena at the intermetallic anodes high-voltage (>4.3V) model and composite cathodes.

COLLABORATIONS: Vince Battaglia (LBNL), Chunmei Ban (NREL), Guoying Chen (LBNL)

Milestones

- 1) Determine the origin of fluorescent species that are produced at high-energy Li-ion cathodes. (Dec. 13) **Complete**
- 2) Resolve SEI-layer chemistry of Si-model single-crystal anodes -collaboration with the BATT Anode Group. (Mar. 14) **Ongoing**
- 3) Characterize interfacial phenomena in high-voltage composite cathodes - collaboration with the BATT Cathode Group. (Jun. 14) **Ongoing**
- 4) Go/No-Go: Stop development of *in situ* near-field techniques, if the preliminary experiments fail to deliver adequate surface-bulk selectivity. Criteria: Demonstrate feasibility of *in situ* near-field techniques to study interfacial phenomena at Li-battery electrodes. (Sep. 14) **Ongoing**

Progress Report

In the first quarter of FY2014 the effect of Ni and Mn dissolution and migration from $\text{LiNi}_{0.5}\text{Mn}_{1.5}\text{O}_4$ cathode toward the graphite anode and the mechanism of their interaction with the SEI layer was studied. The nature and distribution of Ni and Mn species incorporated in the SEI layer at the graphite anode were probed using optical fluorescence microscopy and XAS.

Fluorescence spectroscopy measurements were carried out both *in situ* on binder- and carbon additive-free $\text{LiNi}_{0.5}\text{Mn}_{1.5}\text{O}_4$ and LiMn_2O_4 spinel electrodes and *ex situ* on graphite electrodes from a cell that was cycled 625 times against $\text{LiNi}_{0.5}\text{Mn}_{1.5}\text{O}_4$ composite electrodes. While the electrochemical data of the LiMn_2O_4 electrode did not reveal significant fluorescence rise despite reversible redox of Mn(IV)/(III), as mentioned in the previous report, the $\text{LiNi}_{0.5}\text{Mn}_{1.5}\text{O}_4$ electrode exhibited a strong fluorescence signal rise correlated with the Ni electro-catalytic activity. Interestingly, *ex situ* fluorescence measurement performed on pristine electrodes is free of fluorescence, whereas graphite and $\text{LiNi}_{0.5}\text{Mn}_{1.5}\text{O}_4$ cycled electrodes exhibit non-uniform fluorescence patterns. A plausible explanation of the observed fluorescence must involve formation of fluorescent organometallic compounds by reaction between Ni-metal ions and the electrolyte decomposition products. As the concentration of the metal-ion centers increases, the fluorescence intensity rises.

In this case, Mn metal ions do not form fluorescent species, XANES measurements were carried out on the cycled graphite to analyze the oxidation state and local bonding of Ni and Mn in the SEI layer. The normalized XANES spectra for five different locations are very similar which indicates that the chemical state and structure of the Ni or Mn species are identical throughout the whole measurement area. A direct comparison of the Ni/Mn K-edge transmission XANES spectra with reference spectra indicates that (II) is the dominant valence state of Ni and Mn in the SEI layer and that their molecular environments are very similar to that of metal oxalate as opposed to $\text{LiNi}_{0.5}\text{Mn}_{1.5}\text{O}_4$ (Fig. 1).

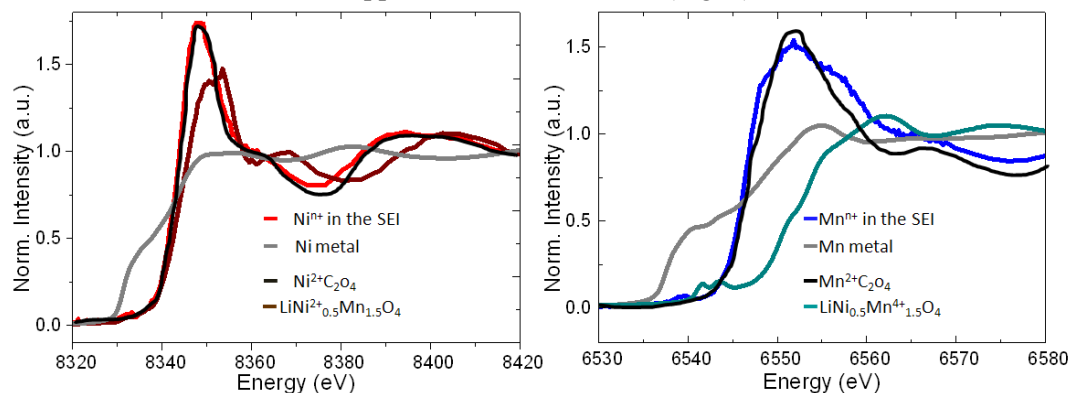


Figure 1. Normalized Ni and Mn K-edge transmission XANES spectra of the cycled graphite electrode compared with references.

These results support the general idea of Ni and Mn dissolution from $\text{LiNi}_{0.5}\text{Mn}_{1.5}\text{O}_4$ and their transport across the electrolyte toward the anode. However, the observed fluorescence suggests that Mn and Ni do not diffuse/migrate as free Mn(II) and Ni(II) ions, which are then incorporated into the SEI layer through the ion-exchange mechanism with mobile Li^+ .

This preliminary data provide a more consistent picture of the chemical-cross-talk between the cathode and anode in Li-ion cells and of the mechanisms of these side reactions and their impact on the Li-ion cell's electrochemical performance. Further investigations concerning the identification of the fluorescence compounds in Li-ion systems are underway (milestone 3), as well as the determination of the influence of electrolyte composition and Si crystal orientation on SEI formation and their impact on the Li-ion system's long-term stability (milestone 2).

Advanced *In situ* Diagnostic Techniques for Battery Materials

PROJECT OBJECTIVE: The primary objective of this proposed project is to develop new advanced *in situ* material characterization techniques and to apply these techniques to support the development of new cathode and anode materials for the next generation of Li-ion batteries (LIBs) for PHEVs. In order to meet the challenges of powering the PHEV, LIBs with high energy and power density, low cost, good abuse tolerance, and long calendar and cycle life must be developed.

PROJECT IMPACT: In the Multi Year Program Plan (MYPP) of Vehicle Technology Program (VTP), the goals for battery were described as: “Specifically, lower-cost, abuse-tolerant batteries with higher energy density, higher power, better low-temperature operation, and longer lifetimes are needed for the development of the next-generation of HEVs, PHEVs, and EVs.” If this project is successfully carried out, the knowledge learned from diagnostic studies and collaborations with US industries and international research institutions through this project will help US industries to develop new materials and processes for new generation of Li-ion batteries in their efforts to reach these VTP goals.

OUT-YEAR GOALS: For the Si-based anode materials, the capacity fading, which is caused by the pulverization of the Si particles during cycling, needs to be resolved. In order to overcome these barriers, fundamental understanding of the physical and chemical changes of the cathode and anode materials in the bulk and at the surface are critical. This project will focus on applying integrated advanced *in situ* diagnostic characterization techniques to investigate these issues, through collaborative efforts with synthesis groups and industrial end users.

COLLABORATIONS: The BNL team will work closely with material synthesis groups at ANL (Drs. Thackeray and Amine) for the high-energy composite; at UT Austin (Prof. Manthiram) for the high-voltage spinel; and at PNNL (Drs. Liu and Zhang) for the Si-based anode materials. Such interaction between the diagnostic team at BNL and synthesis groups of these other BATT members will catalyze innovative design and synthesis of advanced cathode and anode materials. The team will also collaborate with industrial partners at General Motors (Dr. Wu), Duracell (Dr. Bae), and Johnson Controls (Drs. Cho and Bonhomme) to obtain feedback information as battery end users.

Milestones

- 1) Complete the studies of the kinetic properties of $\text{Li}_{1.2}\text{Ni}_{0.15}\text{Co}_{0.1}\text{Mn}_{0.55}\text{O}_2$ [$0.5\text{Li}(\text{Ni}_{0.375}\text{Co}_{0.25}\text{Mn}_{0.375})\text{O}_2 \bullet 0.5\text{Li}_2\text{MnO}_3$] high energy density cathode materials during constant current charge using XAS. (Dec. 13) **Complete**
- 2) Complete the development of using quick XAS technique to study the kinetic properties of $\text{Li}_{1.2}\text{Ni}_{0.15}\text{Co}_{0.1}\text{Mn}_{0.55}\text{O}_2$ [$0.5\text{Li}(\text{Ni}_{0.375}\text{Co}_{0.25}\text{Mn}_{0.375})\text{O}_2 \bullet 0.5\text{Li}_2\text{MnO}_3$] high energy density cathode materials during constant voltage charge. (Mar. 14) **Ongoing**
- 3) Complete the *in situ* XRD studies of Fe-substituted high voltage spinel during charge-discharge cycling. (Jun. 14) **Ongoing**
- 4) Complete the *in situ* XAS studies of Fe-substituted high voltage spinel during charge-discharge cycling. (Sep. 14) **Ongoing**

Progress Report

In the first quarter of FY2014, progress toward our milestones was made. BNL focused on studying the rate-capability-related structural changes of high energy density $\text{Li}_{1.2}\text{Ni}_{0.15}\text{Co}_{0.1}\text{Mn}_{0.55}\text{O}_2$ cathode materials with layered structures during constant current cycling using synchrotron-based XAS, milestone (a).

To elucidate the changes of the electronic transitions and local structure of the Li-rich layered $\text{Li}_{1.2}\text{Ni}_{0.15}\text{Co}_{0.1}\text{Mn}_{0.55}\text{O}_2$ material, *in situ* XAS spectra at Mn, Co, and Ni K-edges were collected during the first cycle and second charge under a constant current of 21 mA g^{-1} . Figure 1a shows the 1st-charge curve of the $\text{Li}_{1.2}\text{Ni}_{0.15}\text{Co}_{0.1}\text{Mn}_{0.55}\text{O}_2/\text{Li}$ cell during *in situ* XAS experiments. The selected scan numbers of the corresponding XAS spectra are marked on the charge curve. The normalized Mn, Co and Ni K-edge XANES spectra of $\text{Li}_{1.2}\text{Ni}_{0.15}\text{Co}_{0.1}\text{Mn}_{0.55}\text{O}_2$ electrode during charge are shown in Fig. 1b. In general, the threshold energy position of the K-edge XANES spectra of transition metals in oxides is sensitive to their oxidation states while the shape of the peaks is sensitive to the local structural environment of the absorbing element. The K-edge XANES spectra for Ni shown in Fig. 1b exhibit the entire rigid edge shift towards higher energy continuously until the charging voltage reached 4.4V (scan 6, marked by dash line), indicating the oxidation of the Ni^{2+} to close to Ni^{4+} in this charging region. Upon further charging up to the voltage plateau, only slight change of the XANES profile can be observed in comparison to the 4.4 V charged state, with no further change of the K-edge energy position, which indicates very little further oxidation of Ni in this voltage range. The interpretation of Mn and Co K-edge spectra changes in this system is much more complicated. For Mn, the shape of the XANES spectra continuously changes during charge, but the inflection point of the K-edge spectra stays at an almost constant value of approximately 6556 eV throughout the whole charging process, implying that the oxidation state of Mn may remain close to Mn^{4+} throughout the charging process. These feature variations of the Mn K-edge at various states of charge are similar to those of conventional layer-structured materials. All of the XANES shape changes at the Mn K-edge are mainly caused by the variation of local structure during Li deintercalation. Similar to the Mn XANES feature, the shape of the Co K-edge spectra continuously changes but the energy position of the absorption edge basically does not shift at all. Previous work has proposed that the charge compensation for the Li deintercalation process in a similar cathode system could be achieved mainly at both oxygen and cobalt sites simultaneously. Figure 1c presents the Fourier transformed (FT) EXAFS spectra of Mn, Co, and Ni collected *in situ* during initial charging. The first peak corresponds to the metal-oxygen interaction and the second peak is related to the metal-metal interaction, as labeled in each spectrum. The most significant changes in intensity are observed at the first peak of the metal-oxygen bonding for all Mn, Co, and Ni during initial charge. A closer inspection reveals that the Ni-O and Co-O peaks completed most of their intensity changes when the voltage reached 4.4V. After that, during further charging through the voltage plateau region, they only exhibit slight changes. In contrast, the Mn-O peak continues its intensity changes in the voltage plateau above 4.4V all the way to the end of charge at 4.8V. This suggests that in the voltage slope region (3 to 4.4V), the delithiation reaction is mostly related to the oxidation of Ni and Co, while in the voltage plateau region, it is mostly related to the Mn sites during initial charge.

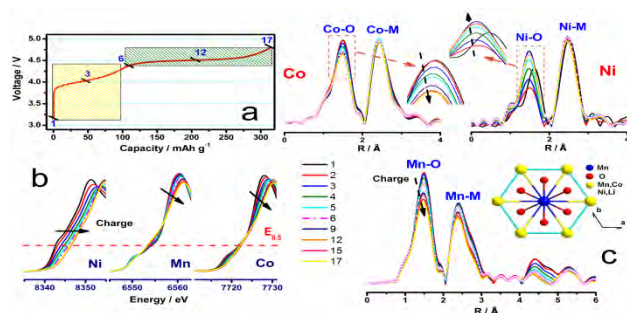


Figure 1. (a) The first charging curve of $\text{Li}_{1.2}\text{Ni}_{0.15}\text{Co}_{0.1}\text{Mn}_{0.55}\text{O}_2$ during *in situ* XAS experiment (under constant current), selected XAS scan numbers are marked on the charge curves; (b) Normalized XANES spectra and (c) Magnitude of Fourier transformed Mn, Co and Ni K-edge spectra collected during initial charge. Inset is the schematic view of the coordination environment around transition metal ions.

NMR and Pulse Field Gradient Studies of SEI and Electrode Structure

PROJECT OBJECTIVE: The formation of a stable SEI is critical to the long-term performance of a battery, since the continued growth of the SEI on cycling/aging results in capacity fade (due to Li consumption) and reduced rate performance due to increased interfacial resistance. Although arguably a (largely) solved problem with graphitic anodes/lower voltage cathodes, this is not the case for newer, much higher capacity anodes such as Si, which suffer from large volume expansions on lithiation, and for cathodes operating above 4.3 V. Thus it is essential to identify how to design a stable SEI. The objectives are to identify major SEI components, their spatial proximity, and how they change with cycling. SEI formation on Si vs. graphite and high voltage cathodes will be contrasted. Li^+ diffusivity in particles and composite electrodes will be correlated with rate. The SEI study will be complemented by investigations of local structural changes of high voltage/high capacity electrodes on cycling.

PROJECT IMPACT: The first impact of this project will be an improved, molecular based understanding of the surface passivation (SEI) layers that form on electrode materials, which are critical to the operation of the battery. Second, direct evidence will be provided for how additives to the electrolyte modify the SEI. Third, also provided will be insight to guide and optimize the design of more stable SEIs on electrodes beyond LiCoO_2 /graphite.

OUT-YEAR GOALS: The goals of this project are to identify the major components of the SEI as a function of state of charge and cycle number different forms of silicon. This includes determining how the surface oxide coating affects the SEI structure, establishing how the SEI on Si differs from that on graphite and high-voltage cathodes, determining how the additives that have been shown to improve SEI stability affect the SEI structure, and exploring the effect of different additives that react directly with exposed fresh Si surfaces on SEI structure. Via this program, new NMR-based methods will be developed for identifying different components in the SEI and their spatial proximities within the SEI, which will be broadly applicable to the study of SEI formation on a much wider range of electrodes. These studies will be complemented by studies of electrode bulk and surface structure to develop a fuller model with which to describe how these electrodes function.

COLLABORATIONS: Brett Lucht, Rhode Island, Kristin Persson, LBNL, Jordi Cabana, UICC, Stan Whittingham, Binghamton, Shirley Meng, UCSD, Stephan Hoffman, Cambridge

Milestones

- 1) Identify major components (LiF , phosphates, carbonates and organics) in Si SEI by NMR methods. (Dec. 13). **Complete**
- 2) Correlate presence of SEI components with cycle number and depth of discharge of Si. Complete preliminary TOF-SIMS measurements to establish viability of approach. (Mar. 14) **Ongoing**
- 3) Identify SEI components in the presence of FEC and VC in Si and determine how they differ from those present in the absence of additives. (Jun. 14) **Study not yet initiated.**
- 4) Go/No-Go: Stop Li^+ PFG diffusivity measurements of electrodes. Criteria: If experiments do not yield correlation with electrochemical performance. (Sep. 14) **PFG studies initiated.**

Progress Report

A new approach for performing *in situ* NMR of Si nanowires has been developed, which allows for an *in situ* study of the whole electrode structure over multiple charge-discharges. Si nanowires grown *via* CVD methods were used (as shown by Chan, C. K. *et al.* “High-performance lithium battery anodes using silicon nanowires” *Nat Nanotechnol.* 3, 31-35, (2008)), but instead of growing the Si wires on stainless steel, the typical support, they were grown on commercially-available carbon supports, providing an extremely effective, binder-free model system for *in situ* NMR studies (Fig. 1).

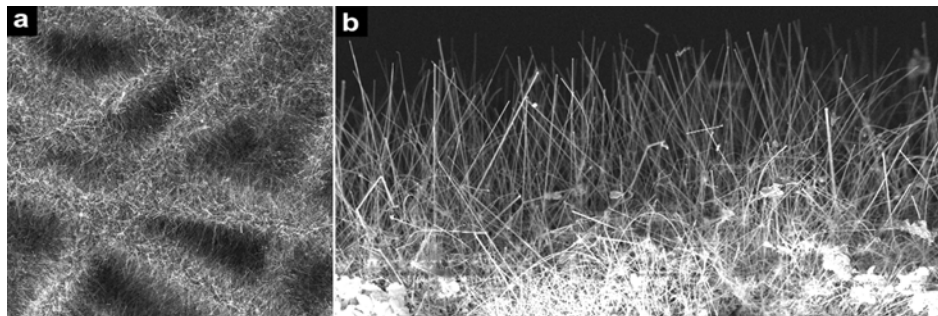


Figure 1. Approx. 60 nm Si wires grown on a carbon fiber support.

The method allows for studies of the wires beyond the 1st cycle (required to convert the crystalline Si into an amorphous phase), which was not possible in earlier studies (in part due to problems associated with maintaining electrical contact between the Si particles and the current collector within the earlier *in situ* NMR design). The approach has been used to-date to identify the previously unobserved electrochemical signature associated with the over-lithiation of *c*-Li_{3.75}Si below 50 mV and investigate the origin of the large hysteresis seen on charging a fully discharged electrode. Spectra of sufficient quality are obtained with only *ca.* 0.5 mg of Si allowing key electrochemical signatures to be mapped onto distinct structural changes. Specifically, by performing NMR studies under SPECS (stepped potential electrochemical spectroscopy) (Fig. 2) it was identified structurally how the Si local environments are affected by the mode of cycling. The method also provides a robust method for studying the SEI and the effect of different additives on SEI growth, which is currently being pursued.

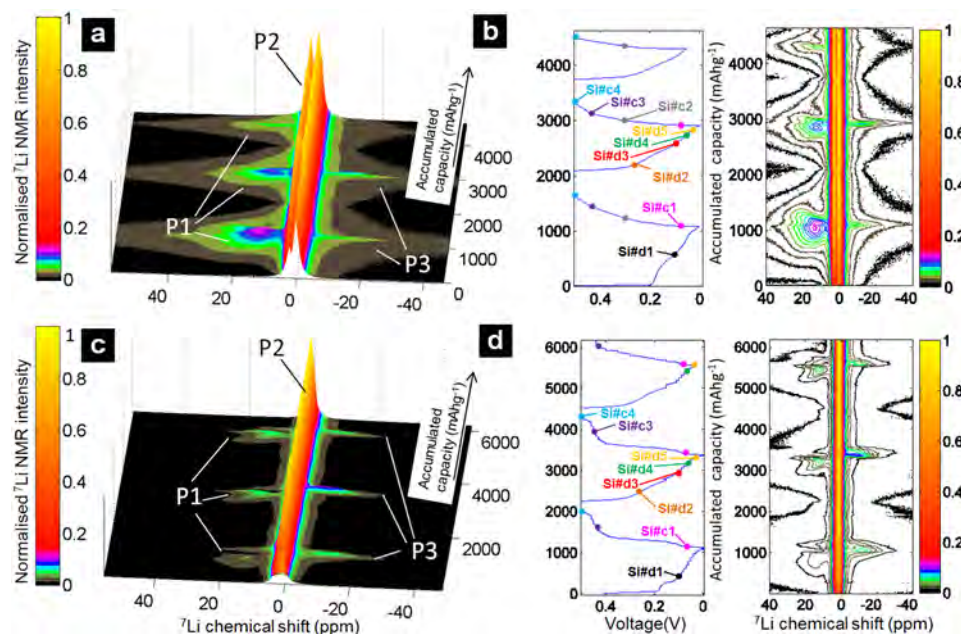


Figure 2. Galvanostatic (a, b) and SPECS with 50 mV steps (c, d) cycling of Si nanowires. The formation of small Si clusters (P1 resonance) and the overlithiated crystalline phase Li_{15+x}Si (P3) are clearly seen by ⁷Li NMR. If all the amorphous phase is converted to Li₁₅Si (c and d) then the system takes a different path on charge, Li₁₅Si reacting to form a low Li content amorphous Si phase (P1 is largely absent).

Simulations and X-ray Spectroscopy of Li-S Chemistry

PROJECT OBJECTIVE: Lithium-sulfur cells are attractive targets for energy storage applications as their theoretical specific energy of 2600 Wh/kg is much greater than the theoretical specific energy of current Li-ion batteries. Unfortunately, the cycle-life of Li-S cells is limited due to migration of species generated at the S cathode. These species, collectively known as polysulfides, can transform spontaneously, depending on the environment, and it has thus proven difficult to determine the nature of redox reactions that occur at the sulfur electrode. The objective of this project is to use X-ray spectroscopy to track species formation and consumption during charge-discharge reactions in a Li-S cell. Molecular simulations will be used to obtain X-ray spectroscopy signatures of different polysulfide species, and to determine reaction pathways and diffusion in the sulfur cathode. The long-term objective of this project is to use the mechanistic information to build high specific energy lithium-sulfur cells.

PROJECT IMPACT: Enabling rechargeable Li-S cells has the potential to change the landscape of rechargeable batteries for large-scale applications beyond personal electronics due to: (1) high specific energy, (2) simplicity and low cost of cathode (the most expensive component of current Li-ion batteries), and (3) earth abundance of sulfur. The proposed diagnostic approach also has significant potential impact as it represents a new path for determining the species that form during charge-discharge reactions in a battery electrode

OUT-YEAR GOALS: Year 1 Goals: Simulations of sulfur and polysulfides (PSL) in oligomeric polyethylene oxide (PEO) solvent. Prediction of X-ray spectroscopy signatures of PSL/PEO mixtures. Measurement of X-ray spectroscopy signatures PSL/PEO mixtures. Year 2 Goals: Use comparisons between theory and experiment to refine simulation parameters. Determine speciation in PSL/PEO mixtures without resorting to adhoc assumptions. Year 3 Goals: Build an all-solid lithium-sulfur cell that enables measurement of X-ray spectra *in situ*. Conduct simulations of reduction of sulfur cathode. Year 4 Goals: Use comparisons between theory and experiment to determine the mechanism of sulfur reduction and Li₂S oxidation in all-solid Li-S cell. Use this information to build Li-S cells with improved life-time.

COLLABORATIONS: Tsu-Chien Weng, Dimosthenis Sokaras, and Dennis Nordlund (Stanford Synchrotron Radiation Lightsource, SLAC National Accelerator Laboratory)

Milestones

- 1) Complete simulations of PSL/PEO mixtures including calculation of solvation free energy and X-ray spectra; compare spectra with experimental measurements. (Dec. 13) **Complete**
- 2) Go/No-Go: Viability of the use of X-ray spectroscopy to study speciation of lithium sulfides in Li-S cells. Criteria: Determine speciation using X-ray spectra. (Mar. 14) **Ongoing**
- 3) Build *in situ* cell for generating polysulfides by electrochemically driven redox reactions and measuring X-ray spectra. (Jun. 14) **Ongoing**
- 4) Synthesize an electron- and ion-conducting polymer binder for the sulfur cathode. (Sep. 14) **Ongoing**

Progress Report

Milestone 1. The first theoretical calculation of the sulfur K-edge XAS of isolated Li_2S_x species solvated in tetraglyme was performed (Fig. 1). Comparison to experimental spectra enables determination of the Li_2S_x species in the solvent. It was determined that the electronic and geometric properties of dissolved Li_2S_x give rise to the spectral differences seen experimentally. The differences between theory and experiments arise primarily due to the presence of mixtures of Li_2S_x species in the experimental system due to spontaneous disproportionation reactions.

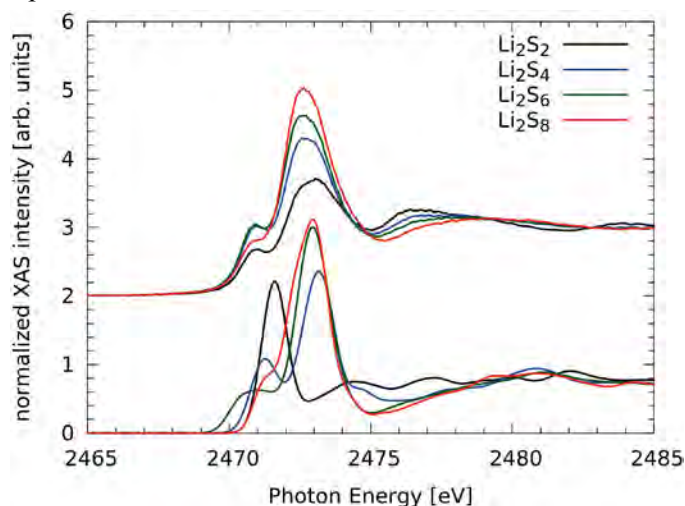


Figure 1. Comparison of the theoretical (lower plots) and experimental (upper plots) sulfur K-edge XAS of dissolved Li_2S_x molecules in tetraglyme.

Milestone 2. In a previous report, it was shown that principal component analysis on XAS data enables quantifying disproportionation reactions in Li polysulfide-containing mixtures.

Milestone 3. Figure 2a shows the schematic for the cell that was developed for *in situ* XAS measurements. Figure 2b shows a picture of the fully built cell. The adapted coin cell design will allow for probing the polymer electrolyte of the Li-S cell during cycling. As polysulfide species are electrochemically generated in the cathode, XAS will be used to probe the rate at which polysulfide dissolution occurs, and determine if one polysulfide species diffuses more rapidly than others. This design is a first step toward probing Li-S charge/discharge reaction mechanisms.

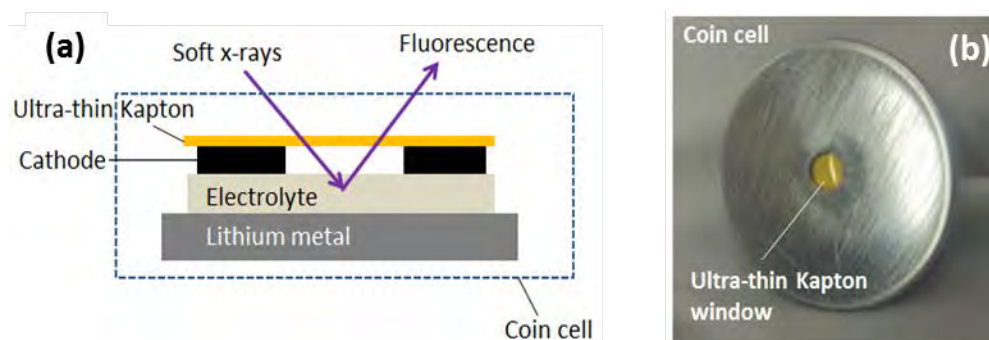


Figure 2. (a) Schematic of Li-S cell for *in situ* XAS studies of cell electrolyte, (b) fully developed *in situ* cell for XAS studies.

Design and Synthesis of Advanced High-Energy Cathode Materials

PROJECT OBJECTIVE: The successful development of next-generation electrode materials requires particle-level knowledge of the relationships between materials' specific physical properties and reaction mechanisms to their performance and stability. This single-crystal-based project was developed specifically for this purpose and it has the following objectives: 1) obtain new insights into electrode materials by utilizing state-of-the-art analytical techniques that are generally inapplicable on conventional, aggregated secondary particles, 2) gain fundamental understanding on structural, chemical and morphological instabilities during Li extraction/insertion and prolonged cycling, 3) establish and control the interfacial chemistry between the cathode and electrolyte at high operating voltages, 4) determine transport limitations at both particle and electrode levels, and 5) develop next-generation electrode materials based on rational design as opposed to more conventional empirical approaches.

PROJECT IMPACT: This project will reveal performance-limiting physical properties, phase-transition mechanisms, parasitic reactions, and transport processes based on the advanced diagnostic studies on well-formed single crystals. The findings will establish rational, non-empirical design methods that will improve the commercial viability of next-generation $\text{Li}_{1+x}\text{M}_{1-x}\text{O}_2$ (M=Mn, Ni and Co) and spinel $\text{LiNi}_x\text{Mn}_{2-x}\text{O}_4$ cathode materials.

OUT-YEAR GOALS:

- Synthesize single-crystal samples of Li transition-metal oxide cathode materials.
- Characterize structural and morphological changes and establish their correlation to rate performance and cycling stability.
- Determine crystal-plane specific reactivity between cathode particles and the electrolyte.
- Measure Li-concentration dependent transport and kinetic properties.
- Define performance-limiting fundamental properties and mechanisms and outline mitigating approaches. Design, synthesize, and evaluate the improved electrode materials.

COLLABORATIONS: R. Kostecki, M. Doeff, K. Persson, V. Zorba, T. Tyliczszak, and Z. Liu (LBNL), C. Grey (Cambridge), B. Lucht (URI), and Y.-M. Chiang (MIT)

Milestones

- 1) Synthesize at least five new cathode crystal samples with at least two new morphologies. (Dec. 13) **Complete**
- 2) Characterize the interface between the high-voltage cathode and the electrolyte. Identify the role of particle surface planes in interfacial reactivity (Mar. 14) **Ongoing**
- 3) Complete the studies on structural evolution during initial Li extraction/insertion and extended cycling. Illustrate the impact of structural changes and phase transformation on rate capability and stability. (Jun. 14) **Ongoing**
- 4) **Go/No-Go:** Continue low-temperature based solvothermal synthesis. **Criteria:** If the crystal samples show similar quality and performance to those made at high temperatures. (Sep. 14) **Ongoing**

Progress Report

Crystal synthesis: The molten-salt method offers great tunability in the size and morphology of the synthesized crystals, but it is desirable to explore other synthesis methods in order to prepare crystals with a variety of physical attributes, particularly those with low-index or metastable surface facets. To this end, two alternative approaches, solvothermal and flux-growth, were investigated in this quarter.

The solvothermal method is known for its simplicity and versatility in preparing well-formed crystals with a wide size range. The low temperature and high pressure conditions typically promote nucleation and crystal growth that favor metastable surface facets, complementing synthesis performed at high temperatures. The choices of solvent, precursors, temperature, and reaction time are key parameters in tuning crystal habits. Here, the approach was successfully modified to synthesize and control crystal morphology of phase-pure spinel $\text{LiMn}_{1.5}\text{Ni}_{0.5}\text{O}_4$ (LMNO) for the first time. Figure 1a shows the plate-shaped LMNO with an average size of 3 to 4 μm . The crystals were synthesized by mixing stoichiometric amounts of amorphous MnO_2 with NiCl_2 and LiOH in ethanol/water (v/v 8:1) followed by thermal treatment in a Teflon-lined Parr autoclave at 250°C for 10 h. In the absence of LiOH , this reaction in water resulted in the formation of a rod-shaped nickel manganese oxide intermediate (MNO). The morphology was largely preserved when immediate lithiation with LiOH was performed in ethanol, which led to the formation of micron-sized, rod-shaped LMNO crystals (Fig. 1b). The size and uniformity of the rods greatly improve with increasing lithiation time. On the other hand, performing the lithiation in water led to the formation of lithiated nanoparticles which, upon thermal annealing, transformed to the thermodynamically favorable, octahedron-shaped LMNO crystals (Fig. 1c). The crystallinity of the MnO_2 has a large impact on morphology, as replacing amorphous with crystalline MnO_2 resulted in the formation of truncated-octahedron-shaped LMNO crystals (Fig. 1d). Mn/Ni ratio was also found to be critical in influencing morphology, and Mn/Ni spinel cubes with an average size of 10 μm were attainable when the ratio was controlled at 1.67:1 (Fig. 1e). All samples shown in Fig. 1 were subjected to post-synthesis annealing at 400°C for 2 h and then 800°C for 6 h in an oxygen atmosphere to improve the oxide quality, particularly with regard to site occupancy and structural ordering. TEM is currently underway to further analyze the properties of the solvothermal synthesized crystals.

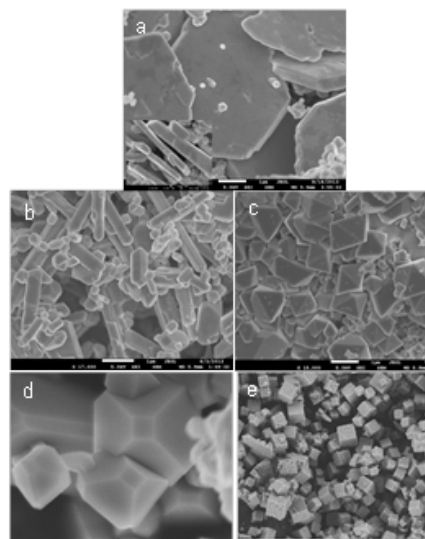


Figure 1. SEM images of solvothermal synthesized LMNO crystals: a) plates, b) rods, c) octahedrons, d) truncated-octahedrons, and e) cubes.

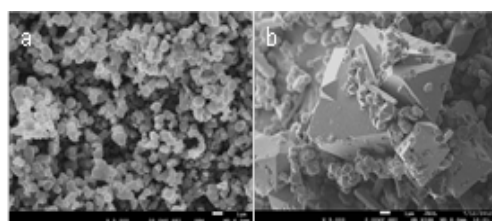


Figure 2. SEM images of NEI LMNO a) before and b) after heating and cooling in a LiCl flux.

In a typical flux-growth synthesis, the pre-synthesized compound was mixed with a flux in an inert atmosphere and heated to elevated temperature to form a melt. Through careful control in the cooling conditions, the sample recrystallizes and is able to form single crystals significantly larger than those from other syntheses. Figure 2 compares the SEM images of a polycrystalline LMNO sample (NEI Corp.) before and after heating in a LiCl flux (8:1 weight ratio). The experiment was carried out by heating the mixture at 750°C for 10 h and then cooling at 5°C/h in a sealed gold tube that was previously evacuated and filled with Ar. Significant crystal growth was observed, and large octahedral-shaped LMNO crystals were obtained (Fig. 2). Experimental conditions will be further adjusted to fine tune the size and morphology of the crystals.

Optimization of Ion Transport in High-Energy Composite Cathodes

PROJECT OBJECTIVE: This project aims to probe and control the atomic-level kinetic processes that govern the performance limitations (rate capability and voltage stability) in a class of high-energy composite electrodes. A systematic study with powerful suite of analytical tools (including atomic resolution scanning transmission electron microscopy (a-STEM) & electron energy loss spectroscopy (EELS), XPS, and first-principles (FP) computation) will be used to pin down the mechanism and determine the optimum bulk compositions and surface characteristics for high rate and long life, and to help the synthesis efforts to produce the materials at large scale with consistently good performance.

PROJECT IMPACT: If successful, this research will provide a major breakthrough in commercial applications of the class of high energy density cathode material for Li-ion batteries. Additionally, it will provide in-depth understanding of the role of surface modifications and bulk substitution in the high-voltage composite materials. The diagnostic tools developed here can also be leveraged to study a wide variety of cathode and anode materials for rechargeable batteries.

OUT-YEAR GOALS: Careful engineering of the surface (coating) and bulk compositions (substitution) of the high-energy composite cathode materials can lead to significant improvement on ion transport and voltage stability. The goals are to establish the STEM/EELS and XPS as quantities diagnostic tools for surface and interface characterization and to enable quick identification of causes of surface instability (or stability) in various types of cathode materials. It is also planned to identify ways to extend the techniques for anode materials, such as Si anode.

COLLABORATIONS:

- Robert Kostecki and Gao Liu (LBNL) – on cathode electrolyte interface diagnosis and anode SEI diagnosis
- Miaofang Chi (ORNL) – on STEM/EELS
- Gabriel Veith (ORNL) – on XPS

Milestones

- 1) Establish the initial suite of surface and interface characterization tools, including STEM/EELS, XPS and FP computation (Dec. 13) **Complete**
- 2) Identify the surface-coated materials (AlF_3 and Li_3PO_4) electrochemical performance matrices, including first-cycle irreversible capacity, discharge energy density, voltage stability upon cycling and rate capabilities. (Mar. 14) **Ongoing**
- 3) Go/No-Go: Stop and change the coating materials if the improvements for rate capability and voltage stability are not significant. Criteria: Characterize coated samples - coating thickness, compositions and morphology before, during, and after cycling. (Jun. 14) **Ongoing**
- 4) Identify ways to extend the STEM/EELS and XPS techniques for anode materials, such as Si anode. (Sep. 14) **Ongoing**

Progress Report

AlF₃ treatment for the Li_{1.2}Ni_{0.2}Mn_{0.6}O₂ lithium excess material. Li_{1.2}Ni_{0.2}Mn_{0.6}O₂ (LNMO) has been synthesized by the hydroxide co-precipitation method without morphology control and treated with Al(NO₃)₃ and NH₄F to theoretically form a 1 wt% AlF₃ coating. A comparison of the cyclic capacity of the 1st and 60th discharge profiles for treated and untreated LNMO are provided in Fig. 1a. After 60 cycles, it is evident that the treatment does not prevent voltage fade. With treatment, the initial coulombic efficiency improved from 75.1 to 82.7% and the initial discharge capacity improved to 259 mAh g⁻¹, but the treatment also resulted in faster capacity fade. A rate study compared the rate performance of untreated (Fig. 1b) and treated (Fig. 1c) LNMO. At a current density of 500 mA g⁻¹ (2C) the treated LNMO delivered a specific discharge capacity of 181 mAh g⁻¹ which is an improvement over untreated LNMO. Characterization of the AlF₃-treated LNMO was carried out using XPS and a-STEM. XPS results indicate the presence of only Al-O bonds which shows that little or no AlF₃ was synthesized by the treatment process. TEM also reveals partial/incomplete coating on LNMO. a-STEM and the image Fast-Fourier-Transform (FFT) show that LNMO's surface structure changed after the treatment. FFT of the a-STEM image near the surface of the LNMO particle indicates the presence of the spinel-like structure. The results show that the AlF₃ treatment, while beneficial for 1st cycle efficiency and rate, may not be the best choice for improving the performance of Li excess cathodes. Strategies to change the bulk structure of Li excess layered materials must be considered.

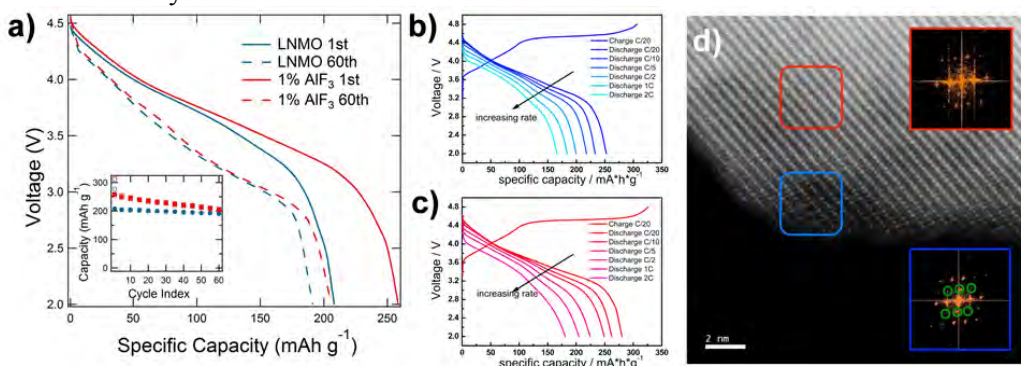


Figure 1. a) Voltage profiles and cyclic capacity of untreated (blue) and 1 wt% AlF₃ treated (red) LNMO at C/10 with 2.0-4.8 voltage range. b, c) Rate profiles for untreated LNMO (blue) and treated LNMO (red). d) a-STEM and FFT of uncycled treated LNMO.

Morphologically controlled Li_{1.2}Ni_{0.2}Mn_{0.6}O₂ with a gradient transition metal composition. In the previous quarterly report, it was shown that morphology control without coatings may be a better option for preventing voltage fade. In order to determine if the performance of morphologically-controlled LNMO could be improved further, LNMO with a radially-gradient composition was synthesized *via* the urea hydrolysis method. Figure 2a provides a SEM image of a focused-ion-beam (FIB) cross-sectioned LNMO particle. EDX was used to map the transition metals in the material. The ratio of Mn/Ni signals at points 1 to 4 is 0.96, 5.7, 3.17, and 2.91, respectively. The changing Mn/Ni ratio suggests particles with a Ni-rich outer surface layer. EDX mapping and line scans (Figs. 2b, 2c) also suggest gradient distribution of Mn and Ni. The electrochemical performance of such a radially gradient spherical LNMO is now under investigation.

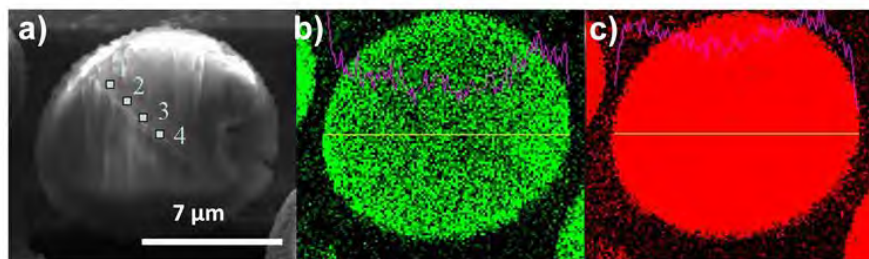


Figure 2. a) Cross sectional SEM image of a LMNO particle synthesized by the urea hydrolysis method with labeled EDX point scan locations. b) EDX mapping for Ni. c) EDX mapping for Mn.

Analysis of Film Formation Chemistry on Silicon Anodes by Advanced *In Situ* and *Operando* Vibrational Spectroscopy

PROJECT OBJECTIVE: Understand the composition, structure, and formation/degradation mechanisms of the SEI on the surfaces of Si anodes during charge/discharge cycles by applying advanced *in situ* vibrational spectroscopies. Determine how the properties of the SEI contribute to failure of Si anodes in Li-ion batteries in vehicular applications. Use this understanding to develop electrolyte additives and/or surface modification methods to improve Si-anode capacity loss and cycling behavior.

PROJECT IMPACT: A high capacity alternative to graphitic carbon anodes is Si, which stores 3.75 Li per Si vs. 1 Li per 6 C yielding a theoretical capacity of 4008 mAh/g vs. 372 mAh/g for C. But Si anodes suffer from large first-cycle irreversible capacity loss and continued parasitic capacity loss upon cycling leading to battery failure. Electrolyte additives and/or surface modification developed from new understanding of failure modes will be applied to reduce irreversible capacity loss, and improve long term stability and cyclability of Si anodes for vehicular applications.

OUT-YEAR GOALS: N/A

COLLABORATIONS:

- Chunmei Ban (NREL) Functionalization of Si by Atomic Layer Deposition (ALD): Effect of functionalization on electrolyte reduction.
- Gao Liu (LBNL) Surface electrochemistry of electrolyte additives on model Si electrodes.

Milestones

- 1) Develop method to attach Si nanostructures to the electrode substrate used in our spectroelectrochemical cell. (Dec. 13) **Delayed, due Sep. 14**
- 2) Determine the oxidation and reduction potentials and products of at least one electrolyte additive provided by Gao Liu's group. (Mar. 14) **Ongoing**
- 3) Determine role of the Si nanostructure on the SEI formation structure and properties. (Jun. 14) **Ongoing**
- 4) Go/No-Go: Feasibility of surface functionalization to improve SEI structure and properties. Criteria: Functionalize a model Si-anode surface and determine how SEI formation is changed. (Sep. 14) **Ongoing**

Progress Report

In Q1, the effect of coatings on thin film Si electrodes and the additive effect (VC, FEC comparison) on Si nanoparticles on SEI composition were investigated. Si films of two different thicknesses (45 and 550 nm), with and without molecular layered deposition (MLD) treatment, were provided by Chunmei Ban, NREL. The electrochemical testing and fabrication of the Si-nanoparticle composite electrodes was performed by Hui Zhao, a postdoc in Gao Liu's group, LBNL. The composite electrode composition was 50%, with 20% carboxymethyl cellulose and 5% polyvinyl alcohol as binder, and 25% additive carbon. All of the electrochemical testing was done using standard coin half-cells in EC/DEC/LiPF₆ electrolyte (v/v=1:1). After cycling, the cells were disassembled in a glove box and the cell components analyzed *ex situ* by ATR-FTIR using procedures developed at LBNL.

Figure 1(a) shows the *ex situ* spectra of two different thin film Si electrodes, with/without MLD treatment after 5 cycles between 1V to 0.05V. A strong peak (1663 cm⁻¹) is observed, besides residual electrolyte features, which could be attributed to Li ethylenedicarbonate (LiEDC), and the broad peak at around 1400 to 1500 cm⁻¹, which is from Li₂CO₃. Based on the relative absorption, it was found that a thinner Si film has less

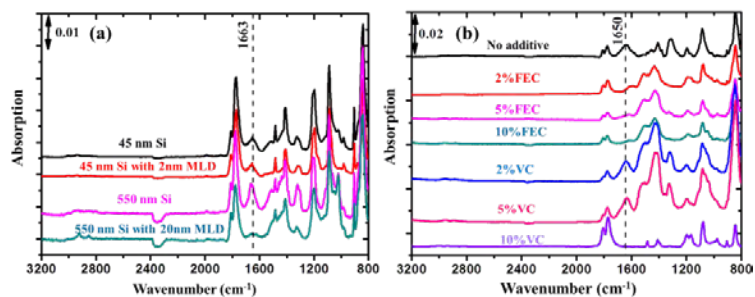


Figure 1. *Ex situ* IR spectrum on (a) Si thin films after 5 cycles at 1/24 C rate. (b) Si nanoparticle electrode with different additive conditions after 100 cycles.

LiEDC and Li₂CO₃, which is probably due to less cracking and thus less SEI species generated. Compared to pristine Si samples, MLD treatment seems to serve as an artificial film which is a barrier to electrolyte reduction; thus less species were generated on the thin Si films with the MLD coating. For thicker Si film, the effect of the MLD coating (which is proportionally thicker) is more pronounced, *i.e.*, producing less SEI.

From battery cycling results with the same type of Si nanoparticle electrodes, the higher the FEC concentration, the longer the cycling life; however for VC additive, a contradictory trend is observed. For better understanding of the additive effect on battery cycling life, *ex situ* IR test on nanoparticle composite electrodes were performed (Fig. 1b). For the control experiment, the composite electrode without any additive, the SEI composition is different from that observed in Fig. 1a for the Si thin films. A new feature, attributable to the SEI, is only captured around 1650 cm⁻¹, perhaps indicating a mixture of LiEDC and Li oxalate. However, for VC additive, and as the concentration of VC increases, this feature absorption decreases, and a new feature at 1400 to 1500 cm⁻¹ attributed to Li₂CO₃ appears. Paradoxically, at 10% VC only electrolyte features remain. From these results alone, high concentrations of VC appear to inhibit the formation of a stable SEI on the Si nanoparticles, which would correlate with the higher capacity fade observed in the cycling tests. According to recent literature [1], VC additive preferentially reacts with the EC anion radical, thus suppressing the 2e⁻ reduction of EC to LiEDC. This reaction path leads mostly to gases, *e.g.*, ethylene and CO₂. For the FEC additive, the SEI appears to be formed almost entirely from Li₂CO₃. Although one can find many reports in the literature of Li₂CO₃ as an SEI component on Li-ion battery anodes, these are the first results reported of Li₂CO₃ formation on such electrodes. In the literature this is attributed to air exposure on handling, but the protocol here was exactly the same used by this group with graphite composite electrodes and in Fig. 1a with binder-free pure Si thin film electrodes. As the Si nanoparticle size was the same order magnitude as the thin films, the difference in SEI composition is not attributed to the stress-related phenomena, *e.g.*, fresh surface created by cracking. The possible role of the binder and/or carbon black needs to be determined to make these results for FEC meaningful.

[1] Ushirogata K., et al, J. Am. Chem. Soc.2013, 135, 11967–1197

Electrode Materials Design and Failure Prediction

PROJECT OBJECTIVE: The goal of this project is to use continuum-level mathematical models along with controlled experiments on model cells to (i) understand the performance and failure models associated with next-generation battery materials, (ii) design battery materials and electrodes to alleviate these challenges. The focus of the research will be on two systems, Si-based anodes and Li-sulfur cells. In Si anodes, the challenges associated with the large volume change and the associated stress effects will be studied. In the Li-S system, the focus will be on the concept of using ceramic single-ion conducting glass layers for Li protection, along with quantification of the losses associated with such a design and its impact on the performance of the chemistry. A theoretical study of the impact of polarization losses on the energy density will be conducted.

PROJECT IMPACT: Silicon-anode-based Li-ion cells and Li-S cells promise to increase the energy density and decrease the cost of batteries compared to the state-of-the-art. If the performance and cycling challenges can be alleviated, these systems hold the promise for meeting the *EV-Everywhere* targets.

OUT-YEAR GOALS: At the end of this project, a mathematical model will be developed that can address the power and cycling performance of next-generation battery systems. The initial focus will be on Si anodes and Li-S cells, although the project will adapt to newer systems, if appropriate. The models will serve as a guide for better design of materials, including mechanical properties to reduce stress in Si anodes, and the kinetics and solubility needed to decrease the morphological changes in S cells and increase the power performance.

COLLABORATIONS: None this quarter.

Milestones

- 1) **Go/No-Go:** Stop materials testing. **Criteria:** Stop materials testing if unsuccessful at obtaining reproducible results for mechanical property values of binder and conductive material composites saturated in electrolyte. (Dec. 13) **Go for materials testing.**
- 2) Incorporate material property values and behavior measured for binders saturated with electrolyte into simulations of model systems. (Feb. 14) **Ongoing**
- 3) Quantify polarization losses at liquid/SIC interface for different electrolytes. (Mar. 14) **Complete.**
- 4) Determine possible reasons for dynamic nature of polarization loss in liquid/SIC interface (*e.g.*, interfacial vs. bulk.). (Jun. 14) **Ongoing**
- 5) Quantify the impact of the interfacial polarization loss between the liquid/SIC by estimating the energy density of a Li-S cell for a given power to energy ratio. (Sep. 14) **Ongoing**

Progress Report

Quantifying polarization loss at single-ion conductor/liquid electrolyte interface: The Li-S system promises a significant increase in energy density when compared to existing Li-ion systems. To prevent self-discharge of the cell, resulting from polysulfide migration to the Li anode, and to limit dendrite growth on the Li anode, the use of ceramic single-ion conductors (SIC) has been proposed. The SIC allows transfer of Li-ions without transfer of the polysulfides, due to their unity transference number. It is therefore necessary to quantify the polarization loss at the SIC/liquid electrolyte interface. A novel methodology to account for polarization loss at the SIC/liquid electrolyte interface was developed. Constant current cycling experiments were first performed in a custom Li-Li symmetric diffusion cell in the absence of the SIC. Thereafter, the SIC was incorporated in the cell such that it was sandwiched between two electrolyte chambers. Figure 1 (red and blue dots) shows the I-V plot extracted from these cycling experiments with and without a SIC. The solid black line shows the model predictions of a Li-Li symmetric cell with SIC (without polarization loss). The model accounts for the ohmic drop in the SIC and concentration polarization effects in the liquid electrolyte that happen when a SIC is incorporated in a Li-Li symmetric cell. The difference between the experimental data for the cell with SIC (red dots) and the model predictions (black line) gives the polarization loss at different current densities. This completes the March milestone.

Stress and strain in Si electrodes: In the last year, the modeling efforts have been focused on simulating the volume change and stresses in a single Si particle covered with a binder. In this quarter, this has been expanded to simulate the lithiation/delithiation of this particle in a sea of other particles. The simulation code now has been reworked into Cartesian coordinates, and the boundary conditions have been modified to produce a periodic domain, meant to approximately represent particles dispersed in a porous matrix. Figure 2 shows material displacement in an example simulation.

Equipment for mechanical testing of binder materials submerged in solvent has been designed and fabricated, and a tentative testing procedure has been established. Simple but effective equipment designs have been developed to be easily adaptable to common commercially-available tonometer equipment, so that the material testing procedures can be easily adopted by other research groups as necessary. Only small volumes of solvent are needed to keep the samples submerged. Care has been taken to ensure that material samples can be brought quickly and easily into proper alignment for consistent testing. Procedures for obtaining fairly consistent material samples have also been created as well, and will be further refined. The initial tests have been sufficiently encouraging to justify continued work towards the February milestone for incorporating material properties obtained by these tests into the existing simulation code.

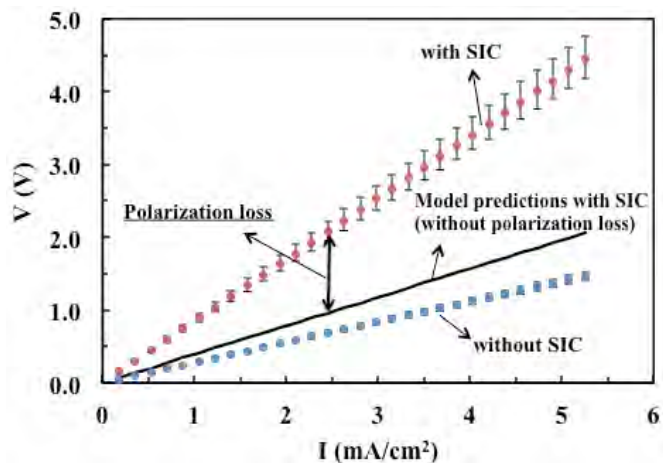


Figure 1. Experimental I-V curves for a Li-Li symmetric cell with and without SIC for 0.5M LiPF₆ in EC:DEC (1:1). Also shown are model predictions (solid line) for a Li-Li symmetric cell with SIC (without polarization loss).

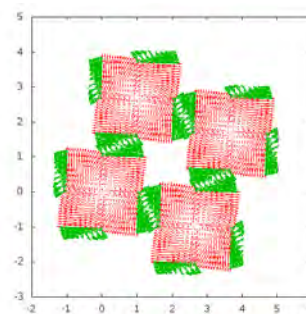


Figure 2. Displacement of active material (red) and binder (green).

Predicting and Understanding Novel Electrode Materials from First-Principles

PROJECT OBJECTIVE: The aim of the project is to model and predict novel electrode materials from first-principles focusing on 1) understanding the atomistic interactions behind the behavior and performance of the high-capacity Li excess and related composite cathode materials, and 2) predict new materials using the recently developed Materials Project high-throughput computational capabilities at LBNL. More materials and new capabilities will be added to the Materials Project Lithium Battery Explorer App (www.materialsproject.org/apps/battery_explorer/).

PROJECT IMPACT: The project will result in a profound understanding of the atomistic mechanisms underlying the behavior and performance of the Li-excess as well as related composite cathode materials. The models of the composite materials will result in prediction of voltage profiles and structural stability – the ultimate goal being to suggest improvements based on the fundamental understanding that will increase the life and safety of these materials. The Materials Project aspect of the work will result in improved data and electrode properties being calculated to aid predictions of new materials for target chemistries relevant for ongoing BATT experimental research.

OUT-YEAR GOALS: During years 1-2, the bulk phase diagram will be established – including bulk defect phases in layered Li_2MnO_3 , layered LiMO_2 ($M = \text{Co}, \text{Ni}, \text{and Mn}$), and LiMn_2O_4 spinel to map out the stable defect intermediate phases as a function of possible transition metal rearrangements. Modeling of defect materials (mainly Li_2MnO_3) under stress/strain will be undertaken to simulate effect of composite nano-domains. The composite voltage profiles as function of structural change and Li content will be obtained. In years 2-4, the project will focus on obtaining Li-activation barriers for the most favorable TM migration paths as a function of Li content as well as electronic DOS as a function of Li content for the most stable defect structures identified in years 1-2. Furthermore, stable crystal facets of the layered and spinel phases will be explored, as a function of O_2 release from surface and oxygen chemical potential. Within the Materials Project, hundreds of novel Li-intercalation materials will be calculated and made available.

COLLABORATIONS: Gerbrand Ceder (MIT), Clare Grey (U Cambridge, UK). Mike Thackeray (ANL), Guoying Chen (LBNL)

Milestones

- 1) Finalize low-T phase diagram including relevant bulk Li, O, and Mn and defect phases in layered Li_xMnO_2 , spinel Li_xMnO_3 , and spinel $\text{Li}_x\text{Mn}_2\text{O}_4$ (Dec. 13) **Complete**
- 2) Over-charge mechanism processes: oxygen migration paths and activation barriers obtained in lowest energy defect structures; oxygen redox potentials obtained (Mar. 14) **Ongoing**
- 3) Go/No-Go: On over-charge mechanism. Criteria: Oxygen release, migration or oxygen redox process; process down select based on data. (Jun. 14) **Ongoing**
- 4) Obtain composite voltage profiles as function of structural change and Li content. (Sep. 14) **Ongoing**

Progress Report

Work has continued on the layered Li_2MnO_3 - one of the components in the layered-layered and layered-spinel composite cathode materials. To elucidate the activation process as well as the structural evolution of Li_2MnO_3 as a function of charge and discharge, an exhaustive search of different structure and chemical deviations of the compound has been performed, using first-principles methods and a ternary cluster expansion. It was found that the original structure is thermodynamically unstable towards transformation and deformation to spinel-like domains, especially at low Li content.

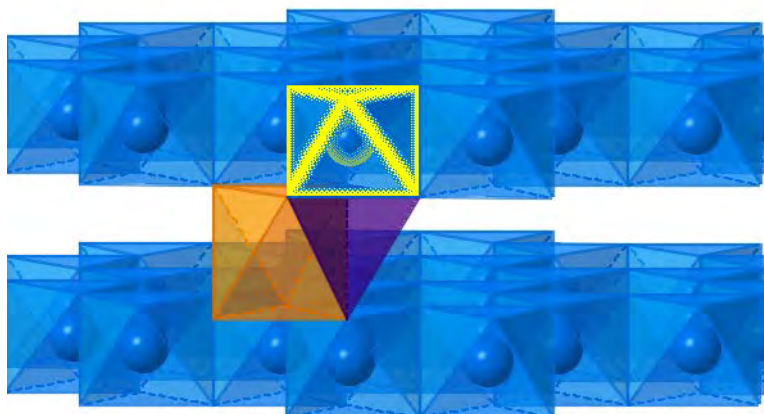


Figure 1. An example of a Mn migration path in Li_xMnO_3 .

As part of the structural transformation, ionic migration patterns are investigated. The degree of ionic migration is determined by thermodynamic as well as kinetic factors, which means that the migration could be slow enough for material to retain its original structure during fast Li-extraction even if the structure is thermodynamically unstable. In this respect, Mn as well as O migration mechanisms (see example in Fig. 1) are calculated to characterize the transformation. The elastic band method is employed for several different hypothesized Mn and O migration paths at several different Li contents and different functionals. The charge and positions of the ions along the transformation paths have been analyzed, as well as included larger supercells to benchmark the conclusions. For the structurally-transformed structures, a voltage profile was developed that highlights the voltage depression of the material as the transformation occurs.

First-Principles Calculations of Existing and Novel Electrode Materials

PROJECT OBJECTIVE: Identify the structure of layered cathodes that leads to high capacity. Clarify the role of the initial structure as well as structural changes upon first charge and discharge. Give insight into the factors that control the capacity and rate of Na-intercalation electrodes, and make suggestions for novel Na-intercalation cathode materials. Generate insight into the behavior of alkali-intercalating electrode materials.

PROJECT IMPACT: The project will lead to insight in how Li excess materials work and ultimately to higher capacity cathode materials for Li-ion batteries. The project will also lead to definite conclusions as to whether Na-ion batteries can exceed Li-ion batteries in energy density.

OUT-YEAR GOALS: Higher capacity Li-ion cathode materials, and novel chemistries for higher energy density storage devices.

COLLABORATIONS: Clare Grey (U Cambridge, UK), Kristin Persson (LBNL)

Milestones

- 1) Identify at least three ordered states in Na_xMO_2 compounds that can be verified with experiments. (Dec. 13) **Complete**
- 2) Obtain computed voltage curve of Li_2MO_3 compound where $\text{M} = \text{Mn}$ or other metal. (Mar. 14) **Ongoing**
- 3) Go/No-Go: If voltage curves of Na compounds with less than 0.5V error cannot be modeled. Criteria: Obtain voltage curves for all the O_3 Na_xMO_2 compounds where M is at least five distinct 3d metals. (Jun. 14) **Ongoing**
- 4) Complete ground state study in Li-Ni-Mn-O and Li-Co-Mn-O system. (Sep. 14) **Ongoing**

Progress Report

The Li migration in Li-excess materials has been investigated. Using cation-disordered Li-excess Mo/Cr oxide ($\text{Li}_{1.211}\text{Mo}_{0.467}\text{Cr}_{0.3}\text{O}_2$) as a prototype material, it was possible to gain a fundamental understanding of Li transport in general Li transition metal (TM) oxides.^[1] In rocksalt-like Li-TM oxides, Li migration between two octahedral sites proceeds *via* a tetrahedral activated state (*o-t-o* diffusion, Fig. 1A).^[2] The activation barrier for this process is mainly determined by the electrostatic repulsion between the tetrahedral Li and the species (cation or vacancy) on its two face sharing sites (Fig. 1C). In stoichiometric layered materials, exactly one face-sharing site is a TM site, while the second one is a Li site. The Li migration barrier for such a 1-TM diffusion channel is correlated with the TM valence and the Li-TM separation that varies with the height of the Li slab (*ca.* 2.6–2.7Å).^[3] This model for cation-disordered structures was generalized by taking into account all possible cation arrangements around the tetrahedral site, namely 0-TM, 1-TM, and 2-TM channels (Fig. 1B-C).^[1] It was found that due to spatial constraints in disordered materials (slab distances *ca.* 2.4Å) the majority of 1-TM and 2-TM channels are not active at room temperature, but 0-TM channels can support facile Li migration. However, around 10% Li excess is required to achieve a sufficiently large concentration of 0-TM diffusion channels to form a percolating 0-TM network (Fig. 2).^[1]

This new insight into Li percolation allows for definition of clearer boundaries for the expected capacity of new Li-excess cathode materials, by evaluating the percentage of the Li contents that is accessible *via* 0-TM migration as a function of the composition (Fig. 2). It also opens up the entirely new compound space of disordered materials, which have so far mainly been disregarded as cathode materials. Currently, studies continue on the implications of Li percolation for further relevant cation-ordered phases (spinel and $\gamma\text{-LiFeO}_2$), which will effectively complete understanding of Li migration in general Li metal oxides.

^[1] J. Lee et al., *Science* (2014), online first. [2] A. Van der Ven and G. Ceder, *Electrochem. Solid State Lett.* **3** (2000) 301-304; A. Van der Ven and G. Ceder, *J. Power Sources* **97-98** (2001) 529-531. [3] K. Kang and G. Ceder, *Phys. Rev. B* **74** (2006) 094105.

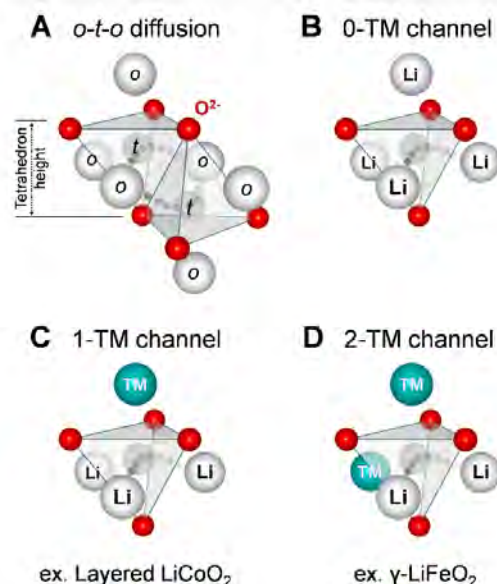


Figure 1. A. Li migration between two octahedral sites *via* a tetrahedral activated state. B-C. The three different diffusion channel types that occur in cation-disordered Li metal oxides. The figure has been reproduced from Ref. [1].

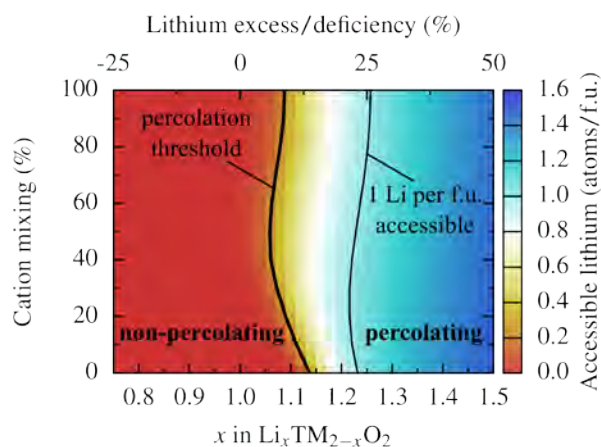


Figure 2. 0-TM percolation and accessible Li contents as function of the composition and the degree of disorder (cation mixing) in layered Li transition metal oxides ($\text{Li}_x\text{TM}_{2-x}\text{O}_2$). The figure visualizes the results of Monte-Carlo percolation simulations.^[1]

First-Principles Modeling of SEI Formation on Bare and Surface/Additive Modified Silicon Anode

PROJECT OBJECTIVE: This project aims to develop fundamental understanding of the molecular processes that lead to the formation of a SEI layer due to electrolyte decomposition on Si anodes, and to use such new knowledge in a rational selection of additives and/or coatings. The focus is on SEI layer formation and evolution during cycling and subsequent effects on capacity fade through two concatenated problems: 1) SEI layers formed on lithiated Si surfaces, and 2) SEI layers formed on coated surfaces. Key issues that this project addresses include the dynamic evolution of the system and electron transfer through solid-liquid interfaces.

PROJECT IMPACT: Finding the correspondence between electrolyte molecular properties and SEI formation mechanism, structure, and properties will allow the identification of new/improved additives. Studies of SEI layer formation on modified surfaces will allow the identification of effective coatings able to overcome the intrinsic deficiencies of SEI layers on bare surfaces.

OUT-YEAR GOALS: Investigating the SEI layer formed on modified Si surfaces involves analysis of the interfacial structure and properties of specific coating(s) deposited over the Si anode surface, characterization of the corresponding surface properties before and after lithiation, especially how such modified surfaces may interact with electrolyte systems (solvent/salt/additive), and what SEI layer structure, composition, and properties may result from such interaction. This study will allow identification of effective additives and coatings able to overcome the intrinsic deficiencies of SEI layers on bare surfaces. Once the SEI layer is formed on bare or modified surfaces, it is exposed to cycling effects that influence its overall structure (including the anode), chemical, and mechanical stability. Elucidating such effects using a molecular level approach will help establish their relationship with capacity fading, which will lead to revisiting additive and/or coating design.

COLLABORATIONS: Within the BATT Program collaboration is with Chunmei Ban, NREL. Work consists in modeling the deposition-reaction of trimethylaluminum and glycerol on Si surfaces and their reactivity. Other collaborations related to the reduction of solvents on Si surfaces are in place with Kevin Leung and Susan Rempe, from Sandia National Labs.

Milestones

- 1) Identify reaction pathways and activation energies for electrolyte reduction on lithiated Si surfaces, both clean and covered with surface oxides and/or with selected SEI products. (Dec. 13) **Complete**
- 2) Quantify electron transfer from a lithiated Si surface covered by a model SEI layer to the electrolyte; develop theory/algorithms accounting for voltage effect on electrolyte reduction reactions. (Mar. 14) **Ongoing**
- 3) Characterize reactivity of additives; identify reaction pathways and interactions of reaction products with electrolyte components; assess aggregation effects. (Jun. 14) **Ongoing**
- 4) Go/No-Go: Continuation of a coarse-grained Kinetic Monte-Carlo Approach for assessing long-time evolution (order of days) of SEI films. Criteria: Continuation will be based on the demonstrated effectiveness of the technique. (Sep. 14) **Ongoing**

Progress Report

Milestone 1: *Ab initio* molecular dynamics (AIMD) simulations were used to identify mechanisms of reduction of EC, FEC, and VC on Si surfaces at various degrees of lithiation, where the low-coordinated surface Si atoms are saturated with O, OH, or H functional groups. The lowest Si-content surfaces were represented by quasi-amorphous LiSi_4 and LiSi_2 ; intermediate lithiation was given by LiSi crystalline facets; and the highest Li content was studied through $\text{Li}_{13}\text{Si}_4$ surfaces. It was found that EC reduction mechanisms depend significantly on the degree of lithiation of the surface. On LiSi surfaces, EC is reduced according to two different $2e^-$ mechanisms (one simultaneous and one sequential), which are independent of specific surface functionalization or nature of exposed facets. On the less lithiated surfaces the simultaneous $2e^-$ reduction were found more frequently. In that mechanism, the EC reduction is initiated by the formation of a C-Si bond that allows adsorption of the intact molecule to the surface, and is followed by electron transfer and ring opening. Strongly lithiated $\text{Li}_{13}\text{Si}_4$ surfaces were found to be highly reactive. Reduction of adsorbed EC molecules occurs *via* a $4e^-$ mechanism yielding as reduction products CO^{2-} and $\text{O}(\text{C}_2\text{H}_4)\text{O}^{2-}$. Direct transfer of two electrons to EC molecules in liquid phase was also possible, resulting in the presence of $\text{O}(\text{C}_2\text{H}_4)\text{OCO}^{2-}$ anions in the liquid phase. FEC reactions were found much less dependent on the degree of lithiation and exhibiting more varied reaction pathways than EC. The initial bond-breaking events and products of $1e^-$ and $2e^-$ reactions are qualitatively similar, with a fluoride ion detached in both cases. On highly lithiated Si surfaces, multi-electron mechanisms were found. Si surfaces with very low degrees of lithiation were also evaluated and the reduction mechanisms were found to be very dependent on the geometry of Li adsorption. A new mechanism for the role of VC in forming an effective SEI layer is currently being investigated. Another essential electrolyte component is the salt. One of the most used salt components is LiPF_6 whose decomposition yields one of the most important SEI products, LiF . To understand its decomposition process, AIMD simulations were carried out for a 1M solution of LiPF_6 in EC solution. In contact with the LiSi surface, the salt molecule becomes promptly dissociated and the PF_5 anion reduction is detected after 2.83 ps. The reduction leads to a total decomposition of the anion into its atomic components. Typical LiF distances are between 1.72 and 2 Å, suggesting the initial nucleation of LiF bonds. Continuation of the AIMD simulation allows observation of the next steps. Within the following 10 ps, no further EC reduction over the surface section containing the LiF fragments was observed. However, the area that was not covered by LiF kept reducing EC molecules and some of the EC decomposition fragments described above appeared readily on the surface.

Milestone 2: Electrodes were modeled through three degrees of lithiation: Si, LiSi , and Li. AIMD simulations demonstrated the rapid formation of LiF on the surface of lithiated Si anodes having an irregular structure in the initial stages of nucleation, and showed the possible continuation of the EC reduction on parts of the surface that were not covered by LiF . Based on the structure obtained from the AIMD simulations, model SEI layers made of LiF fragments were constructed in various thicknesses and configurations, and by analogy, Li_2O model films were also built. It was found that at the same thicknesses and similar configurations, the LiF films offer a higher resistance to electron transfer than Li_2O films. In each case, the resistance of the films is also larger if the fragments are separated at Van der Waals distances. As expected, increasing the thickness increases the film resistance; however, at large film thicknesses in the order of 10 Å there was still a finite although small current. Thus, this analysis proves useful for testing electron transfer through various SEI configurations. Future reports will address the effect of the SEI cluster geometry and composition, and those of the interfaces SEI film/electrode and SEI/electrolyte.

Milestone 3: Current work addresses reactions among intermediate species and aggregation effects. The results will be the basis for a coarse-grained model to be developed in the near future.

A Combined Experimental and Modeling Approach for the Design of High Current Efficiency Si Electrodes

PROJECT OBJECTIVE: The use of high-capacity Si-based electrode has been hampered by its mechanical degradation due to the large volume expansion/contraction during cycling. Nanostructured Si can effectively avoid Si cracking/fracture. Unfortunately, the high surface to volume ratio in nanostructures leads to unacceptable amount of SEI formation and growth, thereby low current/coulombic efficiency and short life. Based on mechanics models it was demonstrated that the artificial SEI coating can be mechanically stable despite the volume change in Si, if the material properties, thickness of the SEI, and the size/shape of Si are optimized. Therefore, the objective of this project is to develop an integrated modeling and experimental approach to understand, design, and make coated Si anode structures with high current efficiency and stability.

PROJECT IMPACT: The validated model will ultimately be used to guide the synthesis of surface coatings and the optimization of Si size/geometry that can mitigate SEI breakdown. The optimized structures will eventually enable a negative electrode with a 10x improvement in capacity (compared to graphite) while providing a >99.99% coulombic efficiency, which could significantly improve the energy/power density of current LIB.

OUT-YEAR GOALS: To develop a well-validated mechanics model that directly imports material properties either measured from experiments or computed from atomic simulations. The predicted SEI-induced stress evolution and other critical phenomena will be validated against *in situ* experiments in a simplified thin-film system. This comparison will also allow fundamental understanding of the mechanical and chemical stability of artificial SEI in electrochemical environments and the correlation between the coulombic efficiency and the dynamic process of SEI evolution. Thus the size and geometry of coated Si nanostructures can be optimized in order to mitigate SEI breakdown, thus provide high current efficiency.

COLLABORATIONS: None this quarter.

Milestones

- 1) Compare the basic elastic properties of ALD coatings (*e.g.*, Al₂O₃) computed from MD simulations with ReaxFF and measured by AFM and acoustic wave for method validation. (Dec. 13) **Complete**
- 2) Predict the interface strength of given coatings on Si substrate from QM calculations and compare with nanoindentation and scratch tests. (Mar. 14) **Ongoing**
- 3) Develop a continuum frame work to model SEI deformation and stability on Si film and compare with *in situ* MOSS measurement. (Jun. 14) **Ongoing**
- 4) Go/No-Go: Stop hard coating core-shell structure design. Criteria: If no mechanically-stable coating can be identified after searching in ALD-coating property design space using the continuum model. (Sep. 14) **Ongoing**

Progress Report

- 1) **MD calculation of the modulus of ALD- Al_2O_3 structures:** A 2D-melt method was developed to generate amorphous ALD- Al_2O_3 coating structures of different densities. These structures are considered semi-disordered, being disordered in-plane (t), maintaining an oxygen peak periodicity of 1.2 Å along the film growth direction (n), and forming local Al-O tetrahedral structures. The Young's moduli were computed along both the $\langle n \rangle$ and $\langle t \rangle$ directions, at different film thicknesses and densities. It was found:
 - a. E_n along the film growth direction is always higher than E_t in the in-plane direction;
 - b. The modulus does not vary with film thickness; this means experimentally one can measure the modulus from a thicker ALD-film.
 - c. E increases linearly with film density (Fig. 2). Since the modulus of the coating is one of the more important parameters for its mechanical stability on a Si electrode, it is important to correlate deposition conditions with film density.
- 2) **Experimental measurements:** This quarter the group verified the growth rate and density of ALD coated Al_2O_3 coatings using X-ray reflectometry and ellipsometry. The same techniques will be used to characterize the SEI layer. The typical growth rate at 80°C is around 1.5 nm/cycle and density is around 3.26 g/cm³. The values have been applied to calibrate the modulus of Al_2O_3 coatings measured *via* a laser acoustic wave system providing a modulus of around 170±5 GPa.
- 3) **Compare experiments and modeling:** For the same density (3.26g/cm³), the atomic modeling predicted modulus is *ca.* 130 GPa, which is lower than the experimental values (*ca.* 170 GPa). For the next stage, the continuum mechanics model will be developed to understand the effect of Al_2O_3 coating on the mechanical failure in Si thin films and particles, and will be validated with *in situ* electrochemical-nanomechanical experiments including *in situ* nanoindentation.

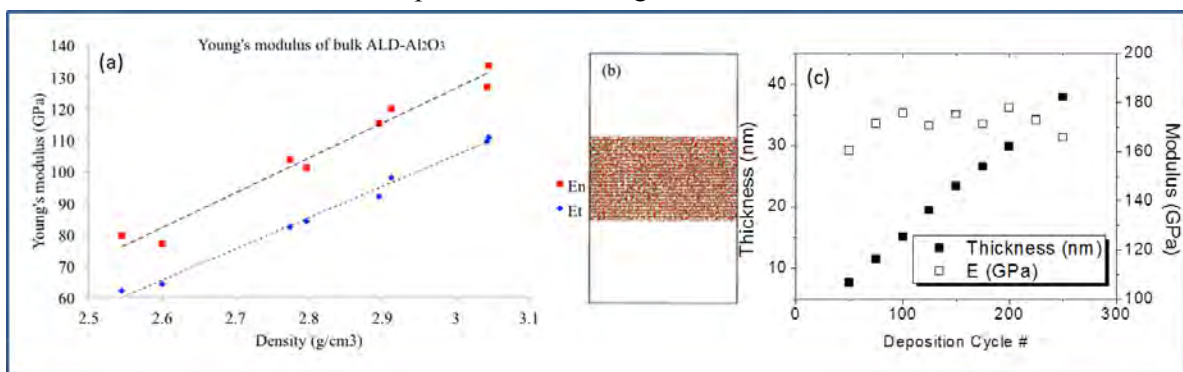


Figure 1. (a) MD predicted Young's modulus as a function of Al_2O_3 film thickness, (b) a typical atomic structure to represent ALD- Al_2O_3 , (c) Experimentally measured the cycle # vs. thickness and calibrated modulus.

- 4) Also this quarter a model Si system was developed for *in situ* AFM to monitor the formation of the SEI on Si electrodes. The initial results showed that the initial, rapid SEI formation can be stabilized before significant Li insertion begins, and that the rate at which this occurs varies significantly with the nature of surface. The initial cycling conditions also have a substantial impact on the SEI, with faster rates leading to smoother, thinner SEI films.

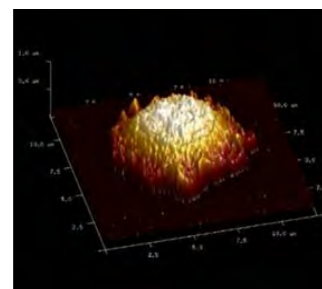


Figure 2. *In situ* AFM image shows SEI is unable to sustain the Si volume expansion.

Predicting Microstructure and Performance for Optimal Cell Fabrication

PROJECT OBJECTIVE: This work uses microstructural modeling coupled with extensive experimental validation and diagnostics to understand and optimize fabrication processes for composite particle-based electrodes. The first main outcome will be revolutionary methods to assess electronic and ionic conductivities of porous electrodes attached to current collectors, including heterogeneities and anisotropic effects. The second main outcome is a particle-dynamics model parameterized with fundamental physical properties that can predict electrode morphology and transport pathways resulting from particular fabrication steps. These two outcomes will enable the third, which is an understanding of the effects of processing conditions on microscopic and macroscopic properties of electrodes.

PROJECT IMPACT: This work will result in new diagnostic tools for rapidly and conveniently interrogating electronic and ionic pathways in porous electrodes. A new mesoscale 3D microstructure prediction model, validated by experimental structures and electrode-performance metrics, will be developed. The model will enable virtual exploration of process improvements that currently can only be explored empirically.

OUT-YEAR GOALS: This project was initiated April 2013 and concludes March 2017. Goals by fiscal year are as follows.

1. Fabricate first-generation micro-four-line probe and complete associated computer model.
2. Assess conductivity variability in electrodes; characterize microstructures of multiple electrodes.
3. Fabricate four-line ionic conductivity probe; complete first-gen dynamic particle packing (DPP) model.
4. Fabricate N-line probe for anisotropic film conductivity; validate DPP model; assess effect of processing variables.
5. Use conductivity predictions in full electrochemical model; evaluate effect of innovative processing conditions.

COLLABORATIONS: Karen Thomas-Alyea of A123 and Andrew Jansen of ANL both provided battery materials. Transfer of our technology to A123 to improve their electrode production process is in the planning stages. A modeling collaboration with Simon Thiele of the University of Freiburg was continued.

Milestones

- 1) Measure variability and average electronic conductivity for five candidate electrode compositions using four-line probe. (Dec. 13) **Complete**
- 2) Measure microstructure of three candidate electrodes using SEM/FIB. (Mar. 14) **Ongoing**
- 3) Determine appropriate set of descriptors or metrics that effectively characterize previously observed microstructures. (Jun. 14) **Ongoing**
- 4) Go/No-Go: Discontinue current four-line probe geometry. Criteria: If measurement variability is not significantly less than sample-to-sample variability. (Sep. 14) **Ongoing**

Progress Report

Completion of Milestone 1

The measurement apparatus incorporating the micro four-line probe for accurate and repeatable measurements of electronic conductivity of thin-film battery electrodes was improved. This apparatus includes an XYZ stage controlled by a LabView program that enables full automation of measurements. To ensure accurate force application on the electrode, a force sensor is used in a PID feedback loop for controlling stage position. Electrical source and measurement equipment is also incorporated. New measurement protocols were established to ensure that samples are not damaged by the probe and to minimize Joule heating during the measurement. Figure 1 shows a schematic of the updated apparatus.

Non-proprietary commercial-grade battery electrodes were provided for characterization by A123 and ANL. Five samples, four cathodes and one anode, were measured and characterized using the micro four-line probe apparatus. The average conductivity results are consistent with expected conductivity values for the electrode materials. Table 1 gives a summary of the data. Figure 2 gives an idea of the spatial variation of conductivity for one of the samples. These results indicate that spatial variations in electrode conductivity can be significant on a mm length scale, and are highly dependent on the composition and processing of the electrode.

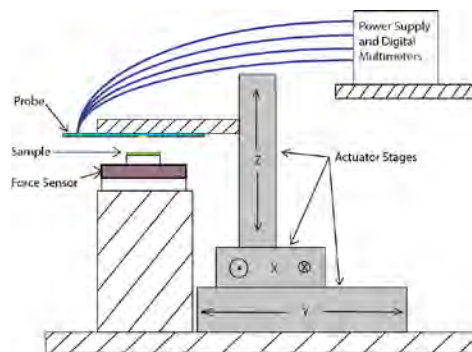


Figure 1. Schematic representation of the micro four-line probe measurement apparatus.

Table 1. Average bulk electronic conductivity of five commercially made electrodes, along with spatial standard deviation for 16 locations covering a 3 mm x 3 mm grid on each electrode.

Sample (Source)	Conductivity (mS/cm)
NCM (A123)	77.7 ± 29.5
LFP (A123)	14.2 ± 1.3
Graphite Anode (A123)	4010 ± 845
Toda 523 (ANL)	229.7 ± 33.4
Toda HE5050 (ANL)	14.0 ± 1.6

Figure 2. A representative conductivity map for the NCM (A123) sample, showing local conductivities varying from 35 to 134 mS/cm. The conductivity value at each location is determined from 20 repeated measurements in which the probe is lifted off the surface and placed again with the same amount of force. Conductivity results at each location are highly repeatable with the apparatus.

